# Deliverable 4.1

# Transport Modelling Approaches for Emerging Mobility Solutions: Supply and Demand Models

# Table of Contents

# Table index

# Figure Index

# Summary sheet

| | |
|---|---|
| **Deliverable No.** | 4.1 |
| **Project Acronym** | Momentum |
| **Full Title** | Modelling Emerging Solutions for Urban Mobility |
| **Grant Agreement No.** | 815069 |
| **Responsible Author(s)** | Santhanakrishnan Narayanan (TUM) |
| | Constantinos Antoniou (TUM) |
| | Athina Tympakianaki (Aimsun) |
| | Jordi Casas (Aimsun) |
| | Mark Brackstone (Aimsun) |
| | Maria Chatziathanasiou (CERTH) |
| | Natalia-Maria Konstantinidou (CERTH) |
| | Josep Maria Salanova Grau (CERTH) |
| | Georgia Aifandopoulou (CERTH) |
| | Rodric Frederix (TML) |
| | Willem Himpe (TML) |
| | Kris Vanherle (TML) |
| | Joren Vanherck (TML) |
| | Ignacio Martín (Nommon) |
| | Javier Burrieza (Nommon) |
| | Antonio D. Masegosa (UDEUSTO) |
| | Jenny Fajardo Calderín (UDEUSTO) |
| | Pablo Fernández Muga (UDEUSTO) |
| **Peer Review** | Tamara Djukic (Aimsun), Evripidis Magkos (CERTH), Oliva García (Nommon) |
| **Quality Assurance Committee Review** | General Assembly |
| **Date** | 03/06/2021 |
| **Status** | Draft |
| **Dissemination level** | Public |

| | |
|---|---|
| **Abstract** | The general objective of this document is to describe the models and algorithms developed to incorporate emerging mobility solutions into strategic transportation models, both in terms of supply and demand. The main outcomes of this document are the following: (i) A list of modules, which encompasses the various developments required to model emerging mobility solutions, (ii) A set of models and algorithms for modelling different aspects of the emerging mobility solutions, and (iii) An intermediate modelling framework, which integrates the principles of agent-based approaches within the traditional four-step approach. |

| | |
|---|---|
| **Version** | Issue 1 Draft 2 |
| **Work Package No.** | 4 |
| **Work Package Title** | Modelling of Emerging Mobility Solutions |
| **Programme** | Horizon 2020 |
| **Coordinator** | EMT Madrid |
| **Website** | www.h2020-momentum.eu |
| **Starting date** | 01/05/2019 |
| **Number of months** | 36 |

# Project partners

| Organisation | Country | Abbreviation |
|---|---|---|
| EMPRESA MUNICIPAL DE TRANSPORTES DE MADRID SA | Spain | EMT |
| NOMMON SOLUTIONS AND TECHNOLOGIES SL | Spain | NOMMON |
| DIMOS THESSALONIKIS | Greece | THESS |
| ETHNIKO KENTRO EREVNAS KAI TECHNOLOGIKIS ANAPTYXIS | Greece | CERTH |
| STAD LEUVEN | Belgium | LEUVEN |
| TRANSPORT & MOBILITY LEUVEN NV | Belgium | TML |
| STADT REGENSBURG | Germany | REGENSBURG |
| TECHNISCHE UNIVERSITAET MUENCHEN | Germany | TUM |
| AIMSUN SLU | Spain | AIMSUN SLU |
| POLIS – PROMOTION OF OPERATIONAL LINKS WITH INTEGRATED SERVICES, ASOCIATION INTERNATIONALE | Belgium | POLIS |
| UNION INTERNATIONALE DES TRANSPORTS PUBLICS | Belgium | UITP |
| UNIVERSIDAD DE LA IGLESIA DE DEUSTO ENTIDAD RELIGIOSA | Spain | UDEUSTO |

Version: Issue 1 Draft 2

# Document history

| Version | Date | Organisation | Main area of changes | Comments |
|---------|------|--------------|---------------------|----------|
| Issue 1 Draft 1 | 09/05/2021 | TUM | Initial version | |
| Issue 1 Draft 2 | 03/06/2021 | TUM | All sections | Consortium internal review |

# List of acronyms

| | |
|---|---|
| **ABM** | Activity-Based Model |
| **ADP** | Approximate Dynamic Programming |
| **AEMET** | Spanish Meteorological Agency |
| **AI** | Artificial Intelligence |
| **AIC** | Akaike Information Criterion |
| **BIC** | Bayesian Information Criterion |
| **BS** | Bike-sharing |
| **CO** | Carbon monoxide |
| **COP** | Combinatorial OPtimization |
| **CO2** | Carbon dioxide |
| **COPERT** | COmputer Programme to estimate Emissions from Road Transport |
| **CS** | Car-Sharing |
| **DARP** | Dial-A-Ride Problem |
| **DB** | Destination Based approach |
| **DBSCAN** | Density-Based Spatial Clustering of Applications with Noise |
| **DR** | Drivers Routes |
| **DRT** | Demand Responsive Transport |
| **DTA** | Dynamic Traffic Assignment |
| **DUE** | Dynamic User Equilibrium |
| **EMEP** | European Monitoring and Evaluation Programme for air pollutants in Europe |
| **EU** | European Union |
| **Euro 0 – Euro 6** | Euro Emission Standards |

| | |
|---|---|
| **EV** | Electric Vehicle |
| **FCD** | Floating Car Data |
| **HBEFA** | Handbook Emission Factors for Road Transport |
| **ICT** | Information and Communication Technology |
| **IPF** | Iterative Proportional Fitting |
| **IPU** | Iterative Proportional Update |
| **JDFs** | Junction Delay functions |
| **JSON** | JavaScript Object Notation |
| **KPI** | Key Performance Indicator |
| **LMS** | Landelijk Model Systeem |
| **LPG** | Liquefied Petroleum Gas |
| **MAE** | Mean Absolute Error |
| **MCMC** | Markov Chain Monte Carlo |
| **MDP** | Markov Decision Processes |
| **MDP-RL** | Reinforcement Learning on Markov Decision Processes |
| **MIP** | Mixed Integer Programming |
| **MSE** | Mean Square Error |
| **NN** | Neural Network |
| **NOx** | Nitrogen Oxides |
| **OD** | Origin-Destination |
| **OSPM** | Operational Street Pollution Model |
| **OTF** | Outsourcing Taxi Fleet |
| **PDVRP** | Pickup and Delivery Vehicle Route Problem |
| **PEMS** | Portable emissions measurement system |
| **PHEV** | Plug-in Hybrid Electric Vehicle |

| | |
|---|---|
| **PM** | Particulate matter |
| **PR** | Passengers Routes |
| **PT** | Public Transport |
| **RL** | Reinforced Learning |
| **RMSE** | Root Mean Square Error |
| **RS** | RideSharing |
| **RSP** | RideSharing Problem |
| **$R^2$** | Coefficient of determination |
| **SB** | Simulation-Based |
| **SCAG** | Southern California Association of Governments |
| **SL** | Statistical Learning |
| **SMOTE** | Synthetic Minority Over-sampling TEchnique |
| **SP** | Stated Preference |
| **SR** | Synthetic Reconstruction |
| **SUE** | Stochastic User Equilibrium |
| **TAG** | Transport Analysis Guidance |
| **TPF** | Turn Penalty Function |
| **TSP** | Traveling Salesman Problem |
| **VDF** | Volume Delay Function |
| **vkm** | vehicle-kilometre |
| **VOC** | Volatile Organic Compounds |
| **VRP** | Vehicle Routing Problem |
| **WS** | Waiting strategies |

# Executive Summary

The overall goal of the MOMENTUM project is to develop a set of mobility data analysis and exploitation methods, transport models and planning and decision support tools able to capture the impact of emerging transport modes, such as shared mobility services, and ICT-driven behavioural changes on urban mobility, in order to support local authorities in the task of designing the right policy mix to exploit the full potential of emerging mobility solutions.

The general objective of Deliverable 4.1 is to describe the models and algorithms developed to incorporate emerging mobility solutions into strategic transport models, both in terms of supply and demand. From this general objective, the specific goals posed for this Deliverable are:

- Elucidate the modular approach followed for the development of the different models for new mobility solutions.
- Present the models and algorithms developed or enhanced according to the test cases proposed in D2.2, along with the consideration for the benefits to cities outside the MOMENTUM case studies.
- Introduce a new modelling approach designed to combine the agent-based principles within the strategic four-step approach.
- Summarize the opportunities for modelling the emerging mobility solutions, based on the developed models and methods.

The main outcomes of Deliverable 4.1 are the following:

- A list of modules, which encompasses the various developments required to model emerging mobility solutions. This could be used as a basis by the future researchers for extending the research on modelling frameworks for emerging mobility solutions.
- A set of models and algorithms for modelling different aspects of the emerging mobility solutions. This set of models and algorithms include:
  - Induced demand: (i) Demand elasticity calculation and (ii) Estimation of irregular and infrequent trips of station based round trip sharing systems
  - OD: OD matrix clustering
  - Mode choice: (i) Disaggregate mode choice model and (ii) Data-driven shared mobility demand prediction
  - Synthetic population: Generation of synthetic population, along with destination choice
  - Fleet management: (i) Planning algorithms and (ii) Models for operational aspects
  - Car-ownership: (i) Aggregate model and (ii) Disaggregate model
  - Traffic assignment: (i) Assignment method for urban environments and (ii) Hybrid dynamic traffic assignment model
  - Emission: (i) Static emission model and (ii) Dynamic emission model
- An intermediate modelling framework, which integrates the principles of agent-based approaches within the traditional four-step approach, providing an opportunity for cities to evaluate and integrate shared mobility systems, and form long term planning strategy.

Version: Issue 1 Draft 2

# 1. Introduction

## 1.1. Scope and objective

The overall goal of the MOMENTUM project is to develop a set of mobility data analysis and exploitation methods, transport models, and planning and decision support tools, which can capture the impact of emerging transport modes (such as shared mobility services) and ICT-driven behavioural changes on urban mobility, to support local authorities in the task of designing the right policy mix, to exploit the full potential of emerging mobility solutions.

To achieve this general goal, one of the objectives set is to develop new modelling approaches that are able to ascertain the impact of emerging mobility concepts and solutions. This means that changes required to incorporate emerging mobility solutions into strategic transportation models, both in terms of supply and demand, have to be formulated and explanatory and predictive models have to be constructed. Furthermore, methods to include inherent uncertainty in the developed models must be designed. This document falls under the purview of the aforementioned goals.

Deliverable 4.1 describes the models developed in MOMENTUM, which are able to capture and mimic user interaction and behaviour with emerging mobility services in the strategic transport models, both in terms of supply and demand. Thus, Deliverable 4.1 aims to:

- Elucidate the modular approach followed for the development of the different models for new mobility solutions.
- Present the models and algorithms developed or enhanced according to the test cases proposed in D2.2, along with the consideration for the benefits to cities outside the MOMENTUM case studies.
- Introduce a new modelling approach designed to combine the agent-based principles within the strategic four-step approach.
- Summarize the opportunities for modelling the emerging mobility solutions, based on the models and approach designed and developed.

## 1.2. Structure of the document

The remainder of this report is divided into seven sections.

- The modular approach followed for the development of the different models is described in Section 2.
- An intermediate modelling approach, which integrates the disaggregate approach of the agent-based models within the traditional strategic approach, is elucidated in Section 3.
- Section 4 includes the presentation of four modules, namely (i) induced demand (section 4.1), (ii) OD (Section 4.2), (iii) synthetic population (Section 4.3) and (iv) mode choice (Section 4.4).
- Fleet management related algorithms are presented in Section 5.
- Traffic assignment (Section 6.1) and car ownership (Section 6.2) modules are included in the subsequent section.
- Section 7 contains the Emission module.
- Finally, main conclusions are summarised in Section 8.

## 1.3. Applicable documents

Applicable documents:

[I] MOMENTUM D1.2 Data Management Plan and Open Data Policy, November 2019

[II] MOMENTUM D2.2 Specification of MOMENTUM Test Cases, February 2020

[III] MOMENTUM D3.1 Data Inventory and Quality Assessment, March 2020

[IV] MOMENTUM D3.2 MOMENTUM Data Repository, June 2020

[V] MOMENTUM D3.3 Methodologies and Algorithms for Mobility Data Analysis, December 2020

# 2. A modular approach

Developments described in this report are based on a modular approach. Different requirements and possibilities for advancing the strategic transport models of the cities are identified and categorized as different modules, as shown in Figure 1. For brevity, the modules are further grouped into four, namely demand, supply, fleet management and sustainability.
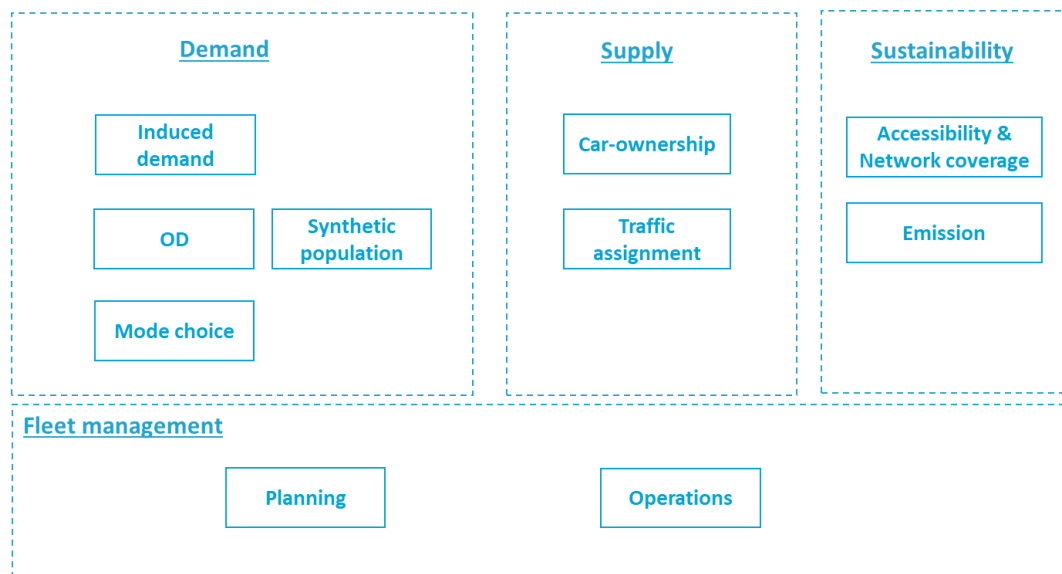


*Figure 1. Modular approach followed for the development of models in MOMENTUM*

The group 'Demand' includes the first three steps of traditional 4-step modelling approach (i.e., trip generation and distribution and mode choice). While cities continue to use the traditional strategic 4-step model, modelling of shared mobility calls for agent-based approaches. Therefore, it is decided to integrate the disaggregate approach of the agent-based models within the traditional strategic 4-step approach, so that cities can continue using their existing models, but with extended capabilities that enable to evaluate shared mobility systems. Therefore, a new module for synthetic population generation is added. Furthermore, introduction of new transport services like shared systems alter the transport supply. As a consequence, the total demand in the network can change. Hence, to reflect this supply-demand interaction (i.e., demand elasticity with respect to a change in supply), another module called 'induced demand' is included.

The fourth step of the traditional modelling approach (i.e., traffic assignment) is included under supply category. Furthermore, a module named 'car-ownership' is also included in this category. With an increasing interest towards sustainable transport in cities, there is a growing concern for private car ownership and use. Hence, a module for car-ownership has been added.

Between supply and demand, a third category called 'Fleet Management' is introduced. When modelling shared mobility systems, it is pertinent to mimic the operations of the shared system operators. Hence this category is created, which contains algorithms for the planning (e.g., to locate stations) and operations (e.g., to assign vehicles to users) of shared mobility services.

Finally, emission calculation and determination of accessibility and network coverage are included under the category 'Sustainability'. There is an increasing interest towards emissions and accessibility from cities, and hence, the aforementioned two measures are added. Under each of the modules, we develop one or more new models. A brief on each of these models is provided in the subsequent sections.

# 3. Modelling schema

Considering the existing literature and the models used by the cities, a new modelling framework is designed to extend the traditional four-step approach, and the same is presented in this section. Existing literature related to modelling of shared mobility generally shows the use of agent and activity-based approaches. For example, Martínez et al. (2017) developed an agent-based model to simulate one-way car-sharing systems in Lisbon. They incorporated operation side of the system, along with a stochastic demand model. Similarly, Ciari, Balac and Axhausen (2016) presented the use of MATSim (an activity-based multiagent simulation system) for modelling car-sharing systems. Another example is the application of agent-based travel demand model MobiTopp by Heilig et al. (2015) for modelling roundtrip-based and free-floating car-sharing systems.

While the **agent-based approaches are seen as a natural way to model shared mobility** (since they offer the possibility of a more realistic representation of the shared mobility), **many European cities continue to use the traditional strategic four-step modelling approach**. Therefore, there is a **need to extend the conventional four-step approach**, to make it more suitable for modelling shared mobility. Existing pertinent literature in this direction include Friedrich, Hartl and Magg (2018); and Friedrich and Noekel (2017). Friedrich and Noekel (2017) focused on the integration of car-sharing systems into the four-step approach, by incorporating the system in the timetable-based PT assignment. This approach does not consider the operation side of the sharing system. In a subsequent research, Friedrich et al. (2018) developed a matching algorithm for ridesharing, which could be integrated within the four-step approach. Demand is based on fixed shares. Thus, a realistic consideration of the mode choice is not implemented.

Literature findings show that there is no substantial research on the integration of shared mobility into the four-step approach. The existing ones focus on single type of shared systems (car-sharing or ridesharing), without a comprehensive approach. In addition, bike-sharing systems and models for deriving pertinent Key Performance Indicators (KPIs), such as car-ownership and induced demand, are not integrated into the four-step approach. Therefore, **a modelling framework, which integrates the disaggregate approach of the agent-based models within the traditional strategic transport modelling approach**, is designed. This new framework, shown in Figure 2, is called 'Intermediate modelling approach', as the approach stands in between the traditional four-step approach and the agent-based approaches.

This new framework will continue to use the existing trip generation and trip distribution steps from the traditional four-step approach for OD matrix generation [indicated as **step (1)** in Figure 2]. Following trip distribution, the OD matrix is disaggregated using socio-demographic data to generate synthetic population and destination choice [**step (2)** in Figure 2]. Based on this synthetic population, the demand for different modes is estimated using mode choice models. The conventional aggregate mode choice models of the cities usually include only conventional modes, and, hence, an updated model that also includes different shared mobility systems is required.

In general, several cities do not have a sufficient data to estimate a mode choice model, which includes all conventional modes and the different shared mobility systems. Wherein data is available, the development of a mode choice model between conventional systems as a whole and the different shared mobility systems could be beneficial, as such a model could be used in other cities. This kind of use is possible, given that it is possible to generalize the demand characteristics of shared mobility systems [e.g., unique profile of users such as younger individuals, possession of Bachelor's degree or higher, and holding of PT passes (Becker, Ciari and Axhausen, 2017; Clewlow, 2016). Hence, the proposed framework has been designed to accommodate such a procedure. In such a case, the calculation of mode share will be a bilevel procedure with the split between conventional systems as a whole and the different shared mobility systems estimated at the top (**step (3)** in Figure 2). The split between the different conventional systems is estimated at the bottom, using the conventional aggregate mode choice model of the city.

**Deliverable 4.1**   New transport modelling approaches   Page **19** of **137**
for emerging mobility solutions

Copyright © 2021 by MOMENTUM   Version: Issue 1 Draft 2
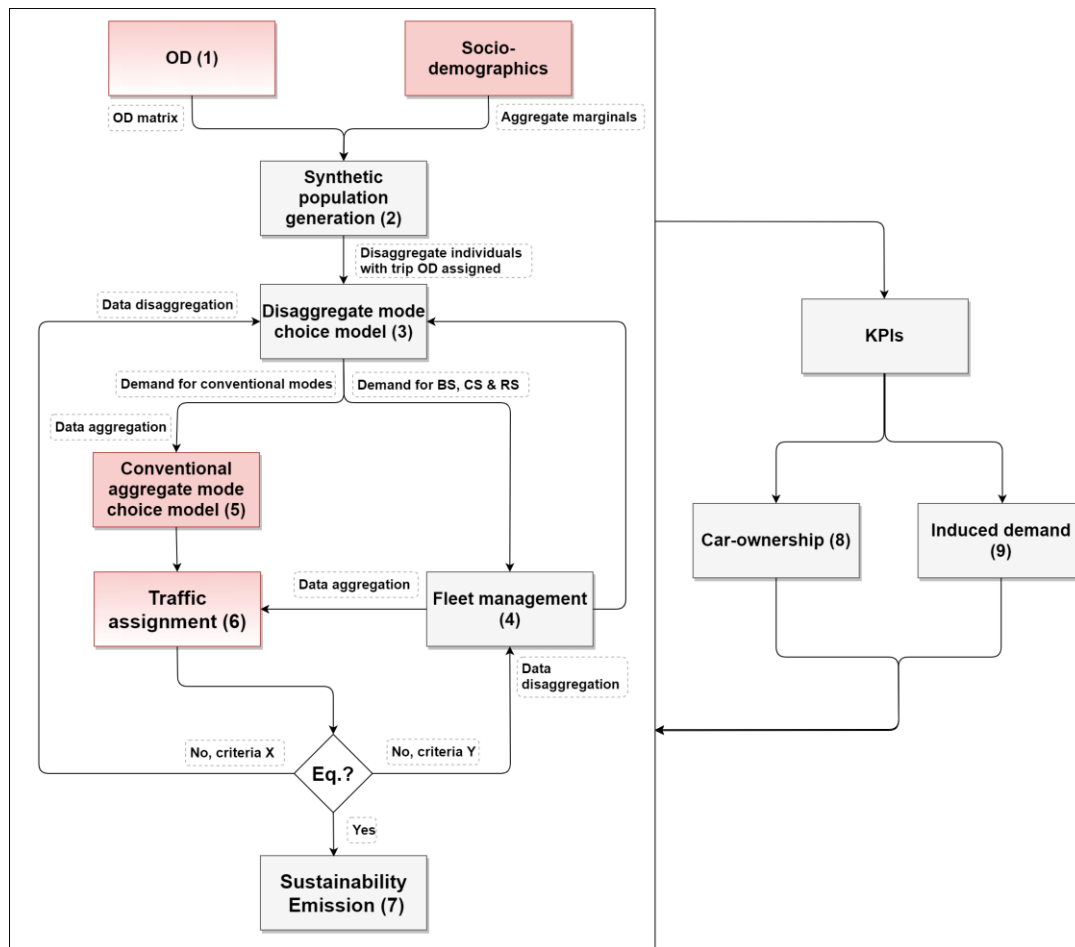
*Figure 2. Intermediate modelling approach*

Note:
1. *BS: Bike-Sharing; CS: Car-Sharing; RS: Ridesharing; Acc.: Accessibility; NC: Network Coverage*
2. *Red colour shaded boxes indicate the existing components in the traditional four-step approach*
3. *Partial red coloured ones are those that are already found in the traditional four-step approach, however, improvements and alternative models are presented in this deliverable (e.g., OD clustering and classification presented in Section 4.2)*
4. *Accessibility and network coverage will be inherent parts of fleet management.*

Once the modal share at the top level is estimated using the disaggregate mode choice model, the disaggregate demand of the shared systems is fed into the fleet management algorithms, which assign vehicles and simulate the operations of the shared vehicles [**step (4)** in Figure 2)]. Initial skim matrix is utilised for the travel times in the first iteration. If there are any unserved demand, they are reassigned to another mode through the disaggregate mode choice model. Once this process is carried out, the trips to be served by the shared vehicles are aggregated. This will be the mode specific demand corresponding to the shared mobility systems. Similarly, the demand corresponding to the conventional modes as a whole is aggregated and fed into the conventional aggregate mode choice model [**step (5)** in Figure 2)]. Thus, the mode specific demand corresponding to the individual conventional modes could be obtained.

Subsequent to the estimation of the mode specific demands of the conventional modes and the shared mobility systems (using the disaggregate and conventional aggregate mode choice models), they are fed into the existing traffic assignment model [**step (6)** in Figure 2)]. Based on the traffic assignment results, it might be required to iterate the sequence from mode choice or fleet management. Models with feedback between traffic assignment

and mode choice steps already exist in literature and it is not something new. Nevertheless, a criterion for iterating from the mode choice step could be based on the extent of change in travel times (smaller changes might not result in a significant change in modal split). Similarly, to iterate from the fleet management step, the criteria could be based on the feasibility of the shared mobility trips (which depends on the updated travel times from the traffic assignment algorithm), and the need for assigning a different vehicle.

Once an equilibrium is reached, post processing is carried out to calculate emissions [**step (7)** in Figure 2)]. Based on this updated modelling sequence, KPIs are calculated, along with estimation of car-ownership [**step (8)** in Figure 2)] and induced demand [**step (9)** in Figure 2)] and the entire modelling sequence could be rerun, with respect to these estimations. Although different equilibrium checks could be introduced (e.g., after estimation of induced demand and car-ownership at the end), they are avoided in view of the convergence issues and to reduce additional complexity. Hence, the decision to rerun the model after estimation of induced demand and car-ownership is left to the discretion of the modeller.

The extensions mentioned above are described in the subsequent sections. The sections are ordered in a way to maintain the grouping (i.e., the four categories) presented in Figure 1. Hence, the structure will differ from the order of steps indicated in Figure 2. Nevertheless, to connect the sections with the step numbers from Figure 2 and to support the reader, the structure is summarized in Figure 3. In addition, to enable easy navigation, links to modules are provided in the header.
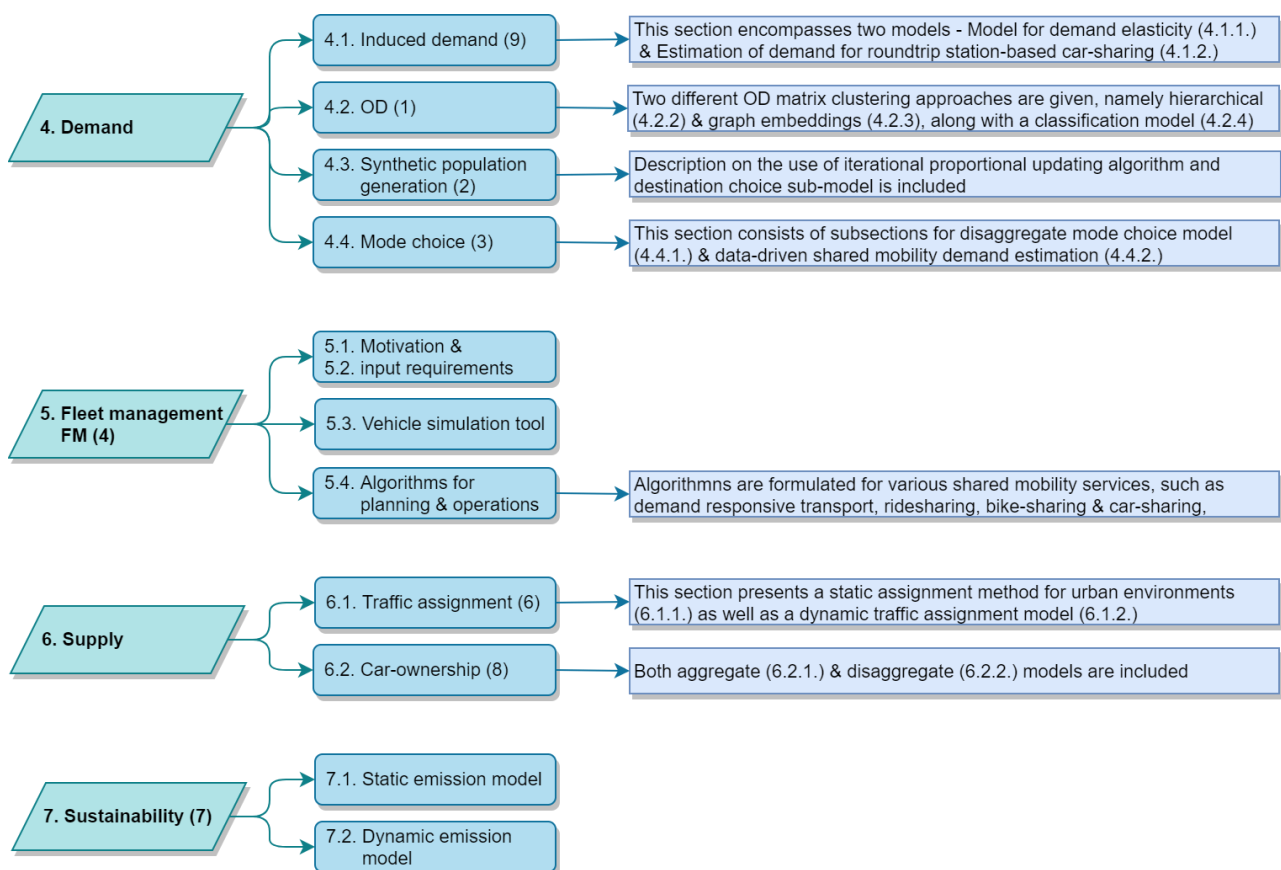


*Figure 3. Structure of Sections 4 to 7*
Note: The numbers in the brackets, i.e., (1), (2), etc., correspond to the numbers in Figure 2.

While demand elasticity model is directly related to induced demand module, the estimation of demand for roundtrip station-based car-sharing system may appear to be inconsistent for inclusion under the module. A round-trip station-based car-sharing system can be introduced in a city to complement public transport, by designing the business model to focus on serving special trips (e.g., trips to furniture stores). The OD matrices generated through the trip generation and distribution steps (in the traditional 4-step approach), usually, do not adequately cover this demand stratum (i.e., special trips). Furthermore, when the car-sharing system is small, the modal split for them is very less (< 50 trips per day), making their use a very rare event, thereby resulting in a situation where it is not possible to account them through the traditional mode choice models. Therefore, the demand has to be additionally estimated using an external approach. Since the demand corresponding to the system is an addition to the trips in the conventional OD matrices, the estimation approach is included as part of induced demand module.

In the traditional 4-step approach, the general OD matrix is usually generated through trip generation and distribution steps. However, with the increasing availability of cell phone data, the generation of OD matrices from such data is rising. In this context, OD matrices can be derived more frequently, such as daily or even hourly. Nonetheless, this generation of OD matrices is based on past mobile phone data. To support the prediction of future OD matrices based on past matrix information, Section 4.2 proposes a machine learning approach to derive representative OD matrices through clustering and use a classifier to assign the most representative matrix available to each day in the future[1].

Disaggregate mode choice model and data-driven shared mobility demand estimation model[1] described in Sections 4.4.1 and 4.4.2 have a substitutional nature, since the use of one negates the need for the other. Mode choice models are the commonly used methods in transport models. However, if one wishes to use shared mobility service data, the data-driven demand model can be used to replace the disaggregate mode choice model. The output of the data-driven demand model is an OD matrix of shared mobility, and the information of this matrix can be fed into the synthetic population module. Since the entry matrix is already mode specific, the output of the synthetic population does not have to pass through the disaggregate mode choice model, rather it can enter directly to the fleet management module.

In a similar fashion, static (Section 7.1) and dynamic (Section 7.2) emission models have a substitution nature. Static traffic assignment models are the usual methods employed in the traditional strategic 4-step approach, and hence, a static emission model is a necessity. Nevertheless, there is a growing interest in dynamic traffic assignment, and aiming at such models, a dynamic emission model has also been developed.

---

[1] Th OD clustering and classification approach and the shared mobility demand estimation model are data-driven approaches and the latter depends on the former. The use of them would result in an alternate (to the intermediate approach shown in Figure 2) framework and a feedback between fleet management module/traffic assignment and shared mobility demand estimation is not possible due to the data-driven nature. Similarly, a feedback between induced demand and  OD generation step cannot be implemented.

# 4. Demand

This section covers the modules for demand related aspects. Models concerning induced demand are presented at first, followed by a section on OD matrix clustering and classification. Then, synthetic population generation and destination choice models are described, and subsequently, models under mode choice module are elucidated.

## 4.1. Induced demand module

### 4.1.1. Demand elasticity

#### 4.1.1.1. Motivation and objective

Under the continuous pressure of congestion, urban mobility ecosystems are in rapid transition. Many new modes of transport become available that shake up classical transport systems. Next to the new modes of transport, also classical sustainable alternatives such as biking and public transport gain in importance. Cities that want to play a pioneering role in this evolution explore how they can adapt their infrastructure to accommodate these changes, for example, by opening part of the car-infrastructure for other transport modes such as shared mobility services. When using traditional transport models (traffic assignment with modal choice) on these supply-side changes, this often leads to overly detrimental predictions on vehicle loss time and queue lengths. In reality, when faced with exorbitant travel times, car drivers often seek and find alternatives that are not accounted for within the model structure, for example departure time shifts, shifts in activity and activity locations, etc. In turn, this leads to cost-benefit analyses that are overly pessimistic, and as a result to valuable changes to the transport infrastructure (e.g., shared mobility infrastructure) not being implemented.

To overcome these drawbacks, the induced demand module implicitly accounts for these alternatives (departure time shifts, shifts in activity and activity locations, etc.) by creating a feedback loop to the demand side, and calibrate this feedback loop based on elasticity estimates that can be found in literature. This approach should be contrasted to activity-based models that can inherently account for such variability but are much more intensive on the computational and data-side.

#### 4.1.1.2. Literature review

The importance and magnitude of demand elasticities—quantifying the relative demand change given the relative change of a variable—in transport systems has long been recognized in literature. A high-level overview of economic demand elasticities is given by Lee, Klein and Camus (1999). It gives a good description of the difference between short- and long-term demand changes. Litman (2017) gives a clear overview concerning generated traffic and how to assess its impact. Geilenkirchen et al. (2010) reviews price elasticities on the transport market and finds that the price-sensitivity for public transport is typically higher than that for car usage. Examples on latent demand upon changes in highway road capacity can be found in van der Loop, van der Waard, and van Mourik (2014). Finally, Williams and Yamashita (1992) investigate the effect of (not) accounting for elastic demand on the user benefits from highway capacity expansions.

In traffic models, route choice and sometimes, modal choices, are already accounted (Cascetta, 2009). However, typically the total demand for a given OD pair is not influenced. When it comes to incorporating variable demand directly into traffic models, the literature is less extensive. We refer to Cantarella et al. (2013) for a detailed literature review. A few large and extended traffic models indicate that they account for variable demand. These include the Dutch Landelijk Model Systeem (LMS) and the UK's Transport analysis guidance (TAG). However, precise implementation descriptions are often not available or a large amount of data and calibration is needed for every model. This makes them expensive in both labour and computational cost, rendering it virtually infeasible

MOMENTUM

Modules: **Induced demand | OD | Synthetic population generation | Mode choice | Fleet management | Traffic assignment | Car ownership | Emissions**

for traffic models of smaller urban areas to incorporate variable demand. Here, we propose a pragmatic way to include variable demand in those smaller-scale traffic models.

### 4.1.1.3. Theoretical framework for variable demand

The goal is to model variable demand $D$ for a given OD pair, given the demand for a base-scenario $D_0$. The OD matrix is assumed to be split according to the time of travel (e.g., peak versus off-peak). The variable demand $D$ is thus the demand for a given OD pair during a given period of the day. Shifts in demand between OD pairs (e.g., shopping at another supermarket) and periods of the day (e.g., delaying a trip to off-peak hours) are accounted for implicitly by making the separate demands variable, but not establishing an explicit coupling between them. Our model focuses on short-term changes in demand, such that shifts between OD pairs and periods of the day are expected to be rather limited. As such, it is sufficient to focus on one separate variable demand in the OD matrix, without considering interactions with other OD pairs or time periods. Those interactions are, however, accounted for during traffic assignment.

The given or computed demand $D$ needs to be distributed over the set of available travel options B (modal choice). Here we start from the well-established discrete choice framework (Train, 2009), and assume that this choice can be described using a logit model. Given the utility $U^i$ for option $i \in$ B, its demand $D^i$ is given by $D^i = P^i D$, where the share choosing for option $i$ is

$$P^i = \frac{e^{U^i}}{\sum_{j \in B} e^{U^j}}.$$

(1)

Note that the utility $U^i$ is the negative of the cost for option $i$. Here, we only account for a single logit level of travel modes to choose from. However, the theoretical framework presented here is straightforward to extend to multiple nested logit levels, in which case $U^i$ represents perceived utility for the complete nest $i$.

The distribution of the demand over the different alternatives $i$ is fully determined by their utilities, for which we assume to have pre-calibrated functional forms. It remains to determine the demand $D$, given the demand of a base scenario $D_0$. In the following subsections, estimates of $D$ using either a linear model, or a discrete choice model are proposed. The calibration of the latter model will be the subject of the next section. All variables representing a quantity during the base scenario will be written with a subscript 0.

#### 4.1.1.3.1. Models for demand elasticity estimation
##### 4.1.1.3.1.1. Multidimensional linear

The most straightforward approach is to construct a linear approximation of the $D$ in terms of the utilities of the alternatives $U^i$. The first order Taylor expansion around the base scenario—corresponding to base demand $D_0$ with base utilities of the alternatives $U_0^i$— gives

$$D = D_0 + \mathbf{1} \cdot \frac{\partial \mathbf{D}}{\partial \mathbf{U}}\bigg|_{T=0} \cdot (\mathbf{U} - \mathbf{U_0}) = D_0 + \sum_{i \in B} \left[ \sum_{j \in B} \frac{\partial D^j}{\partial U^i} \right]\bigg|_{T=0} \left( U^i - U_0^i \right).$$

(2)

Here, the demand vector $\mathbf{D} = [D^i]_i$ and utility vector $\mathbf{U} = [U^i]_i$ were introduced, consisting of the the demands and utilities for the alternatives $i \in$ B, respectively. The Jacobian $\partial \mathbf{D} / \partial \mathbf{U}$ appears because the demand of each alternative $D^i$ depends on the utility $U^j$ of all the possible alternatives $j \in$ B. The expression $f(x)|_{T=0}$ means that the function $f$ should be evaluated with parameters representative for the base scenario.

It is useful to write the new demand as a sum over the demands for the different alternatives $D^j$

$$D = \sum_{j \in B} D^j \quad \text{with } D^j = D_0^j + \sum_{i \in B} \frac{\partial D^j}{\partial U^i}\bigg|_{T=0} (U^i - U_0^i).$$

(3)

### 4.1.1.3.1.2. One-dimensional linear

We assume that the underlying mode-choice model has a logit structure, and that the demand $D$ is a function of an aggregated utility $U$. The latter is defined as the logsum over the utilities of the different alternatives $U^i$:

$$U = \ln \sum_{i \in B} e^{U^i}.$$

(4)

Although the functional form $D(U)$ is unknown, it can be approximated around $U = U_0$ through its first order Taylor expansion:

$$D = D_0 + (U - U_0) \frac{\partial D}{\partial U}\bigg|_{T=0}.$$

(5)

Here, the derivative can further be written as

$$\frac{\partial D}{\partial U} = \frac{\partial D / \partial x}{\partial U / \partial x.} \quad \text{with} \quad \frac{\partial U}{\partial x} = \frac{\sum_{k \in B} \left[ e^{U^k} \frac{\partial U^k}{\partial x} \right]}{\sum_{l \in B} e^{U^l}} = \sum_{k \in B} P^k \frac{\partial U^k}{\partial x}.$$

(6)

### 4.1.1.3.1.3. Logit formulation

In the logit-based model, an additional choice level is added at the highest level. This higher level can be interpreted as the choice *to travel* or *not to travel*, with corresponding perceived utilities $U^t$ and $U^{nt}$. The relative magnitude of these utilities determines which share $P^t$ of a fictitious population $Pop$ decides to travel, i.e., the demand for the OD pair:

$$D = P^t Pop \quad \text{with} \quad P^t = \frac{e^{U^t}}{e^{U^{nt}} + e^{U^t}}.$$

(7)

The travel utility will from now on be written as $U = U^t$ and the exponential of the utility not to travel as $K = e^{U^{nt}}$. Considering the short-term evaluation period, both the fictitious population $Pop$ and the utility not to travel $U^{nt}$ are assumed constant. The base-scenario relation $Pop = D_0/P_0^t$ can then be used to write the demand as

$$D = \frac{P^t}{P_0^t} D_0 = \frac{e^U}{e^{U_0}} \frac{K + e^{U_0}}{K + e^U} D_0.$$

(8)

The utility to travel $U$ and its evaluation for the base-scenario $U_0 = U|_{T=0}$ are given by logsums over possible travel alternatives. They can be estimated using standard calibration techniques, both for the base and the current

scenario. The main challenge that remains, is to get an estimate for $K = \mathrm{e}^{U^{\mathrm{nt}}}$, which is defined in terms of the utility not to travel. It is a priori unknown and needs to be calibrated.

### 4.1.1.3.2.     Properties and comparison between the aforementioned models

The proposed models have their advantages and disadvantages, closely related to their analytical forms.

The multidimensional linear model can be fine-tuned for a specific scenario. For a choice set B of $n$ possible alternatives, there are $n^2$ parameters that can be tuned ($\partial D^j / \partial U^i \big|_{T=0}$ for every combination of $i, j \in$ B). This great adaptability may become a burden to calibrate when the set of alternatives is large. The multidimensional linear model is simple to analyse and it is easy to understand what happens in the model, being advantageous when unexpected behaviour is displayed. However, the linearity in the utilities of the alternatives $U^i$ severely limits the accurateness for large utility changes.

The one-dimensional linear model attempts to naturally incorporate prior knowledge on the logit behaviour for the choice model. It remains linear, but in a single variable (the logsum $U$) that is itself non-linear. This can lead to more natural behaviour, beyond linear in the alternative utilities $U^i$. However, it also means that the effect of relative changes in $U^i$ on the variable demand $D$ is less straightforward to analyse. Results for larger changes in $U^i$ might be better due to the incorporation of the underlying model in the logsum $U$, yielding changes in $D$ that are beyond linear in $U^i$. Having only a single calibration parameter, $\partial D / \partial U|_{T=0}$, means that calibration requires less effort and data (if good calibration is possible). Care must be taken that the calibrated parameter does not contradict the logit choice model. For instance, it is natural to assume that the output of Equation (9) must be positive.

$$
\frac{\partial D}{\partial U}\bigg|_{T=0} = \frac{\partial D / \partial x|_{T=0}}{\partial U / \partial x|_{T=0}}. \tag{9}
$$

Indeed, the overall demand should increase with the logsum utility. $\partial U / \partial x|_{T=0}$ is fully determined through the logit model at hand, while $\partial U / \partial x|_{T=0}$ should be calibrated. One should make sure that the latter two have the same sign at all times, to guarantee compatibility between the calibration and the logit model. In experimental calculations, the one-dimensional linear model has been found to show unrealistic behaviour, with decreasing demands for one alternative when the utility of another alternative decreases. This happens because the share of the former alternative does not increase fast enough as compared to the overall decrease of the demand (due to the utility decrease of the latter alternative). This type of behaviour is not desirable.

Overall, the logit-like model has similar advantages as the multidimensional linear formula. However, it does not exhibit the described unrealistic behaviour. As such, the logit-like model is the preferred model. In the calibration process, it is important to check the condition $K > 0$, which follows immediately from the definition $K = \mathrm{e}^{U^{\mathrm{nt}}}$.

### 4.1.1.4. Calibration

In theory, the described variable demand models can be calibrated based on observations on demand and mode choice changes with respect to changes in attribute $x$. Such data might be obtained through observations, stated- or revealed preference surveys. For the linear models, a simple linear regression can suffice, while for the logit model, state-of-the-art software packages, e.g., Biogeme (Bierlaire, 2020), can be used.

However, in practice, it is not always feasible nor desirable to obtain enough data for a data-driven calibration. Especially when only ballpark estimates for the variable demand are desired, a less resource-consuming estimation method is better. In the next section, we elaborate on one such alternative, based on demand elasticities that can often be found in literature.

#### 4.1.1.4.1.   Elasticity calibration

Assume that variable $x$ is changed, which might influence the utilities $U^j$ of several alternatives. The $x$-elasticity of $D^j$ is commonly defined as

$$\eta_j = \frac{\partial D^j / D^j}{\partial x / x} = \frac{\partial D^j}{\partial x} \frac{x}{D^j}. \tag{10}$$

It quantifies how a relative change in $x$ (e.g., monetary cost or travel time of $i$) leads to a change in demand $D^j$. Using $D^j = P^j D$, the elasticity can be expressed as

$$\eta_j = \frac{x}{D^j} \frac{\partial (P^j D)}{\partial x} = \frac{x}{D^j} \left[ D \frac{\partial P^j}{\partial x} + P^j \frac{\partial D}{\partial x} \right]. \tag{11}$$

The changed demand $D^j$ can thus stem from either be from the demand for other alternatives $D^k$, or from the part of the population that decides (not) to make the travel OD at the time period under study.

The different proposed methods can be calibrated based on these expressions and the values for the elasticity, often readily available in literature. Care must be taken, however, as elasticities typically strongly depend on the present values of demands $D^j$, $x$ and modal split. The calibration parameters for the multi-dimensional linear model are given by

$$\frac{\partial D^j}{\partial U^i} = \left( \frac{\partial U^i}{\partial x} \right)^{-1} \left[ \eta_j \frac{D^j}{x} - \sum_{k \in B \setminus \{i\}} \frac{\partial D^j}{\partial U^k} \frac{\partial U^k}{\partial x} \right]. \tag{12}$$

For the one-dimensional model, the single calibration parameter is

$$\frac{\partial D}{\partial U} = \frac{\left[ \frac{D^j}{x} \eta_j - D \frac{\partial P^j}{\partial x} \right]}{P^j \, \partial U / \partial x}, \text{ where } \frac{\partial U}{\partial x} = \sum_{k \in B} P^k \frac{\partial U^k}{\partial x}. \tag{13}$$

Finally, the calibration parameter for the logit formulation is found to be

$$K = e^{U_0} \left[ \frac{\sum_k P_0^k \frac{dU^k}{dx} \Big|_{T=0}}{\frac{dU^j}{dx} \Big|_{T=0} - \frac{\eta_j}{x_0}} - 1 \right]. \tag{14}$$

Each of these calibration parameters needs to be evaluated for the base-scenario. Detailed derivations can be found in the appendix.

### 4.1.1.5. Proof of concept

In this proof of concept, the use of the three different models proposed above is demonstrated on a simple scenario. Consider a single OD pair with two options to make the travel: option $A$ (e.g., by car) or option $B$ (e.g., by bus). In the base scenario, the overall demand is $D_0 = 1000$, with shares $P_0^A = 0.7$ and $P_0^B = 0.3$. The utility of alternative $A$ is assumed constant, while the utility of alternative $B$ is $U^B(x) = -1 - 0.005x$, where $x$ is a cost that may vary. For the base scenario, the cost is taken to be $x_0 = 100$. The shares of the alternatives and the base-utility of alternative $B$ fixes the utility of alternative $A$. The direct cost elasticity for $B$ and cross-elasticity for $A$ are taken as $\eta_B = -0.4$ and $\eta_A = 0.05$. Finally, $\lambda$ is set to 1.

The predictions of the three different models for the total variable demand, and how modes $A$ and $B$ contribute to it, are shown in Figure 4 for costs $x$ ranging from 0 to 300. For the one-dimensional linear model and the logit-like model, calibration was done once using the direct elasticity $\eta_B$. For the multidimensional linear model, the constantly decreasing $D$ leads to decreasing $D^A$ for large $x$. This was to be expected, as this model is only valid in a small range around $x_0$. In the specific scenario considered here, the one-dimensional linear model and the logit-like model show very similar results. Both using the direct elasticity and the cross-elasticity yields plausible results. The total demand $D$ decreases with increasing cost of alternative $B$. The decrease flattens off as the share of alternative $B$ is reduced. Some travellers that chose alternative $B$ before switch to alternative $A$ when the cost of $B$ is increased. This leads to an increased demand for $A$. The change of $D^B$ is partially compensated by an opposed change in $D^A$, leading to a milder overall demand $D$ change.
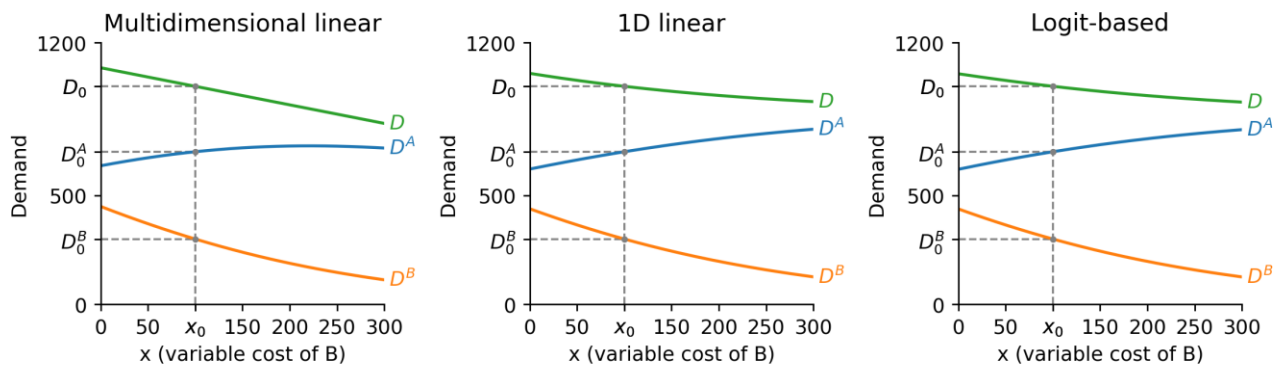


Figure 4. Results for proof of concept, using three different models.

### 4.1.1.6. Application within MOMENTUM

The logit-based induced demand model will be demonstrated in the case study of Leuven.

## 4.1.2. Demand estimation for a roundtrip station-based car-sharing system

### 4.1.2.1. Motivation and objective

Car-sharing systems could be classified as one-way and round-trip systems. While the former can be further divided into free-floating and station-based systems, the latter is a station-based system. In certain cities (e.g., Regensburg), a round-trip station-based system is implemented to complement public transport, by designing the car-sharing business model to focus on serving special trips (e.g., trips to furniture stores). In such cases, the conventional public transport system is meant to cover the regular trips like commuting, and the car-sharing system is meant to cover the special trips, thereby reducing the necessity for car-ownership.

Many European cities, especially small and medium sized cities, continue to use the traditional strategic 4-step modelling approach. The OD matrices from these models, usually, do not adequately cover the demand stratum

(i.e., special trips) of the aforementioned round-trip station-based car-sharing systems. Furthermore, when car-sharing system is small, the modal split for them is very less (< 50 trips per day), making their use a very rare event, thereby resulting in a situation where it is not possible to account them through the traditional mode choice models.

Therefore, the demand has to be additionally estimated using an external approach. Besides demand, it is also required to profile the users of such a system, so that the demand can be linked to individuals. The development of models for these two (i.e., aggregate demand and users) is dealt in this section. Since the demand corresponding to the system is an addition to the trips in the existing OD matrices, the approach mentioned here is included as part of the induced demand module.

### 4.1.2.2. Data sources utilised for model estimation

This analysis is based on the data collected on car-sharing system from Regensburg. The data sources that are available and used in this analysis include station locations, car-sharing system operator data and a household mobility survey.

The operator data consists of information related to trips carried out between November 2016 to November 2019. The data includes details such as booking start and end date, booking start and end time, pick up and return station (same value because of round-trip system), vehicle make and model, distance travelled during the booking. A total of 8,567 trips are recorded in the dataset, which will be used to estimate the demand for the car-sharing system.

The survey was conducted between February 2018 and January 2019, and 2,501 individuals from 1,116 households participated in the survey. The survey contains a question related to frequency of use of the car-sharing system, with the following possible answers: daily or almost daily, 3 to 4 days per week, 1 to 2 days per week, 1 to 3 days per month, 1 or 2 days per quarter, rare and never. This frequency variable is used to obtain a profile of the car-sharing users.

### 4.1.2.3. Methodology

The aim is to develop a data-driven approach for estimating the demand and profile the users of the car-sharing system. This approach uses a multi-method framework, combining a multinomial logit model to find the users, and regression models to estimate the number of trips per day and number of trips per station per day, as shown in Figure 5. The decision to keep an independent variable in the model is based on the p-value (significance level of 0.10) of the corresponding variable, and improvement in the statistical parameters $R^2$ (for linear regression), log-likelihood (for multinomial logit), and AIC and BIC (for Dirichlet regression). Models are developed in a stepwise fashion, first backward (from saturated models), where only variables of high significance are kept, then forward (from empty models), where significant variables are added one after the other.

The dependent variables for the model on number of trips per day and number of trips per station per day are constructed by aggregating the individual trips from the operator data. The dependent variable for the multinomial model is the frequency variable from the household survey. It is to be noted that the frequency categories "Daily or almost daily" and "3 to 4 days per week" have 0 and 1 samples, and hence, they are discarded for the analysis (since a model estimation is not possible). Furthermore, the categories "1-3 days/Month" and "1-2 days Week" are grouped together as "medium frequency users" and the categories "1-2 days/Quarterly" and "rare" as "low frequency users".
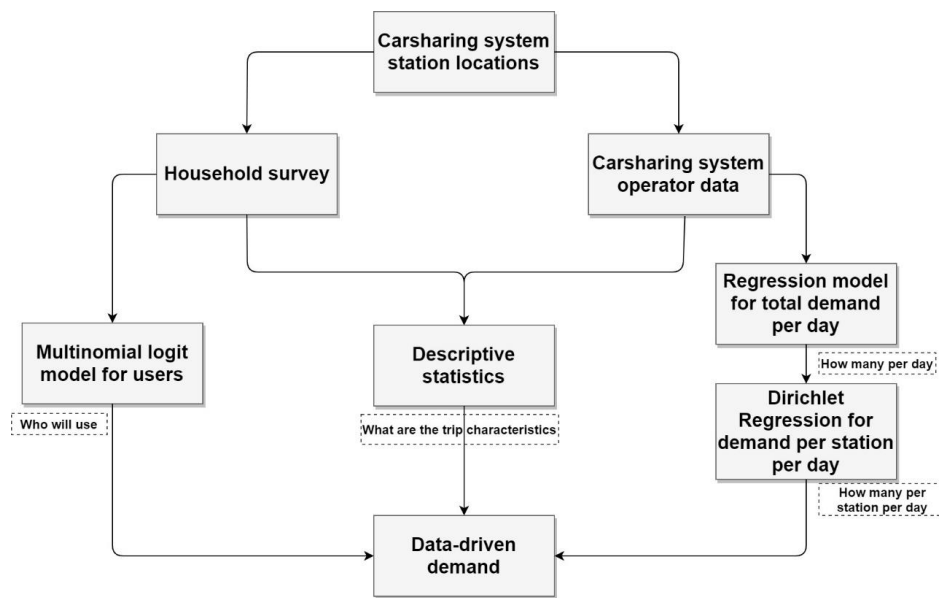
*Figure 5. Demand modelling for roundtrip station-based car-sharing system*

### 4.1.2.4. Analysis results

#### 4.1.2.4.1.    Linear regression model

The objective behind this model is to estimate the daily demand for the whole car-sharing system. The model is estimated in R using the base function lm(). The decision to include an independent variable in the model is based on the p-value (significance level of 0.10) of the variable, and improvement in the statistical parameter (adjusted) $R^2$. The specification of the final model is as follows:

$$TotalDemand = Intercept + StationCount + isFriday + isSaturday + isSunday + isFebruary + isInMarchOrAprilOrMay + isInJuly \qquad (15)$$

The estimates of the regression model and their interpretation are shown in Table 1.

| Variable | Estim. | S.E. | t-stat | Interpretation |
|---|---|---|---|---|
| StationCount | 1.82 | 0.03 | 55.78 | For every new station introduced (with 1 or 2 vehicles), on average, the demand increases by 1.82. |
| isFriday | 0.56 | 0.22 | 2.55 | Highest demand during Friday |
| isSaturday | -0.46 | 0.22 | -2.11 | Lesser demand during Saturday |
| isSunday | -2.58 | 0.22 | -11.87 | Lowest demand during Sunday |
| isFebruary | 1.23 | 0.29 | 4.32 | Higher demand during February |
| isInMarch/April/May | 1.52 | 0.18 | 8.52 | Highest demand during the months March to May |
| isJuly | 0.79 | 0.27 | 2.90 | Higher demand during July |
| Intercept | 0.91 | 0.17 | 5.23 | - |

Adjusted $R^2$: 0.75

*Table 1. Estimation result – Total demand model for roundtrip station-based car-sharing system*

#### 4.1.2.4.2.    Dirichlet regression model

This model is developed to divide the daily demand (estimated through the linear regression model) to the eight car-sharing stations in Regensburg city (i.e., this model finds the shares for individual stations). The model is based on multivariate Dirichlet distribution and is estimated in R using the package 'DirichletReg'. The decision to include an independent variable in the model is based on the p-value (significance level of 0.10) of the variable, and improvement in the statistical parameters AIC and BIC. The final model specification is as follows:

$$
\begin{aligned}
Burgweinting\ (B) &= Intercept + log(TotalDemand) + isSunday \\
Candis\ (C) &= Intercept + log(TotalDemand) + isMonday + isSaturday \\
Dachauplatz\ (D) &= Intercept + log(TotalDemand) + isFriday \\
Koenigswiesen\ (K) &= Intercept + log(TotalDemand) \\
Landratsamt\ (L) &= Intercept + log(TotalDemand) + isWednesday \\
Petersweg\ (P) &= Intercept + log(TotalDemand) + isWednesday \\
Stadtamhof\ (S) &= Intercept + log(TotalDemand) + isTuesday + isSunday \\
Techbase\ (T) &= Intercept + log(TotalDemand)
\end{aligned}
\tag{16}
$$

The estimates of the regression model and their interpretation are shown in Table 2.

| Variable | Estim. | S.E. | z-val | Interpretation |
|---|---|---|---|---|
| TotalDemand (B) | 2.85 | 0.59 | 4.84 | As the penetration of the car-sharing system increases, certain stations attract more customers, e.g., there is a higher share for Candis, when the total demand increases |
| TotalDemand (C) | 3.10 | 0.38 | 8.10 | |
| TotalDemand (D) | 2.07 | 0.38 | 5.40 | |
| TotalDemand (K) | 2.37 | 0.41 | 5.78 | |
| TotalDemand (L) | 1.97 | 0.32 | 6.11 | |
| TotalDemand (P) | 2.77 | 0.36 | 7.57 | |
| TotalDemand (S) | 1.96 | 0.43 | 4.55 | |
| TotalDemand (T) | 3.06 | 0.41 | 7.37 | |
| isMonday (C) | -0.46 | 0.25 | -1.83 | Lower share for Candis on Monday |
| isTuesday (S) | 0.40 | 0.22 | 1.85 | Higher share for Stadtamhof on Tuesday |
| isWednesday (L) | 0.38 | 0.22 | 1.75 | Higher share for Landratsamt on Wednesday |
| isWednesday (P) | 0.51 | 0.18 | 2.88 | Higher share for Petersweg on Wednesday |
| isFriday (D) | -0.35 | 0.21 | -1.67 | Lower share for Dachauplatz on Friday |
| isFriday (S) | 0.33 | 0.20 | -1.63 | Higher share for Stadtamhof on Friday |
| isSaturday (C) | 0.49 | 0.21 | 2.32 | Higher share for Candis on Saturday |
| isSunday (B) | 0.79 | 0.37 | 2.12 | Higher share for Burgweinting on Sunday |
| isSunday (S) | 0.51 | 0.29 | 1.73 | Higher share for Stadthamhof on Sunday |
| Intercept (B) | -7.84 | 1.65 | -4.75 | - |
| Intercept (C) | -7.84 | 1.06 | -7.38 | - |
| Intercept (D) | -4.36 | 1.05 | -4.16 | - |

| Intercept (K) | -6.01 | 1.13 | -5.31 | - |
|---|---|---|---|---|
| Intercept (L) | -4.73 | 0.89 | -5.33 | - |
| Intercept (P) | -6.39 | 1.01 | -6.32 | - |
| Intercept (S) | -4.43 | 1.20 | -3.70 | - |
| Intercept (T) | -7.92 | 1.15 | -6.90 | - |

AIC: -1176; BIC: -1125

*Table 2. Estimation result – Demand distribution model for roundtrip station-based car-sharing system*

### 4.1.2.4.3. Logit model

A multinomial logit model is developed to estimate the car-sharing use frequency (i.e., medium frequency, low frequency and never) for individuals. The decision to include an independent variable in the model is based on the p-value (significance level of 0.10) of the variable and improvement in the log-likelihood value (likelihood ratio test). The final model specification is as follows:

$$
\begin{aligned}
MediumFrequency\ (M) \\
&= Intercept + Age + isStudent + isFullyEmployed + isHalfEmployed \\
&\quad + isBicycleHighFrequencyUser + isPTHighFrequencyUser \\
&\quad + numberOfSharingVehiclesInZone \\
LowFrequency\ (L) \\
&= Intercept + Age + isStudent + isFullyEmployed + isHalfEmployed \\
&\quad + hasLowIncome + hasUniversityDegree + HHBicycles + HHPrivateCars \\
&\quad + isBicycleMediumFrequencyUser + isPrivateCarLowFrequencyUser \\
&\quad + isPTAndCarUser + numberOfSharingVehiclesInZone \\
Never\ &= 0\ (base\ category)
\end{aligned}
\tag{17}
$$

The estimation result is shown in Table 3. As shown in the table, the frequency of use is influenced by the following factors: number of household bikes and cars, income, education, age, employment, frequency of use of conventional modes and the number of sharing vehicles in the district.

| Variable | Estim | S.E. | z-val | Interpretation |
|---|---|---|---|---|
| Age (both M & L) | -0.04 | 0.01 | -4.49 | With increasing age, there is an increasing probability to not use the car-sharing system |
| isStudent (M) | 1.78 | 0.48 | 3.67 | Students have high probability for medium and low frequency use, when compared to the category 'Never' |
| isStudent (L) | 2.09 | 0.39 | 5.30 | |
| isFullyEmployed (M) | 1.57 | 0.48 | 3.30 | Fully employed individuals (≥ 35 hr/week) are more probable to use the car-sharing system |
| isFullyEmployed (L) | 1.65 | 0.39 | 4.19 | |
| isHalfEmployed (M) | 1.97 | 0.55 | 3.57 | Individuals with half employment (b/w 18 to 34 hr/week) have a higher likelihood to use the car-sharing system |
| isHalfEmployed (L) | 1.57 | 0.47 | 3.33 | |
| hasLowIncome (L) | 0.72 | 0.37 | 1.94 | Low-income population (< €1500/month) is more likely to be a low frequency user. The low-income population may not have the capacity to own a private car and may be using the car-sharing system |

| | | | | |
|---|---|---|---|---|
| | | | | for special trips for which PT is not suitable, e.g., transporting goods from furniture stores. This could imply that the car-sharing enhances transport equity. |
| hasUniversity Degree (L) | 0.59 | 0.27 | 2.20 | Possession of university degree enhances the chances of using the car-sharing system. |
| HHBicycles (L) | 0.17 | 0.05 | 3.35 | With an increase in the number of bicycles in the household, there is an increased probability to use the car-sharing system at low frequency. This could imply that the car-sharing system complements the active mode users. |
| HHPrivateCars (L) | -0.29 | 0.17 | -1.75 | Lower likelihood to use car-sharing system, if there is an increase in the number of private cars in the household. |
| isBicycleHigh FrequencyUser (M) | 1.60 | 0.38 | 4.23 | A higher probability to use the car-sharing system, if an individual is a bicycle user (High frequency: at least for 3 days a week; Medium Frequency: once a week or at least once a month). This could also imply that the car-sharing system complements active mode users. |
| isBicycleMedium FrequencyUser (L) | 0.53 | 0.24 | 2.23 | |
| isPTHighFrequency User (M) | 1.10 | 0.36 | 3.10 | Similar interpretation to that of 'isBicycleHigh FrequencyUser', implying that the car-sharing system complements PT users, i.e., the car-sharing system is used for trips for which PT is not suitable. |
| isPrivateCarLow FrequencyUser (L) | 0.65 | 0.33 | 1.99 | Individuals who use their private cars at low frequency (once a quarter or year) are more probable to use the car-sharing system, which could mean that it is possible to reduce car-ownership in the city in the long run. |
| isPTAndCarUser (L) | -0.77 | 0.35 | -2.18 | Lower likelihood to use the car-sharing system, when an individual uses both PT and private for at least once a week. Following could be the reason: PT is used whenever possible, and private car when PT is not adequate, i.e., there exists a group who do not use car-sharing, but their private cars, when PT is not suitable for their trips. |
| numberOfSharing VehiclesInZone (M) | 0.27 | 0.08 | 3.28 | More the number of car-sharing vehicles, higher is the likelihood to use the system. Thus, introduction of new car-sharing vehicles will have a positive effect. |
| numberOfSharing VehiclesInZone (L) | 0.14 | 0.06 | 2.21 | |
| Intercept (M) | -5.65 | 0.56 | -10.16 | - |
| Intercept (L) | -4.01 | 0.49 | -8.25 | - |

McFadden $R^2$: 0.16; Log-likelihood: -522.1

*Table 3. Estimation Result – Use frequency model for roundtrip station-based car-sharing system*

#### 4.1.2.4.4.    Trip characteristics

This section is aimed at showing the distribution of travel distances of the trips from the different car-sharing stations in Regensburg. Figure 6 shows that the distribution varies between the stations. These distributions will be used as basis to assign trip distance and activity location for the sharing trips.
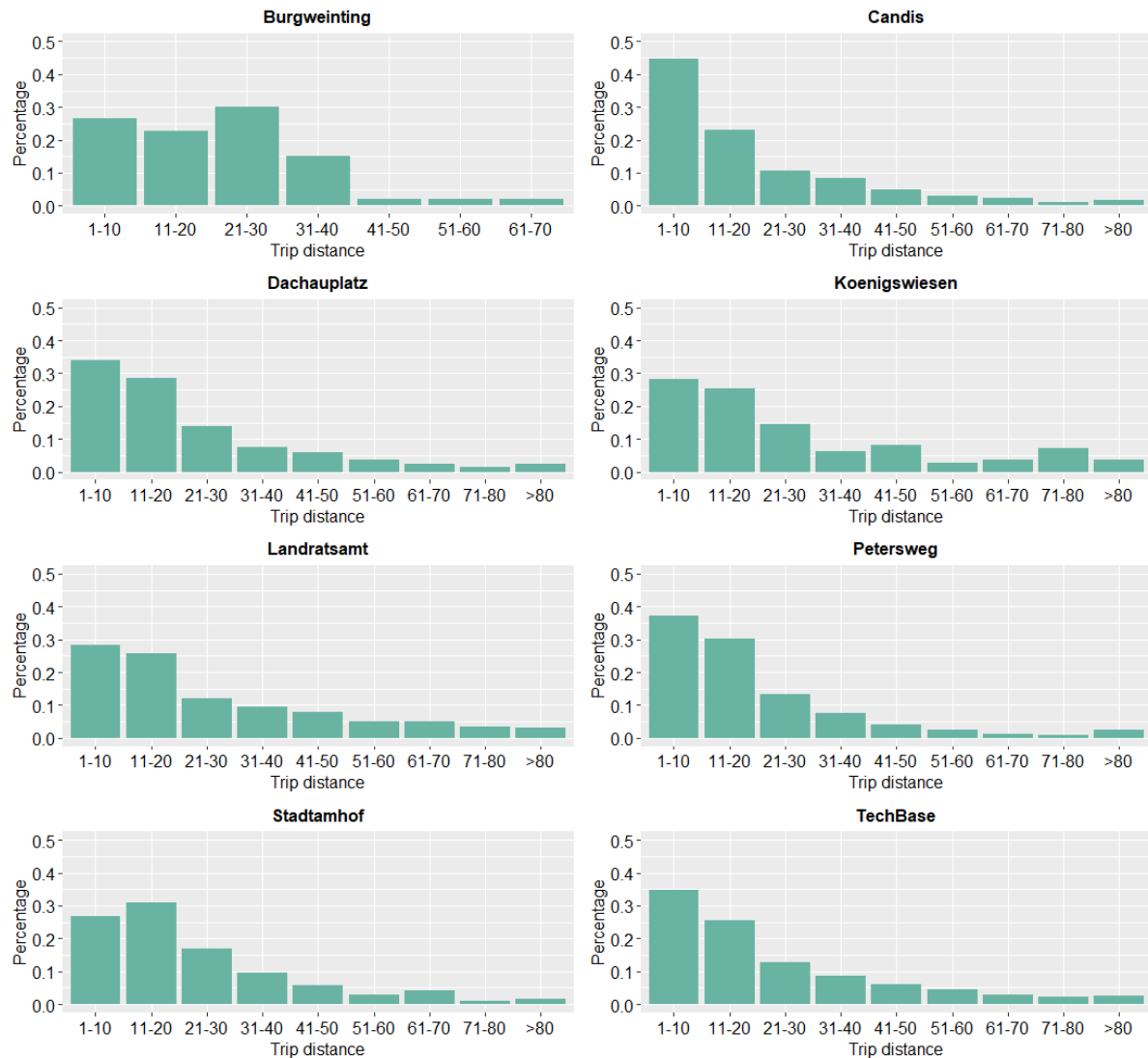


*Figure 6. Trip length distribution for roundtrip station-based car-sharing system in Regensburg*

### 4.1.2.5. Application within MOMENTUM

Within MOMENTUM, the aforementioned car-sharing system is unique to the city of Regensburg, and hence, the approach mentioned in this section is developed from Regensburg data and also will be applied to Regensburg case study. The outputs from the regression models will be utilised to estimate the demand. The outputs from the multinomial logit model will be used to assign car-sharing use frequency to a synthetic population and then the individuals will be randomly sampled based on the assigned frequency and linked to the demand estimated by the regression models.

It is to be noted that a user would have visited an activity location such as a furniture store during the booking period, although the user picks up and leaves the vehicle at the same station. Such an activity location needs to

be found to split the roundtrip into two individual trips. Therefore, the distribution of the trip distance obtained from the operator data will be used to assign the activity zone (i.e., the sampled distance and the distance between the origin station zone and other zones will be compared and the assignment will be made). Furthermore, since the time at the activity location is unknown and the travel speed for deriving such a time from the total booking duration is also unknown, a random selection from an interval of 30 minutes to 2 hours will be used as the time at the activity location.

## 4.2. OD module - OD matrix type classification and selection for typical days

### 4.2.1. Motivation and objectives

General mobility within a city is typically characterised through an OD matrix. For a given zoning system of study area, it indicates the number of trips by mode between OD pairs in the network. A static OD matrix is typically defined for a single day for specific time period and mode, and is usually estimated by means of household surveys, traffic counts or modern emerging data sources such as mobile phone records.

One of the issues regarding OD matrix estimation is that it typically relies on data that is necessarily collected in the past and, therefore, OD matrix information for upcoming dates under study can only be obtained through the use of simulation models or a combination of past matrices of similar days, usually hand-picked based on experience. The closer the structure and volumes of the selected matrix are to the traffic conditions of the day under study, the more reliable the results from the models will be. The traffic conditions of a specific day may depend on a variety of factors, such as the day of the week the weather, the existence of events, etc.

This section presents a methodology for OD matrix selection based on machine learning that allows to automatically select a representative matrix for a given day in the near future according to different variables (day of week, weather, etc.). Figure 7 shows the proposed workflow.
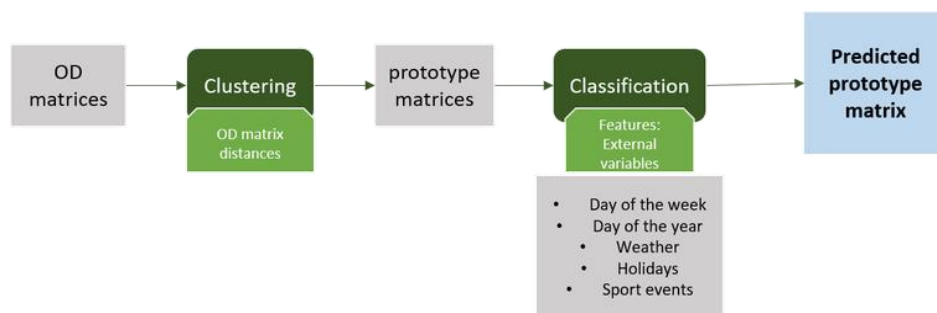


*Figure 7. Workflow of the proposed classification model*

As the figure shows, the initial step consists of the clustering of existing OD matrices according to their similarities in terms of trip volume and trip-zone structures. For this purpose, the similarity metric developed in previous stages of the project will be used (for further detail on the similarity measure, the reader might refer to Section 2 of Deliverable 3.3: "Methodologies and Algorithms for Mobility Data Analysis" of the present project). For this clustering, due to its easiness of interpretation, the hierarchical clustering will be used. The matrices assigned to each cluster will be aggregated by means of averaging into "prototype matrices", which correspond to the approximated matrix that corresponds to each cluster.

Then, using the clusters, a classification machine learning algorithm has been developed for the prediction of the cluster assigned to a given OD matrix using as input features variables related with the date of the matrix, weather or potential events. In this way, the classifier will predict to which cluster, the study day corresponds to and,

consequently, assign to it the most probable matrix or average matrix, built as the average of all the matrices belonging to the same cluster.

In the context of the MOMETNUM project, beyond the advantages already discussed about having a demand matrix as representative of the study day as possible, a better selection of the representative OD matrix will result in a better estimation of the share mobility demand obtained from data based predictive models, which takes as input the information of general OD matrices for shared mobility demand estimation. This model is discussed in Section 4.4.2.

The next sections describe in detail the exploration of clustering levels and the classification experiments and results. For the development of such models historical OD matrices for Madrid for all the days in October 2018, February, April, June, July and October 2019 and February 2020 obtained from mobile phone records were used. The matrices correspond to the city of Madrid with a zoning based on the transport zones defined by the Madrid transport authority.

## 4.2.2.  Hierarchical clustering

The initial step of the proposed method consists of the clustering of a series of historical OD matrices according to the similarities observed between them. Such similarities are obtained by applying the similarity metrics developed in the context of the project and discussed in Deliverable 3.3: "Methodologies and Algorithms for Mobility Data Analysis".

In this case, we have used the agglomerative clustering algorithm provided by Scikit-learn (version 0.23.2) in Python (version 3.7), to perform hierarchical clustering based on Ward aggregation algorithm. This type of clustering initially defines a tree-like structure that hierarchically represents all the distances between elements to be clustered, clearly identifying the degree of similarity of each pair of entities (either single elements or already clustered groups of elements). In this tree-like structure, called dendrogram, each element has a horizonal line that is connected to others by a vertical line at the point (x-axis value) that corresponds to the actual distance between them.

The number of clusters to be considered is defined by means of a cut-off distance provided to the agglomerative clustering algorithm. Every pair of elements whose distance (the vertical line connecting them) is below this cut-off distance will belong to the same cluster. For the correct determination of such distance, a series of levels has been defined according to the complexity and the number of clusters each cut-off distance introduces for the matrix dendrogram. Where to fix the cut-off distance is decided in an iterative process where the characteristics of the resulting clusters for each cut-off are evaluated. Depending on the problem under study, this evaluation can be quantitative using stablished metrics such as the silhouette score or qualitative which is the case of the current problem. The following sections provide a descriptive analysis of the clustering schemes for different cut-off distances for Madrid for a set of OD matrices calculated with mobile phone data for the months of October 2018, February, April, June, July and October 2019 and February 2020.

### 4.2.2.1. Level 0

The Level 0 clustering scheme (a) represents the higher-distance cut-off in the Figure 6 and yields the least clusters of all the schemes. Before Level 0, there is just a very big separation between two large groups, which corresponds to weekends (top) vs weekdays (bottom). Within Level 0, we can separate those two groups as follows:

- **Weekend group**: The top group is formed mainly by weekends and equivalent groups. It is divided into three sub-groups:
    - o  1. The largest one, at the top of this group (black) contains most Saturdays in the dataset as well as Sundays of two months: October 2019 and February 2020.

- o 2. The middle one (yellow) contains most of the Sundays for all the months prior to October 2019 within the dataset.
  - o 3. The smallest one (pink) corresponds to the four days of Easter in April 2019.
- **Weekday group**: The bottom group is composed of the different weekdays in different arrangements. At this level there are three main sub-groups:
  - o 4. Top sub-group (cyan) contains most weekdays of October 2019 and February 2020. Aggregation inside is observed by weekdays, except for Fridays, that are grouped together and equidistant to the other groups.
  - o 5. Middle sub-group (red) corresponds to the 5 weekdays of the last week of February 2020, which is possibly separated due to the limitations of mobility (mainly tele-work in many large companies) that arose due to the COVID-19 pandemic.
  - o 6. Bottom sub-group (green) corresponds to all the weekdays from remaining months (except October 2019 and February 2020). There are interesting inner patterns that will be explored at deeper levels.
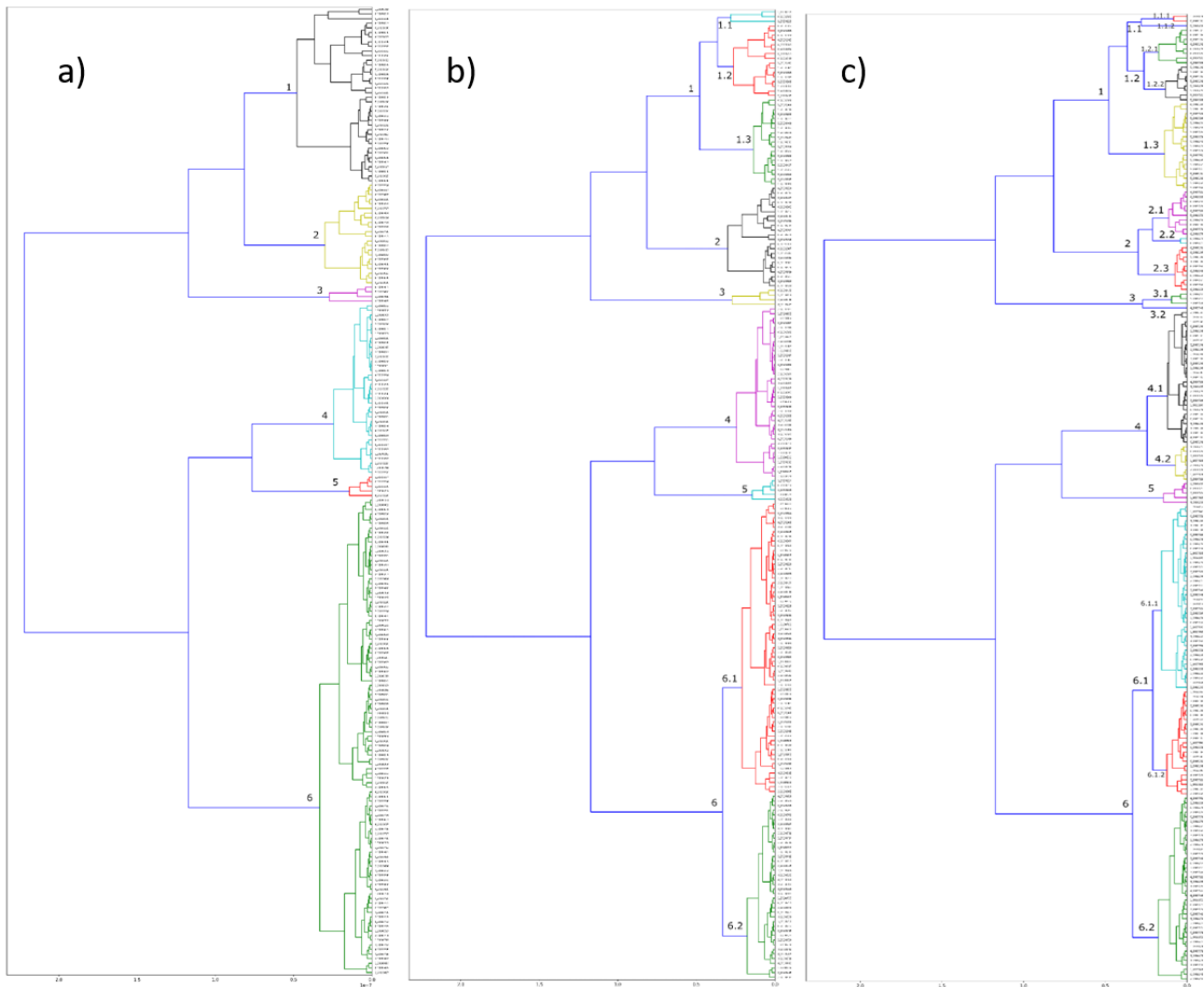


*Figure 8. Dendrogram coloured a) according to Level 0 clusters, b) according to Level 1 clusters, c) at the Level 2 cut-off distance*

Version: Issue 1 Draft 2

### 4.2.2.2. Level 1

At this Level 1 (Figure 8b) the use of a smaller cut-off distance yields more clusters (9) that appear when further partitioning pre-existing groups at Level 0. The most relevant new groups are the following ones:

- **Sub-groups derived from group 1**: Initially, group 1 contained together Saturdays and Sundays of October 2019 and February 2020 with the rest of Saturdays in the dataset. At this level, the next sub-groups have appeared:
  - 1.1. The small top subgroup (cyan) is a very small day containing two outliers and a Saturday (which is an outlier itself, as it is paired with weird days). These days correspond to those outliers observed at Level 0:
    - February 19th, 2019 (Tue): No rain, some wind gusts (not very powerful). A quick Google search suggests there is no remarkable event.
    - October 22nd, 2018 (Mon): Again, no rain, some wind gusts and nothing on the news.
    - February 29th, 2020 (Sat): can be explained due to the impact of COVID-19 caution adopted by citizens.
  - 1.2 The middle subgroup (red) now includes all Saturdays and Sundays of October 2019 and February 2020 in two clearly separated sub-groups.
  - 1.3 The bottom subgroup (green) includes all Saturdays of the remaining months along with a single Sunday:
    - October 28th, 2018 (Sun). The most remarkable event is a couple of races that could be relevant for the separation.
- **Sub-groups derived from cluster 6**:
  - 6.1. The top sub-group (red) contains most days from October, February, and June 2019 and almost half of April's. There are two outliers, October 31st, 2019, and July 2nd, 2019.
  - 6.2. The bottom sub-group (green) contains most days of July 2019 as well as the other half of April's. In this case, the days that do not match this pattern are the following ones:
    - 7th, 26th, 27th, and 28th, June 2019
    - 1st, 8th, and 22nd, February 2019.

### 4.2.2.3. Level 2

At Level 2 (Figure 8c) the larger cut-off distance makes the dendrogram be further split in up to 14 clusters. The new clusters are mainly new sub-groups detailed below:

- **Group 1.1 is separated into two minimal sub-groups:**
  - 1.1.1. Top sub-group (red): This group comprises a Monday and a Tuesday well separated in time that seem to be strange, as they are within reach of weekends.
  - 1.1.2. Bottom sub-group (blue): This group is just February 29th, 2020, which may be significantly different to other Saturdays due to COVID-19 pandemic effects. Even though at this point there were no public health measures in place yet, many large private companies had already put in place tele-work measures to ensure business continuity.
- **Group 1.2 has been separated into two sub-groups**:
  - 1.2.1. Sub-group 1.2.1 (green) contains all Sundays from October 2019 and February 2020.
  - 1.2.2. Sub-group 1.2.2 (black) contains all Saturdays from October 2019 and February 2020.
- **Group 2 is now separated into two different sub-groups**:
  - 2.1 Top sub-group (purple) comprises the Sundays of February 2019, July 2019 and half of April's. There is also one day from October 2018 and a Saturday, July 27th, when it is possible that mobility is more alike to regular Sundays due to the holiday period.
  - 2.2 Middle sub-group (cyan) Comprises only two Sundays July 21st and July 28th different than the rest, possibly due to changes in mobility because of the holiday season.

- o 2.3 Bottom sub-group (red) contains Sundays from June 2019 and October 2018. Also contains a Friday (October 12th, 2018) and a Saturday (October 13th, 2018) that correspond to Spanish national festivity "Día del Pilar" and the day after.
- **Group 3 has been split into two:**
  - o 3.1 Top sub-group (green) Contains the days of the weekend of 20th April 2019 (Sunday and Saturday) and Thursday 18th April, which are the holiday days of Easter)
  - o 3.2 Bottom sub-group (blue) Corresponds to Friday 19th April 2019 alone which is part of Easter as well, but gets separated.
- **Group 4 is now separated in two sub-groups**:
  - o 4.1. The top sub-group (black) is composed by all weekdays of October 2019 and one and a half weeks of February 2020. In general, contiguous, or nearly contiguous days appear closest in terms of distance.
  - o 4.2. The bottom sub-group (yellow) is uniquely composed by February days and precisely the standard working days (Tuesday, Wednesday, and Thursday) of two weeks (11th-13th and 18th-20th) along with a Friday (21st) and a Monday (17th).
- **Group 6.1 is now separated into two different sub-groups:**
  - o 6.1.1. Top sub-group (cyan) is composed by weekdays from February and June 2019 mainly, as well as 9 days of April 2019. There are considerably less Fridays in general. The inner organization is mainly by day of week (Mondays tend to get together with Mondays, etc.).
  - o 6.1.2 Bottom sub-group (red) contains mainly October 2018 dates. Internally, there is a difference between October 2018 dates and the rest, which correspond to days in October and February 2019.

### 4.2.2.4. Summary on hierarchical based clustering of OD matrices

Several levels of clustering based on cut-off distances have been explored. The results show different levels of disaggregation according to the level selected and most of them seem to be reasonably explained taking into account information about each OD matrix date and festivity. In sum, any of the levels described could be used as the building base of the matrix type classification model.

Nevertheless, there are two relevant observations from the clustering data. The first one is that October 2019 and February 2020 seem to be significantly different to the rest of OD matrices and it is worth noting that the algorithm in charge of generating OD matrices experienced changes for those periods. In this light, it is possible that the comparison between these two and the rest has methodological differences and thus, impact the final results of the classification. For that purpose, the classification model will be trained without these months' data.

In addition, it can be clearly observed that Level 2 could be the most appropriate Level to perform classification, as it provides clusters which differences cannot be only explained by direct hypotheses like calendar days and, therefore, interesting for the study of alternative features. However, the number of samples available for some clusters is too low, which could negatively impact on the quality of representative matrices (the resulting average matrices for each cluster). In this light, Level 1 is selected, as it provides a disaggregated enough, is able to split dates beyond the trivial weekday/season rules while keeping the number of cluster members reasonably high.

## 4.2.3. OD matrix clustering based on graph embeddings

### 4.2.3.1. Objective

The aim of this section is to present a novel OD matrix clustering methodology based on Graph Embedding techniques (Goyal and Ferrara, 2018). This methodology also makes use of the structural similarity measure of OD matrices developed in MOMENTUM, but it is mainly based on two concepts: a) the creation of a similarity graph for the set of OD matrices to be compared and b) the application of Graph Embedding techniques. In the following subsections, we will present the proposed methodology and the results obtained.

### 4.2.3.2. Methodology

The proposed clustering methodology is based on the concept of Graph Embedding (Goyal and Ferrara, 2018). The aim of this type of techniques is to find a representation of nodes, arcs, and their features in the form of a feature vector that maintains the properties of the graph structure and information (e.g., adjacent/non-adjacent nodes have close/far representations of each other, respectively).

In our case, the graph $G = (V, E)$ is defined by a set of nodes or vertices $V$ and a set of edges $E$. The set of vertices is defined as $V = \{m \in M\}$, where $M$ is the set of OD matrices to be clustered. Thus, each node in the graph is an OD matrix. The set $E = \{(m_i, m_j) \mid similarity(m_i, m_j) > \mu, m_i \in M, m_j \in M\}$, corresponds to pairs of OD matrices whose similarity exceeds a certain threshold $\mu$. That is, in the graph, two OD matrices will be connected by an edge if they are similar enough. Figure 9 shows an example of such a graph. In this case, the colour of the nodes corresponds to the day of the week.
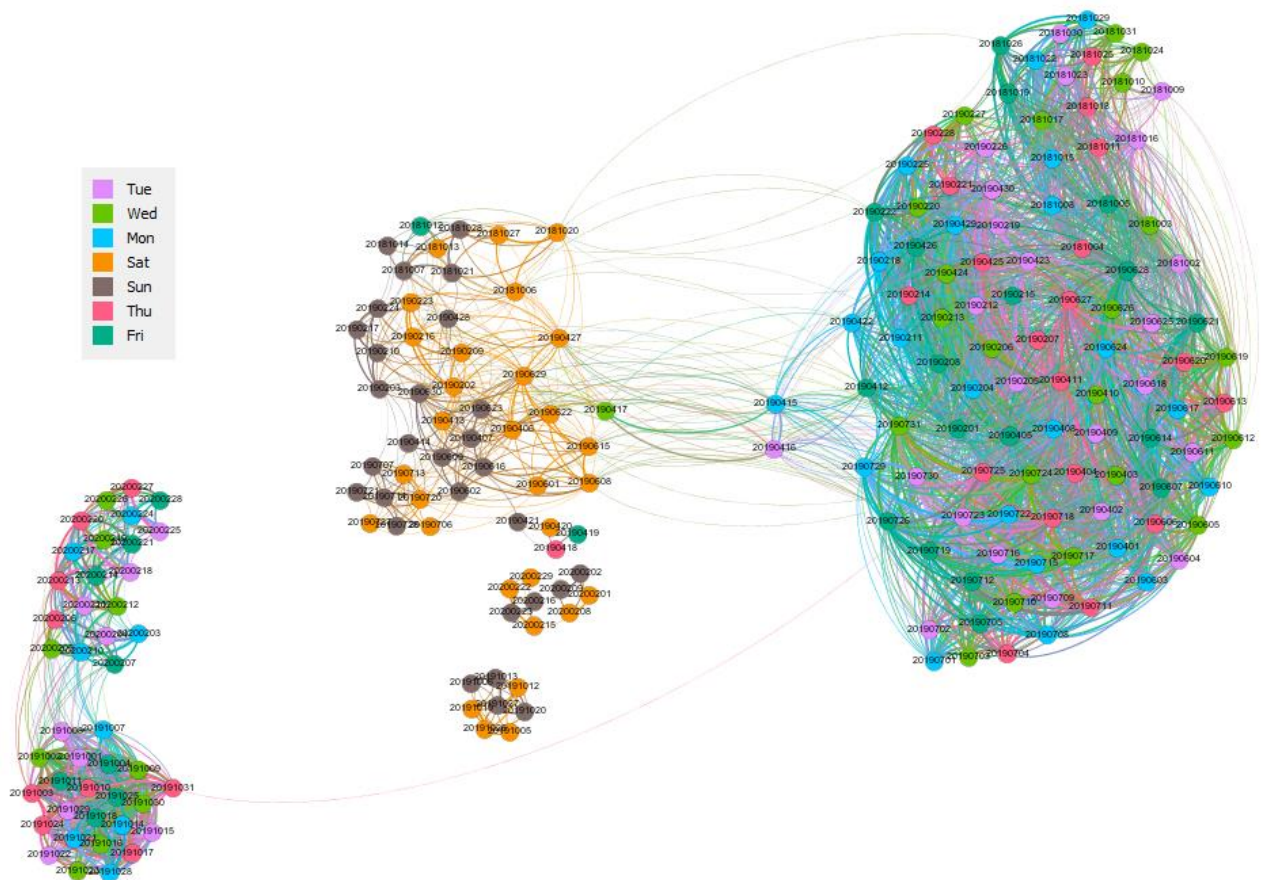


*Figure 9. Example of similarity graph for OD matrices. The colour of the nodes corresponds to the days of the week*

Once the graph has been defined, the next step in the proposed methodology consists of applying the Graph Embedding method. Although there are several proposed approaches in literature, for this task we have used Node2Vec (Grover and Leskovec, 2016), one of the best known and most widely used methods for this purpose both in the scientific literature and in practice. Specifically, this method learns low dimensional representations (embeddings) of the nodes of a graph in a way that preserves the neighbourhood structure (e.g., adjacent nodes) and different equivalences as homophily or structural equivalence. Thus, the result of this stage is a set of vectorial representations of the OD matrices composing the graph $R = \{X_k \mid X_k \in \mathbb{R}^n\}$.

Finally, the last step consists of applying a clustering method on the vector representation of the OD matrices using Euclidean distance to obtain the different clusters of these matrices. In this case, we opted for hierarchical clustering because of its simplicity in defining different levels of grouping.

### 4.2.3.3. Results of the clustering based on graph embeddings

In this section, we are going to show the result of the clustering of the OD-articles using Graph Embeddings. The similarity measure is also the one proposed in D3.3, and specifically, the so-called Approach 1, described in Section 2 of Deliverable D3.3 "Methodologies and Algorithms for Mobility Data Analysis". The threshold for determining when an edge is established between two OD matrices was set at the 70th percentile, i.e., only those OD matrices whose similarity is within the top 30% of the most similar ones are those connected with an edge. The resulting graph is shown in Figure 10. For the sake of understanding, the colours of the nodes correspond to the months analysed.
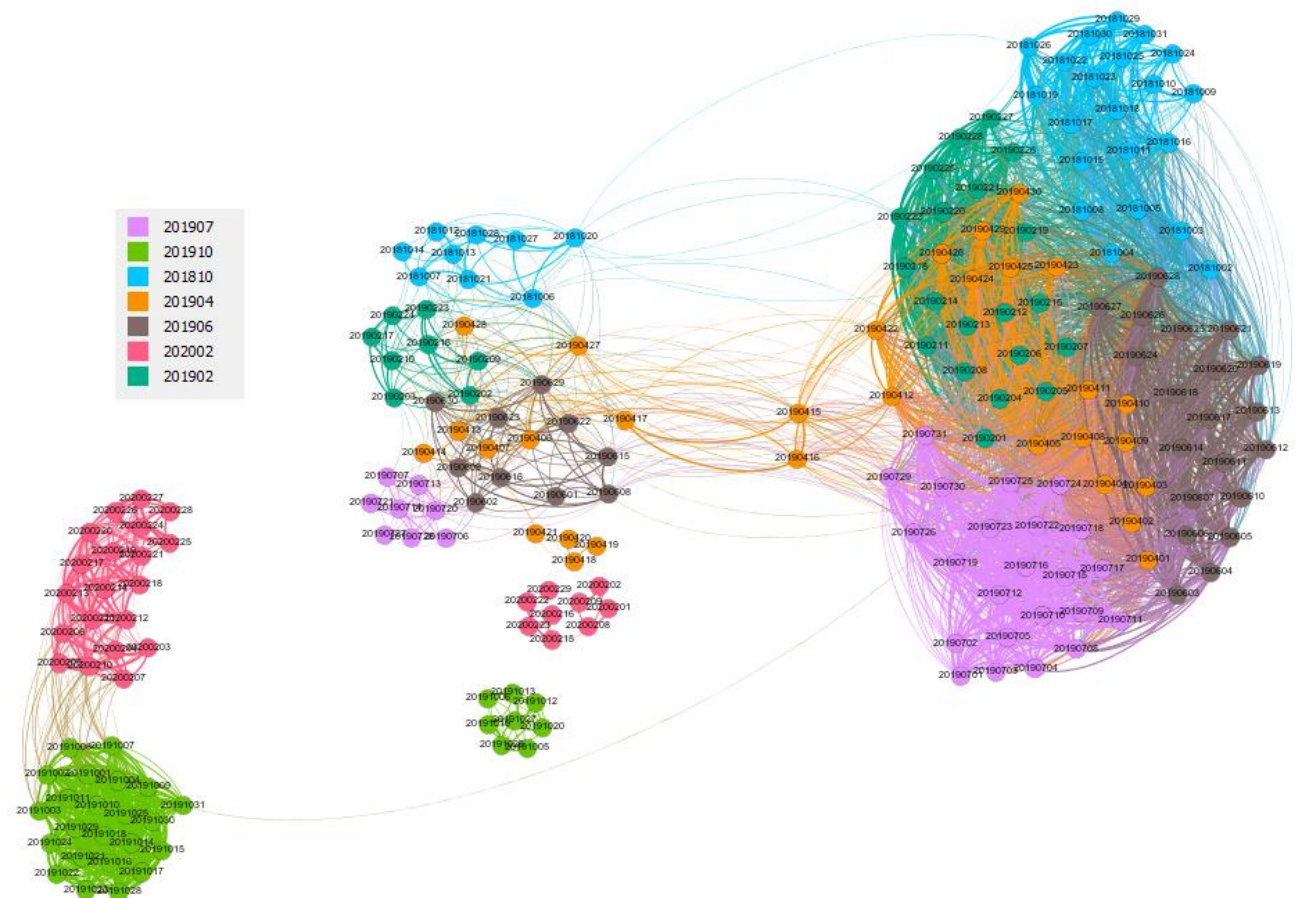


*Figure 10. Graph representation of similarities between OD Matrices according to Approach 1. The colour of the nodes corresponds to the month*

The parameterisation used to apply Node2Vec is shown in Table 4. As indicated in the methodology section, the result of embedding is a vector representation for each OD matrix (in this case of dimension 128). Hierarchical clustering has been applied to this representation using the Ward method based on the Euclidean distance between these representations in order to obtain the different OD matrix clusters.

Regarding the data used and the clustering levels defined, we follow the same approach as the one used for matrix clustering based on the similarity measure. In the following sections, we show the resulting clusters according to different aggregation levels.

| Parameter | Value |
|---|---|
| p | 1 |
| q | 20 |
| number of random walks | 500 |
| random walk length | 10 |
| window size | 10 |
| feature vector dimension | 128 |

*Table 4. Parametrization of Node2Vec algorithm*

### 4.2.3.3.1.   Level 0
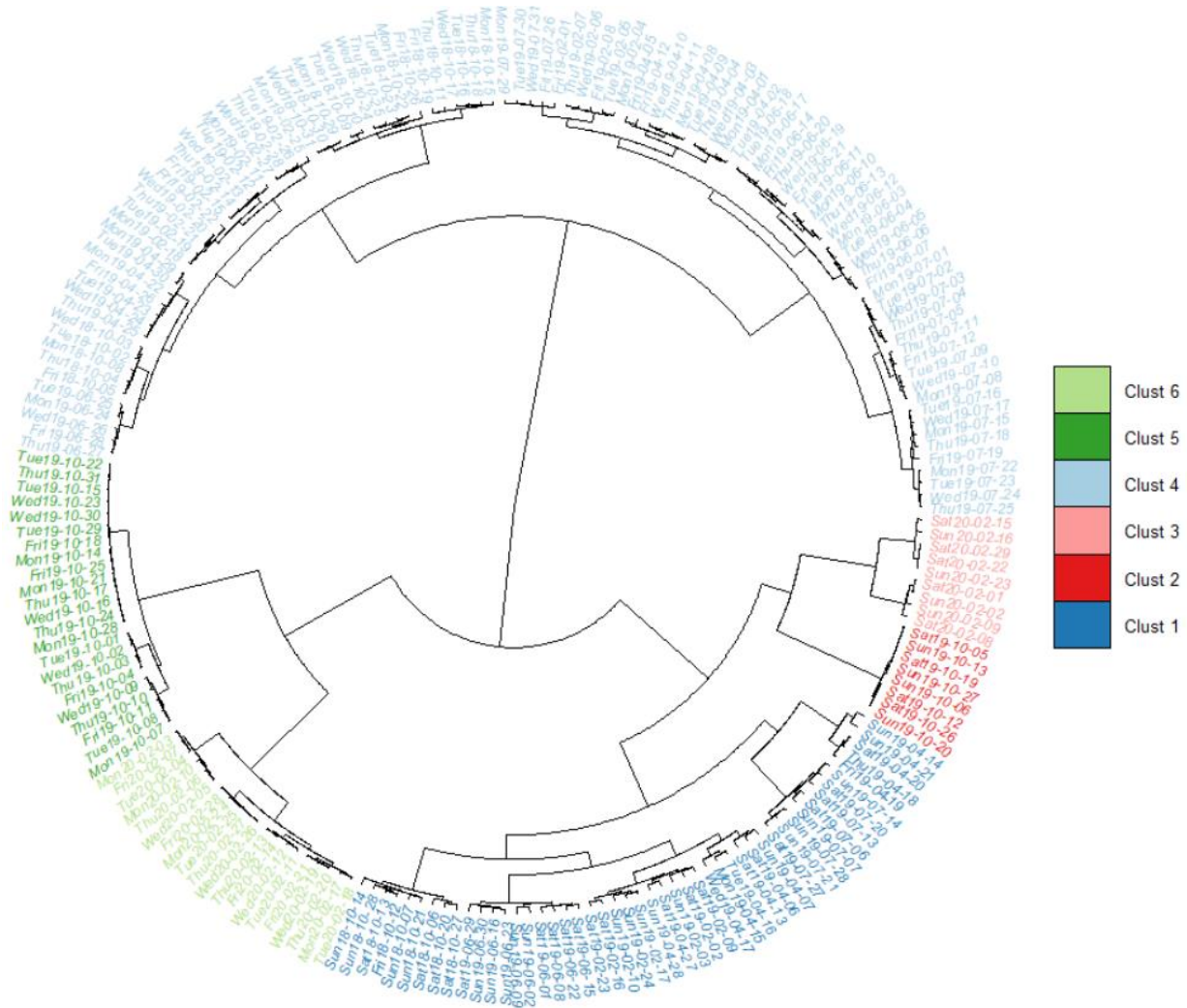


*Figure 11. Phylogram for clusters of OD Matrices in Level 0*

This Level 0 represents a higher level of clustering where the cut-off threshold is set at a high value, and which is shown in Figure 11. In this case, we can observe three large clusters before the Level 0 separation that would correspond to the group of weekends, and two groups of weekdays: one with the months of October 2018, and

Version: Issue 1 Draft 2

February, April, June, and July 2019; and another with October 2019 and February 2020. Within Level 0, we can separate these three groups as follows:

- **Weekend group:** as in the previous clustering (see Section 4.2.2), this group consists mainly of weekends or equivalent days (e.g., holidays). It is further divided into groups, similar to the way the three global clusters are divided:
  - *1. Saturdays, Sundays, and holidays previous to October 2019.*
  - *2. Saturdays and Sundays from October 2019.*
  - *3. Saturdays and Sundays from February 2020.*
- **Weekday group previous to October 2019:** this group includes the weekdays of the first five months studied, which are condensed into a single cluster.
  - *4. Weekdays previous to October 2019.*
- **Weekday group from October 2019:** This last block includes the weekdays of the months of October 2019 and February 2020, each with its respective cluster:
  - *5. Weekdays from October 2019.*
  - *6. Weekdays from February 2020.*

### 4.2.3.3.2.   Level 1
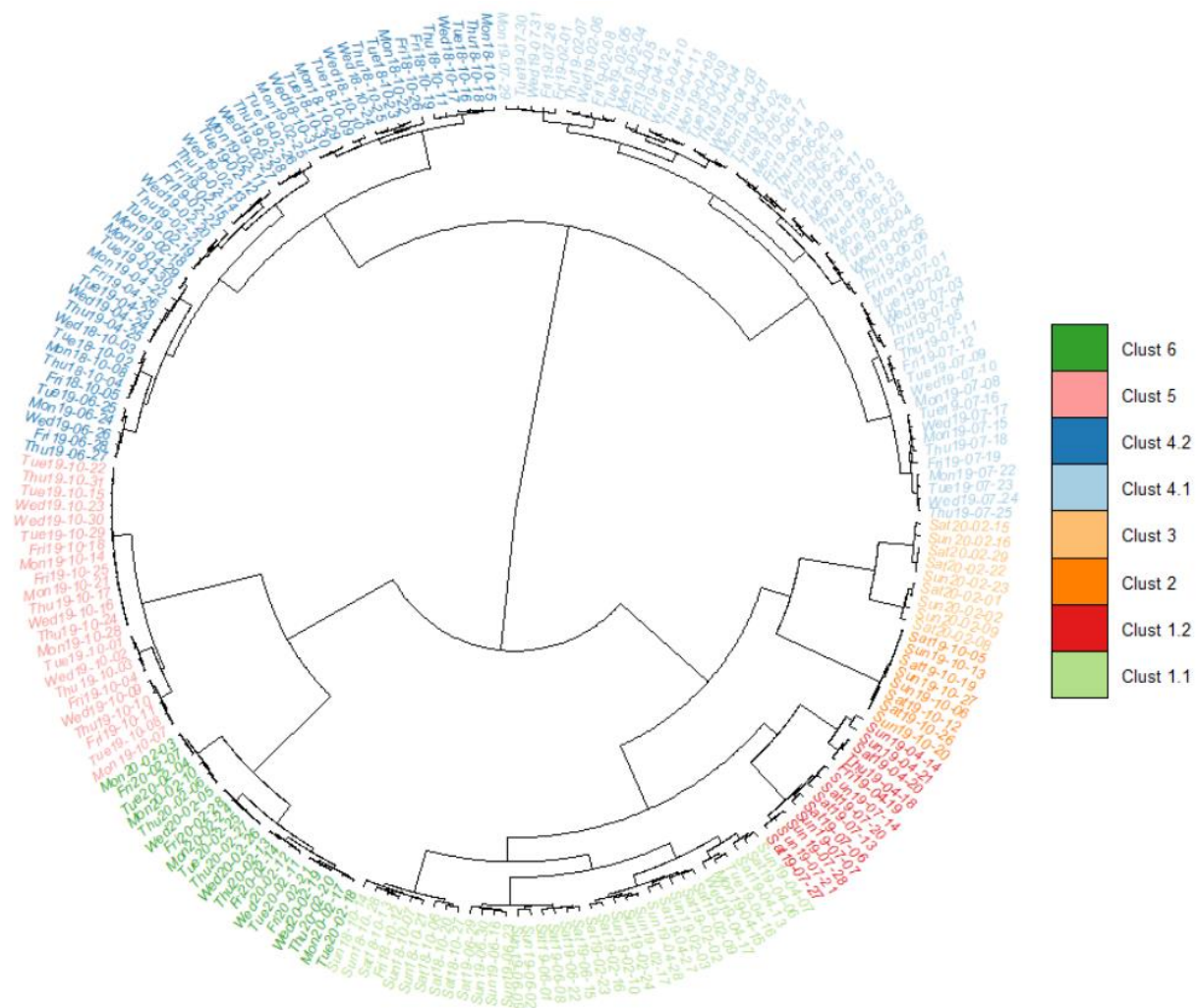


*Figure 12. Phylogram for clusters of OD Matrices in Level 1*

As in clustering presented in Section 4.2.2, by setting a lower threshold for determining clusters, new partitions appear in some of the groups defined at Level 0:

- **Sub-groups derived from cluster 1 "Weekends previous to October 2019".** With this new division, cluster 1 is further split into two sub-groups:
  - *1.1. Weekends and holidays previous to July 2019 (except Easter Holidays 2019).* This group includes Saturdays and Sundays in the months prior to July 2019 with the exception of the weekend relating to the Easter holidays in 2019. In addition to this, there are other relevant exceptions:
    - October 12th, 2019 (Friday): This day corresponds to the Spanish national festivity "Día del Pilar".
    - April 15-17 (Monday, Tuesday, and Wednesday): They are the first three days of Easter Week 2019. Although these three days are working days, educational facilities are closed for holidays that week, so students and a high percentage of workers are usually on vacation on these three days.
  - *1.2. Weekends from July 2019 + Easter Holidays 2019.* This cluster includes the weekends of holiday periods such as July and the four days of Easter in 2019 when a high percentage of locals travel outside the Region of Madrid.
- **Sub-groups derived from cluster 4 "Weekdays previous to October 2019".** Similar to the previous one, cluster 4 is divided into two groups, although in this case with a more balanced distribution. The seasons of the year seem to have some influence on this division as we explain below:
  - *4.1 Weekdays from Spring-Summer.* This sub-group includes all weekdays in July 2019, the first three weeks of June 2019, the first two weeks of April 2019, and the first week of February 2019. Below we analyse the reasons why the above-mentioned days in April and February are included in this sub-group:
    - First two weeks of April 2019: These first two weeks are characterized by stable weather (no rain) and mild/cool temperatures (between 15ºC and 20ºC maximum), so it is reasonable that they fall into this group.
    - *First week of February 2019:* this week is also characterized by stable weather (no rain) and slightly cool temperatures (maxima between 13ºC and 16ºC). In any case, the rest of the weeks of the month have similar weather, so this does not seem to be the reason. As can be seen in Figure 12, the graph shows that this week is right on the borderline with the month of July. For this reason, this subset of OD matrices will be probably borderline cases, which the clustering algorithm has not grouped correctly.
  - *4.2 Weekdays from Autumn-Winter-Spring.* This sub-group includes all weekdays in October 2018, the last three weeks of February 2019, the last week of April 2019 and the last week of June 2019. Below we analyse the reasons why the above-mentioned days in April and June 2019 are included in this sub-group:
    - Last week of April 2019 (April 22-26, April 29-30): This week is characterized by a few days of bad weather, particularly on April 23, 24 and 25, which are rainy days, windy and with slightly low temperatures (maxima between 13ºC and 14ºC). This adverse weather may be the reason why this last week of April falls into this group.
    - Last week of June 2019. This last week is characterized by quite high temperatures (maxima between 32ºC and 40 ºC) which contrast with its inclusion in this group. As the first week of February, this is a borderline case that may have been incorrectly grouped by the clustering method.

4.2.3.3.3.    Level 2
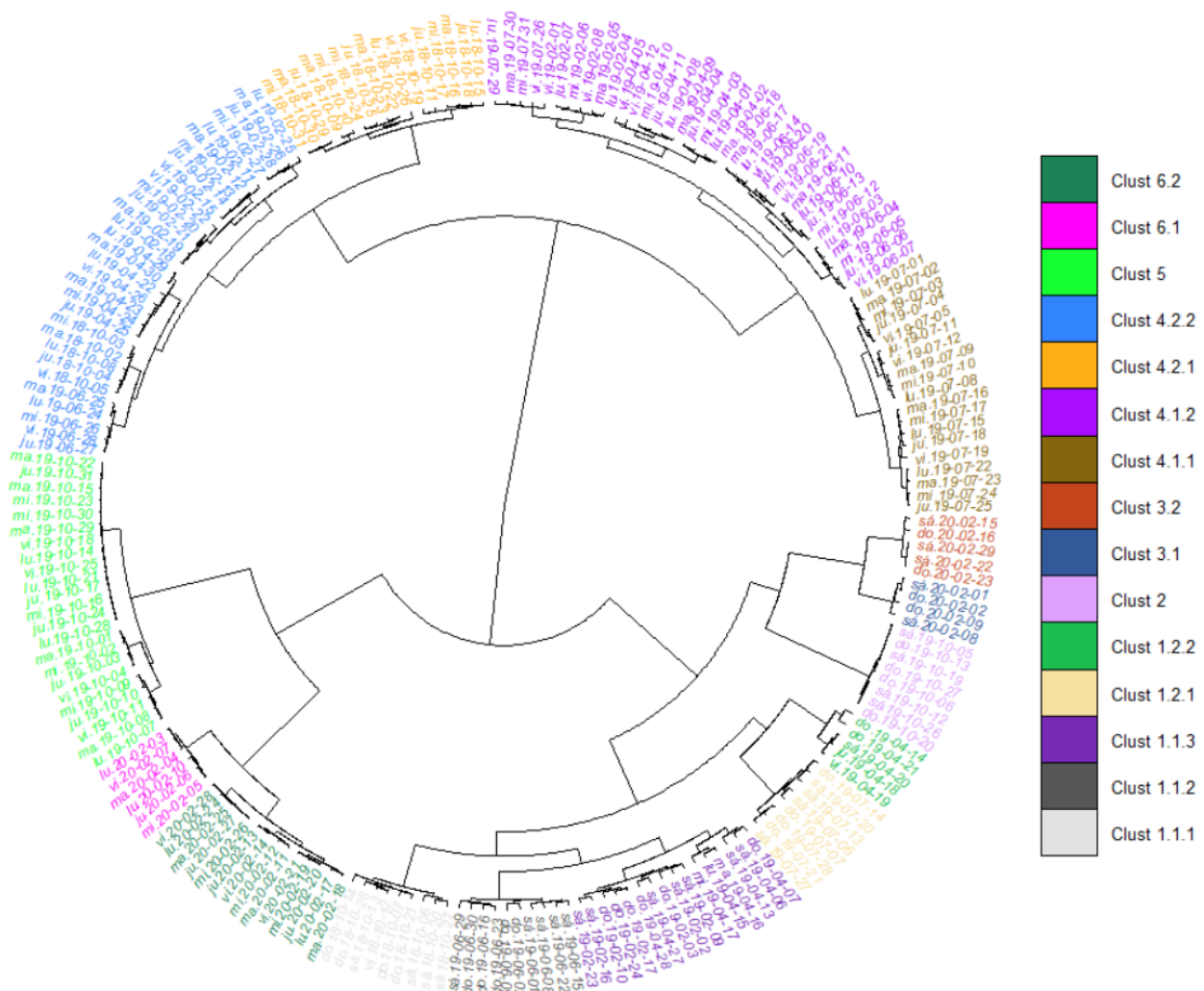


*Figure 13. Phylogram for clusters of OD Matrices in Level 2*

In this Level 2, we do an even more refined clustering by means of a lower cut-off threshold. In total there are 15 clusters, which divide the Level 1 clusters as follows:

- **Sub-groups derived from sub-group 1.1.** Sub-group 1.1 is divided into the following three sub-groups, probably due to climatological reasons:
    - 1.1.1. Weekends and holidays (October 12th) from October 2018.
    - 1.1.2. Weekends from June 2019.
    - 1.2.3. In this case, the group contains all the weekends from February and April 2019, except for the Easter holidays, and the three first days of Easter week for the reasons explained above.
- **Sub-groups derived from sub-group 1.2.** This sub-group has been separated into the following two sub-groups, because of the different characteristics of July versus Easter holidays.
    - 1.2.1. Weekends from July 2019.
    - 1.2.2. Easter holidays 2019.
- **Sub-groups derived from cluster 3.** In this case, the cluster is also divided into two sub-groups corresponding to the first and second half of February 2020. This split is probably due to the effects of the COVID-19 pandemic this month, as explained above.

- o   3.1. Weekends from the first half of February 2020.
- o   3.2. Weekends from the second half of February 2020.
- **Sub-groups derived from sub-group 4.1.** This sub-group, which includes the weekdays of part of the spring and the summer, now differentiates between the weekdays of July and the rest of the months. This behaviour is to be expected as July is a different month in which schools are closed and a significant percentage of the inhabitants of this region are on holidays.
    - o   4.1.1. Weekdays from July 2019 (except 26, 29, 30 and 31)
    - o   4.1.2. This group entails the weekdays from the first three weeks of June 2019, the first two weeks of April 2019, the first week of February 2019 and the last four days of July 2019. In this case, there are two sub-groups that are borderline cases probably misplaced by the clustering algorithm, as we can see in the graph displayed in Figure 13. The last four days from July 2019 it is more reasonable to be included in sub-cluster 1.2.1, and the first week of February 2019, in cluster 1.2.3.
- **Sub-groups derived from sub-group 4.2.** This sub-group, which includes the weekdays in autumn, winter and part of spring, has also been subdivided into two sub-groups, which are described below:
    - o   4.2.1. Weekdays from the last three weeks of October 2018.
    - o   4.2.2. This sub-group comprises the weekdays from the last three weeks of February 2019, the last two weeks of April 2019, the first week of October 2018 and the last week of June 2019. Here, we can find some interesting peculiarities. As said before, some days of the last two weeks of April presented bad weather, so its clustering together with the last three weeks of February makes sense. The graph shown in Figure 13 also corroborates this fact. However, the first week of October 2018 and the last week of June 2019 form a matrix group that is at the border of several clusters. The fact that these two weeks are grouped together is probably due to the good weather during the first week of October 2018, with sunny days and maximum temperatures between 26ºC and 29ºC. In this case, we also believe that the clustering algorithm has wrongly grouped these two weeks together, and it would make more sense for them to be included in sub-group 4.1.2.
- **Sub-groups derived from cluster 6.** In this last cluster, which contained the weekdays of February 2020, two sub-groups have also been generated, which, as in the case of cluster 3, are based on different mobility patterns in the last weeks of February due to the outbreak of the COVID-19 pandemic in this region.
    - o   6.1. Weekdays from the first 10 days of February 2020.
    - o   6.2. Weekdays from the last 20 days of February 2020.

#### 4.2.3.3.4.    Clustering summary

In this section, we have presented a new methodology for OD matrix clustering based on Graph Embeddings. This methodology has been tested on the same data as the clustering performed for OD matrix classification in Section 4.2.2. The analysis of the results has also been based on different levels of aggregation.

In this analysis, similarities and differences have been observed with the clustering based solely on the similarity measure of OD matrices. The main similarities found would be the following:

- At a higher level, the clustering clearly differentiates between weekdays and weekends.
- The months of October 2019 and February 2020 show a different behaviour from the rest, which is due to the change in the OD matrix generation algorithm mentioned above.
- Weekdays that are public holidays are grouped with weekends.
- The weekdays are divided into two large blocks according to the seasons of the year.

The main differences are as follows:

- The clusters provided by this methodology are more legible and natural as they tend to group OD matrices close in time. As it could be seen in Figure 11, Figure 12 and Figure 13, they are grouped by weeks in a large percentage of cases.
- In line with the above, we can find fewer outliers in the clusters. Nevertheless, we have been able to identify subsets of OD matrices that a priori were not well clustered. However, the fact that they are groups of OD matrices and not isolated OD matrices, makes it easier to identify them.
- No clustering by day of the week is observed for weekends, as was the case with the clustering method used in Section 364.2.2. This deserves further study, as it is initially expected that Saturdays and Sundays at certain times of the year will resemble each other.

To summarise, this is a promising matrix clustering methodology since it results in cleaner and more natural clusters. However, some of the differences detected, such as the erroneous clustering of certain sets of OD matrices or the non-clustering by days of the week, call for further research in the future to better understand what the cause of these differences may be. Hence for matrix classification the clusters obtained with the hierarchical approximation will be considered.

## 4.2.4. OD matrix classification and selection

Once a valid clustering scheme has been obtained, the aim of this model is to develop a machine learning classifier capable of assigning each day of study to a representative matrix group based on calendar-based features. This way, the selected OD matrix will be closer to the expected one.

This section provides an overview of a machine learning classification model based on the decision tree algorithm that has been developed using the following months: October 2018, and February, April, June and July 2019; that have been assigned a class according to their OD matrix differences in trip volume and structure. For that purpose, a set of input features mainly derived from the date of each matrix is used and described in the input features section below.

### 4.2.4.1. Architecture of the OD matrix classifier

The proposed classifier system is based on the decision tree classifier algorithm. The decision tree classifier is a machine learning algorithm that learns a set of rules based on the input features to hierarchically determine the category each data sample belongs to. The decision tree algorithm has a set of hyper-parameters that control the shape and complexity of the tree, such as the tree depth or the minimum number of samples to have at each leaf.

These hyper-parameters are adjusted through a 3-fold cross-validation methodology which consists of trying several combinations of hyper-parameters and retaining the best-performing one. Instead of using the entire training dataset once for each combination of parameters, it is split in three chunks. For each combination of parameters, the model is repeated three times considering as testing data a different chunk each time.

This way, each hyper-parameter performance is averaged over the three iterations, which provides robustness against random sampling biases. At the end, the best combination of hyper-parameters is used with the training data to develop the final model that is then validated using a testing data set that has not been used for this purpose.

### 4.2.4.2. Classifier Input Features

The decision tree classifier takes as input a set of features that has been derived from variables that are available before the date of study. These variables mainly correspond to calendar-based items (day of week, day of year,

holidays) and also to predictable or scheduled events (weather or sports events). Table 5 provides a summary of the variables introduced in the model.

| Variable name | Description |
|---|---|
| DoW | Day of week introduced by means of categorical values activated when the date corresponds to that day of the week. Available categories are Monday, weekday, Friday, and Saturday. |
| DoY | Sine and cosine components of the day of the year. Sine and cosine are used instead of the actual day of the year to provide continuity to years. This way, December is close to January of the next year. |
| Days from festivity | Number of days from the last festivity from the day of study. Saturdays and Sundays are considered festivities |
| Days to festivity | Similar to days from festivity, number of days to the next festivity in the calendar. |
| Ta | Daily average temperature observed from the meteorological stations maintained by the Spanish meteorology agency (AEMET). |
| Prec | Daily accumulated precipitation observed at the meteorological stations maintained by AEMET. |
| prec (by hours) | Similar to precipitation, but instead of the whole day accumulation, it is separated in hour ranges (0-6, 6-12, 12-18, 18-24). |
| Wanda | Binary variable that indicates whether there is a football match in Wanda Metropolitano stadium in the given day. |
| Bernabeu | Binary variable that indicates whether there is a football match in Santiago Bernabeu stadium in the given day. |
| Rayo | Binary variable that indicates whether there is a football match in Rayo Vallecano stadium in the given day. |
| local_football | Combination of the previous three that indicates the number of large sport events taking place during the same day. Hour of the events are not taken into account. |

*Table 5. Summary of the features considered for the classification task*

### 4.2.4.3. Performance of the classification model

A model to select the clustering scheme of Level 1 for the months of October 2018 and February, April, June and July 2019 has been trained and validated. In order to measure performance two metrics have been used:

- **Accuracy**: This metric measures the number of matrices that have been correctly predicted by the system. This metric ranges from 0 to 1, being the higher the better.
- **F-score**: The F-score is a performance metric that evaluates how does a model perform like accuracy but taking into account minority classes. By averaging precision (number of predictions from each cluster that are correct) and recall (amount of members of each cluster correctly assigned) F-score provides a robust metric for model performance. As in the case of accuracy, the metric is bound between 0 and 1, being 1 the best performance and 0 the worst one.

One relevant feature of decision tree algorithm is that it provides two descriptive elements of the decision process: feature importance and tree plot. Feature importance provides an approximation to the value that the tree gives to each feature in the prediction task. The tree plot provides a clear diagram of the decision hierarchy

implemented in the classification, which are the complete set of rules followed by the tree when performing predictions.

For the training, available data has been split into 80% training (including hyper-parameter tuning) and 20% testing. The accuracy obtained by that tree is 0.941 in training and 0.867 in testing and the f-score is 0.917 and 0.711 respectively. Table 6 summarises the feature importance values for each feature used in the resulting tree.

|   | Feature name | Feature importance |
|---|---|---|
| 1 | Days from festivity | 0.453794 |
| 2 | Day of Week: Saturday | 0.219578 |
| 3 | Sin component of Day of Year | 0.210476 |
| 4 | Cosine component of Day of Year | 0.058022 |
| 5 | Average temperature | 0.036013 |
| 6 | Day of Week: Friday | 0.022118 |

*Table 6. Feature importance values for relevant variables. Those variables not included in the table have resulted in a value of 0*

The table indicates that only 6 variables have been considered relevant by the model, mainly the days from the last festivity, whether the day of week of given observation is Saturday and the sine component of the day of the year. This suggests that the optimal matrix aggregation is targeted towards work and non-work days with an important component of the season each matrix is observed at. The day of the week seems to be relevant, but just considering the extended weekend (Friday, Saturday, and Sunday).

For more detail, Figure 14 provides the detailed view of the trained tree algorithm.
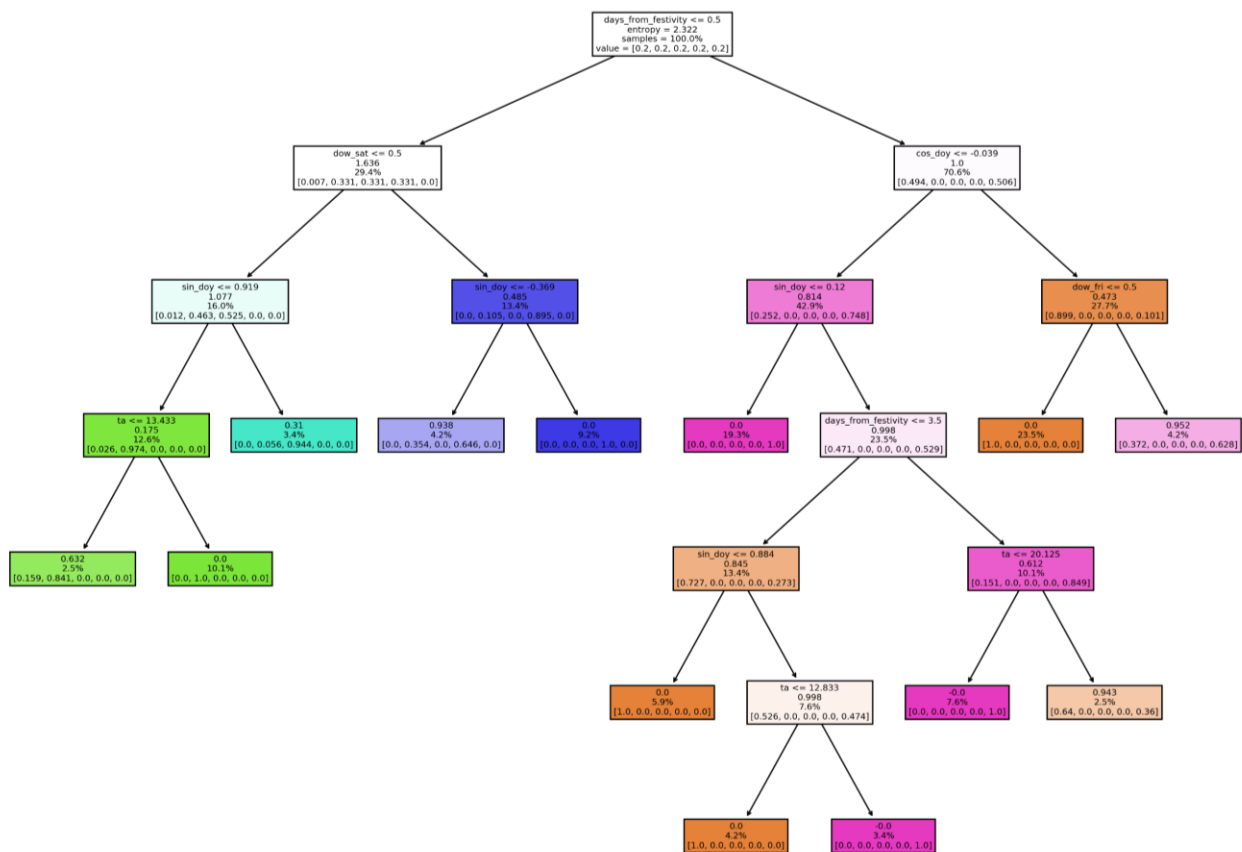
*Figure 14. Schematic of the resulting tree model*

The topmost variable in the tree is days from festivity in a way that it separates working and non-working days from the beginning. This is in line of the generated dendrogram that separates in this way. Regarding the non-working days sub-tree, the relevant variables are whether the non-working day is a Saturday, the sine component of the day of the year and, in some cases, whether the temperature is below 13 degrees (cold versus warm weather).

In the working days sub-tree, it is worth mentioning the relevance of sine and cosine of the day of the year, whether the day of week is Friday and, in some cases the temperature (again cold versus warm weather with two different thresholds.

## 4.2.5. Conclusion

The approach proposed in this section defines a machine-learning methodology for OD matrices selection. In order to generate the initial classes, hierarchical clustering over OD matrices similarity was performed. Once each OD matrix is assigned a cluster, the average cluster matrices are computed by all cluster matrices. Similarly, we have explored a new methodology for clustering OD matrices based on Graph Embeddings that shows promising results attending to the clusters obtained, which break data more naturally and provide more intuitive cluster schemes than hierarchical clustering. In any case, further research is needed to validate this approach within the entire methodology.

Using the labelled data and a set of input features based on upcoming dates and scheduled events that are known prior to the date of study, a Decision Tree classifier has been developed to predict the clustering class to be assigned to each upcoming new date, in order to provide an enhanced approximation of its OD matrix. The resulting model demonstrates very high accuracy and F-score values. Furthermore, it has illustrated which are the

most relevant factors that affect daily mobility similarities, namely working and non-working days, the season of the year and, up to some extent, the observed weather conditions and some specific days of the week such as Saturdays or Fridays.

This model will be useful in the correct prediction of the general mobility to be expected for a given day, which can be used to obtain the potential demand to be expected at the city level to feed models developed in MOMENTUM project with better estimations that will yield more accurate predictions and, consequently, improvements in the design and provision of mobility services by urban planners.

# 4.3. Synthetic population generation

## 4.3.1. Motivation and objective

This section introduces the model for generating the synthetic population. The synthetic population is a key input to agent-based models and microsimulation of urban systems in order to simulate the behaviour of agents on the transportation network as well as their interactions with the infrastructure.

A synthetic population generation refers to creating a representation of disaggregated population by combining aggregated sociodemographic data for the entire population with a sample of disaggregate data such that they match known distributions of key attributes for the general population (Beckman et al., 1996). In other words, a set of household and person attributes need to be combined, whose attribute distributions match those of the general population in small geographic units (e.g., a census tract, traffic analysis zone or TAZ, block group, or block). The main limitation with respect to the synthetic population generation is the availability of disaggregate data of the population. The data are often difficult to collect as well as the sources usually being heterogeneous, which may bring inconsistencies between the available sample data and aggregate distributions.

In the context of the MOMENTUM project, the objective is to synthesise a simplified representation of the actual population, based on sociodemographic and other relevant information (i.e., household and individual attributes), from which the preference of an individual in selecting a new mobility service, as opposed to a traditional transport mode, can be captured. The synthesised population will be then used as input to the mode choice model to estimate the demand for conventional modes as well as emerging mobility services. The main challenge is the data availability of samples of the real population that include information with respect to the behavioural response of a person, especially for new transport modes and services (e.g., bike-sharing system, ridesharing, etc.). To address this limitation, assumptions are made regarding the factors that would affect individuals in choosing a new service, based on sociodemographic and other attributes that characterise them (e.g., no car-ownership or driver's license).

### 4.3.1.1. State-of-the-art methods

In this section, the state-of-the-art approaches of synthetic population generation are briefly reviewed to justify the methodology that is selected within the project.

Various methods have been proposed in the literature for the generation of synthetic population. Data availability and quality is the main limiting factor in population synthesis, leading to the development of different methods. Generally, population synthesis is performed using one of the following methods: Combinatorial OPtimization (COP), Synthetic Reconstruction (SR) and Simulation-Based (SB) (or Statistical Learning, SL) approaches. The methods differ with respect to the input data requirements, procedure employed, or the underlying assumptions to generate a representative synthetic population. We refer the reader to Müller and Axhausen (2011), Hörl and Balac (2020), Yameogo et al. (2021) and Sun et al. (2018) for a thorough state-of-the-art review of population synthesis methods.

One of the main distinguishing data requirements between the three approaches is that COP and SR methods require both disaggregate (sample) data and aggregate data (marginals), while SL methods can synthesise a population using only sample data. Moreover, COP and SR methods can only produce reliable and accurate results when the reference sample size is sufficiently large, whereas for SL methods the sample size is not a critical factor.

COP treats population synthesis as an optimisation problem which optimises the sample weights, on a zone-by-zone basis, to match the zonal marginals (Voas and Williamson, 2000). The main limitations of COP approaches are: 1) the attribute association in the sample data not being preserved by the algorithm and, 2) the computational cost for large population size (Pritchard and Miller, 2012; Yameogo et al., 2021).

SR methods generate the synthetic population by combining joint distributions over different variable (attribute) sets and then drawing from the reference sample using the fitted joint distribution. One of the most widely used SR techniques is the Iterative Proportional Fitting (IPF) (Stephan, 1942) method, which adjusts a contingency table constructed from the sample so as to match known marginal distributions of household or person attributes (Beckman et al., 1996). However, there may be attributes for certain demographic groups that do not exist in the reference sample, especially when dealing with small geographies (for more details see Müller and Axhausen, 2011; Yameogo et al., 2021; Ye et al., 2009). This will produce division by zero for the empty cells during the execution of IPF, leading to undefined results. Moreover, the method does not perform well in matching the distributions of person-level attributes and household distributions simultaneously (Guo and Bhat, 2014; Lim and Gargett, 2013; Müller and Axhausen, 2011; Pritchard and Miller, 2012).

In order to address the inability of the IPF methods to simultaneously estimate both household and individual-level attributes, Ye et al. (2009) proposed the Iterative Proportional Update (IPU) procedure. In particular, the IPU procedure computes weights for the sample of the population such that household and person attributes are simultaneously matched with their respective known aggregate distributions for a specific geographic area (Ye et al., 2009). Furthermore, the IPU method has addressed the zero-cell problem that may occur when applying the IPF method. For a detailed description we refer the reader to Ye et al. (2009). For those reasons IPU is considered a more advantageous method compared to IPF. One limitation of the original IPU method was its limited applicability to only one geographic resolution at a time. Konduri et al. (2016) extended the IPU method to control for a variable of interest at multiple geographic resolutions simultaneously. The IPU algorithm will be described in more detail in the next section, as it has been selected as the main population synthesis approach used in this project.

Farooq et al. (2013) proposed a novel simulation-based approach to synthesise independent populations, instead of determining household weights using the IPF methods and then drawing. They performed Markov chain Monte Carlo (MCMC) simulations, using the Gibbs sampling algorithm, to draw synthetic populations from partial views of the joint distribution of the real population. The main challenge with this approach is identifying the conditional distributions of attributes available from various data sources. Furthermore, SL methods fail to satisfy the conditional distributions while satisfying the marginal distributions of all variables simultaneously (Yameogo et al., 2021).

### 4.3.2.  Methodology

The proposed synthesis process for MOMENTUM involves a combination of different methods and techniques. The main component of the adopted population synthesis process is the IPU approach, and in particular the utilisation of the PopGen standalone package, which will be described in this section.

Nevertheless, there may be attributes (especially for the new mobility services) that are not available in both the census and travel survey data, hence, it would not be possible for the IPU algorithm to map them in the initial population synthesis. In such cases, statistical matching procedures will be used to enrich the synthetic population with additional attributes. Therefore, a sub-model based on statistical techniques is proposed to address the assignment of a specific trip to the synthesised individuals. The sub-model is referred to as the

destination choice model and is also described in this section. This procedure is important and requires careful consideration of the underlying assumptions that need to be made.

### 4.3.2.1. The Iterative Proportional Updating (IPU)

As mentioned in a previous section, the IPU algorithm generates a synthetic population by fitting household and person sociodemographic attributes, available for a sample of the population, with known aggregate distributions of those attributes for a specific geographic area. Depending on the data availability (e.g., census and travel surveys), different attributes can be considered to generate a synthetic population.

The IPU is a heuristic iterative procedure that solves the following optimisation problem for estimating household sample weights so that the given constraints (for both household and person types) are matched:

$$Min \sum_j \left[ \frac{\sum_i d_{i,j} w_i - c_j}{c_j} \right]^2$$

(18)

$$\text{Subject to } w_i \geq 0$$

Where $i$ denotes a sample household, $j$ denotes the constraint (household/person type), $d_{i,j}$ represents the frequency of the constraint $j$ (household/person types) in household $i$. $w_i$ denotes the weight assigned to sample household $i$ and $c_j$ is the value of the constraint $j$.

A brief description of the generalised procedure of the IPU heuristic method is presented in the Annex A2 .

### 4.3.2.2. The PopGen synthesiser

PopGen is an open-source software package (MARG, 2016). The tool was initially created for the Southern California Association of Governments (SCAG) Activity-Based Model (ABM) (Ye et al., 2009). PopGen has been used as a population synthesiser in several studies in the literature, which have demonstrated its advantages and capabilities (He et al., 2020; Jain et al., 2015; Konduri et al., 2016; Ye et al., 2009). One of the main advantages of PopGen is that it employs the IPU algorithm (Ye et al., 2009). PopGen provides the flexibility to synthesise a population at multiple geographic levels (small, medium, or large regions) simultaneously.

Therefore, for the scope of this study, PopGen is utilised as a suitable and practical synthetic population synthesiser across all case studies, due to the availability of the code package as well as the employment of the enhanced IPU methodology.

### 4.3.2.3. Destination choice sub-model

Travel surveys can provide information regarding the mode as well as the trip made by the sample of individuals that participated in the survey. However, the shared mobility services that are investigated in this project are relatively new modes of transport and are not included in the travel surveys. In fact, the mapping of a destination to the trip of a specific individual in the synthetic population is a challenging problem, as it directly depends on the data availability and quality which may not be sufficient in assigning accurately trip attributes to all individuals. Consequently, adequate assumptions using sociodemographic information, attributes such as home location and employment status, need to be made for mapping the synthetic individuals with a trip choice.

This problem has been tackled in the literature using various approaches and techniques, depending on the modelling purpose. For example, He et al. (2020) modelled tour-based mode choice and proposed to simply assign household travel survey agendas to the synthesised population's agendas using socio-demographic information. The authors consider two attributes for the assignment, home location and occupation, and every individual in the synthetic population is assigned with an agenda of a sample individual from the same traffic zone with the

same type of occupation. Following, a mode choice model was used to simulate the modes chosen for each trip in the agendas of the synthetic population. Felbermair et al. (2020) proposed the utilisation of Bayesian networks and Markov Chain Monte Carlo in combination with stratified sampling in order to generate a synthetic population with activities plans using limited survey data. Hörl and Balac (2020) apply a fully data-driven procedure to synthesise a population aiming to establish a baseline into which more sophisticated models can be integrated. The main component of the proposed process is a statistical matching procedure that combines data sets from the census and household travel survey. The proposed synthesis pipeline aims to provide a synthetic travel demand on a person level that can be directly used in agent-based transport simulation.

Within MOMENTUM, sampling techniques and statistical matching procedures (D´Ozario et al., 2006; Hörl and Balac, 2020) will be applied under certain assumptions related to the consistency in the data collected and the correlation of the mutual attributes (obtained from different data sources) with the new unilateral attributes of interest to be added to the synthetic population.

### 4.3.3. Data sources

#### 4.3.3.1. Input data

The required input data for the generation of synthetic population are usually organised according to the data sources, into sample data and census data. For instance, household travel surveys are carried out on a regular basis in many countries. They provide essential information for the households, such as the current car-ownership and number of driving licenses. These data can be useful in estimating potential changes in travel behaviour that may be produced by new mobility services.

Moreover, depending on the data sources available in the case studies, aggregate and disaggregate OD matrices will be used in the population synthesis in order to assign a specific trip to each synthetic individual. Aggregate OD matrices can be obtained from the trip distribution of the traditional travel demand models, while disaggregate OD matrices for a representative sample are also available for some cities, which may include more accurate information than the aggregate OD matrices. For example, OD matrices obtained from mobile data usually include sociodemographic information that can be mapped with the census data.

#### 4.3.3.2. Geographic data

These datasets are associated with one or more geographic zoning systems at which the specific data or attributes are available. Moreover, the available samples may have been obtained from different sources, such as travel surveys, household expenses surveys, etc. A necessary first step in the process of generating a synthetic population is the mapping of the geographic correspondence between the various data sources.

The geographic resolution for which the synthetic population will be generated, depends on the geographic unit for which the census data as well as travel survey and other sample data are provided for each city. Moreover, adequate selection of the geographic areas is also critical for the application of the case studies. The feasibility of implementing and evaluating new mobility modes in simulation, depends on the selection of the geographic resolution for which the demand is generated. For some shared service systems (e.g., bike-sharing), too much of aggregation of an area might be restrictive for the evaluation of the service, while for others, high aggregation level may be sufficient (e.g., car-pooling).

One of the advantages of PopGen is that it enables the geographic correspondence between different resolutions that may exist in the available data. For example, the census data might be fragmented into a higher geographic resolution compared to the sample data or any other data that may be available only at the regional level.

### 4.3.3.3. Control variables

The population synthesis model can produce synthetic households and persons based on the available sample while matching the aggregate known distributions of key variables (attributes), which are usually referred to as control variables. These variables are used as controls by the algorithm for estimating the weights that each sample household and individual is assigned with.

The selection of the control variables of interest depends on the data availability in the census and samples. The variables need to be further divided into adequate categories, based on which representative combinations of household and person attributes will be created. The exact control variables at household and person level as well as the design of the categories to be used in the population synthesis across the case studies, will be identified in WP5 based on the data availability for each city. A preliminary investigation of the available data indicates that meaningful household and person control variables are available in the census data across the cities. An important consideration is to ensure that all control variables that will be selected follow similar patterns for both the aggregate census and disaggregate sample data.

A preliminary investigation of the available data indicates that meaningful household and person control variables are available in the census data across the cities. In particular, the variables to be considered are based on the other developments presented in this deliverable, e.g., mode choice and car-ownership models, which depend on the synthetic population. The identified relevant control variables to be used in the project are provided in Annex A2.

While variables such as household size, number of cars, person´s age, gender, education, and employment status are usually available in census and survey data, and hence, possible to be considered for the PopGen synthesiser, variables such as Public Transport subscription, driver´s license, are required to be assigned through statistical matching. Having mentioned that, the availability of data within each case study may influence this process.

### 4.3.3.4. Outputs

The output of the synthetic population generation module includes the synthesised households and persons for the specific geographic zones in each case study. Subsequently, the synthetic individuals will be used as input for the disaggregate mode choice model to estimate the mode choice for every individual. Finally, the individual demand requests for a specific trip and service will be given as input to the fleet management module in order to plan and operate the demand requests.

## 4.3.4. Application within MOMENTUM

Depending on the data availability for each case study, a combination of the PopGen standalone package and statistical techniques will be applied to synthesise the populations for each city.

# 4.4. Mode choice

## 4.4.1. Disaggregate mode choice model

### 4.4.1.1. Motivation and Objective

With the introduction of shared mobility services, a natural phenomenon is a change in the modal split. Therefore, there is a need for a model, which is capable of capturing this phenomenon. Hence, the objective of this section is to present a mode choice model for shared mobility services, which can estimate the mode share for the shared mobility systems.

### 4.4.1.2. Data source used for model estimation

In general, mode choice models are developed using Stated-Preference (SP) surveys. However, such a data is not available and hence, the development of the mode choice model will be based on a regional household mobility survey dataset from Madrid. This survey is carried out by Madrid regional government between February 2018 and June 2018 and is available at *https://datos.crtm.es.*

The dataset contains information such as household and individual sociodemographic characteristics, along with mobility-related aspects (e.g., mode choice and trip characteristics), for a sample of 85,064 households. Since the sharing systems are only available in certain zones, a reduced sample of 25,464 individuals (based on the traffic zones where sharing systems are available) is used for this research.

### 4.4.1.3. Estimation methodology

The mode choice model presented in this section is a multinomial logit model, and as mentioned in the previous section, the estimation is based on a household travel survey from Madrid. Any household survey, usually, contains details about the trips taken by the respondents, and data that characterize the different available modes (e.g., travel time or cost associated with different modes) will not be available. Similar is the case with the Madrid survey dataset. Hence, it is not possible to estimate a classical multinomial logit mode choice model. Therefore, a personal-level model is decided to be developed. Such a model is not newly implemented in this project, but rather is already found in literature (e.g., Anderson and Simkins, 2012; Cheng et al., 2014; Liang, et al., 2020). Some studies term such a model as generalized multinomial logit model (e.g., Anderson and Simkins, 2012).

The alternatives for mode choice used in this research are the following: (i) Conventional systems-as-a-whole, (ii) Bike-sharing, (iii) Car-sharing, and (iv) Ridesharing. For ridesharing, trips carried out in mobility services such as Uber are taken as proxy. While the mode choice models usually include all kinds of modes (individual conventional and the shared modes), all the conventional modes are considered under single alternative in this research. In general, several cities do not have a sufficient data to estimate a mode choice model, which includes all conventional modes and the different shared mobility systems. Hence, development of a mode choice model between conventional systems-as-a-whole and the different shared mobility systems could be beneficial, as such a model could be used in other cities. This kind of use is possible, given that it is possible to generalize the demand characteristics of shared mobility systems [e.g., unique profile of users such as younger individuals, possession of Bachelor's degree or higher, and holding of PT passes (Becker, Ciari, and Axhausen, 2017; Clewlow, 2016)].

Following the decision on the variable type used in the model (i.e., personal-level attributes), the subsequent concern is on the lower number of samples for the shared mobility services (< 1 %). This could cause problems such as accurate predictions and separation issues. Therefore, it is decided to consider the choice for shared mobility services as a rare event and use a penalized likelihood estimation approach. However, this approach, although negated the issues of accurate predictions and separation issues, still is affected by model insensitivity due to very high-class imbalance. Furthermore, the computation time is enormous. Hence, synthetic sampling based on the technique of SMOTE (Synthetic Minority Oversampling Technique) (Chawla, Bowyer, Hall and Kegelmeyer, 2002) has been carried out. The aforementioned methodology is shown in Figure 15.

Model specification is developed in a stepwise fashion, first backward (from saturated models), where only variables of high significance are kept and then forward (from empty models), where significant variables are added one after the other. The decision to keep an independent variable is based on the p-value (significance level of 0.10) of the corresponding variable and the likelihood ratio test.

**Deliverable 4.1**

New transport modelling approaches
for emerging mobility solutions

Page **56** of **137**

Copyright © 2021 by MOMENTUM

Version: Issue 1 Draft 2
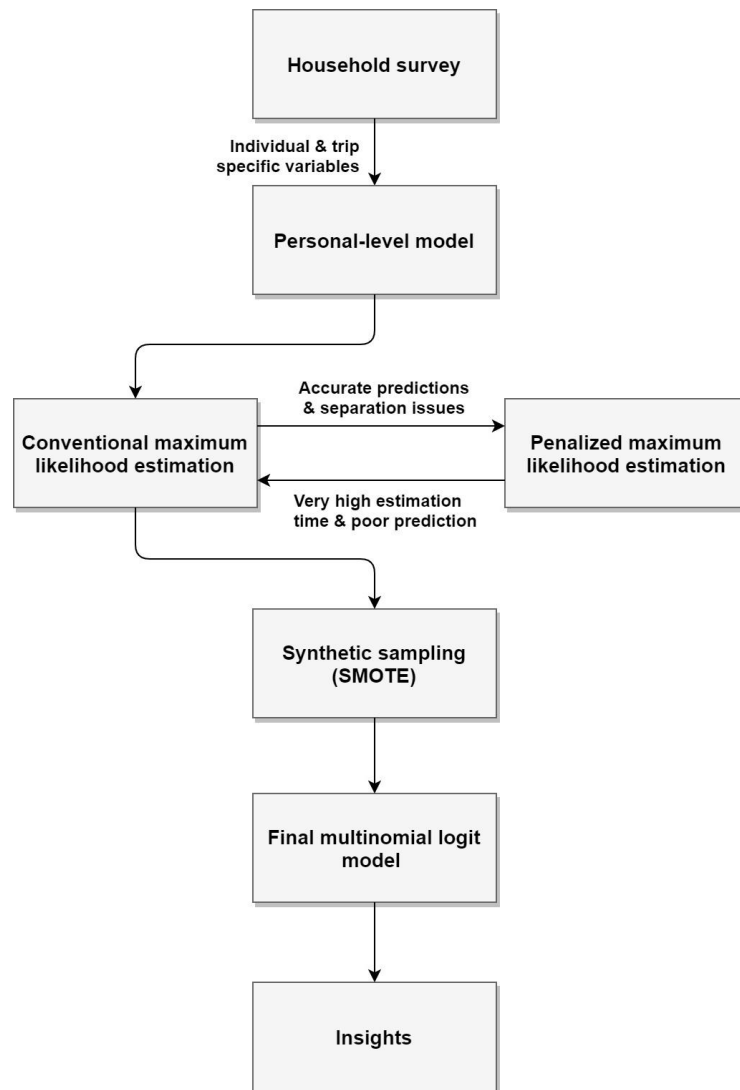
*Figure 15. Methodology – Disaggregate mode choice model*

### 4.4.1.4. Estimation results

The final model specification, which is selected based on the p-value of the independent variables and the likelihood ratio test, is as follows:

$$
\begin{aligned}
Bike-sharing\ (B) \\
&= Intercept + Age20-44 + isMale + hasUnivOrVocationalDegree \\
&+ PTPassDummy + HHCarsNum + TripDistKM \leq 2 + TripDistKM \\
&> 2 And \leq 5 + TravelTimeMins \leq 30 + NumberOfSharingBikesInZone \\
Car-sharing\ (C) \\
&= Intercept + Age20-44 + isMale + hasUnivOrVocationalDegree \\
&+ PTPassDummy + HHCarsNum + TripDistKM > 2And \\
&\leq 5 + TripDistKM > 5And \leq 15 + TravelTimeMins \\
&\leq 15 + TravelTimeMins > 15And \\
&\leq 30 + NumberOfSharingBikesInZone
\end{aligned}
\tag{19}
$$

$$Ride-sharing\ (R)$$
$$= Intercept\ +\ Age20-44\ +\ hasAnyLicense$$
$$+\ hasUnivOrVocationalDegree\ +\ PTPassDummy\ +\ TripDistKM$$
$$> 2And \le 5\ +\ TripDistKM > 5And \le 15\ +\ TravelTimeMins$$
$$\le 15\ +\ TravelTimeMins > 15And \le 30$$
$$Conventional\ systems-as-a-whole\ =\ 0\ (base\ category)$$

The estimation results are shown in Table 7.

| Variable | Estim. | S.E. | z-val | Interpretation |
|---|---|---|---|---|
| Age20-44 (B) | 1.14 | 0.04 | 26.18 | |
| Age20-44 (C) | 1.04 | 0.04 | 24.68 | Individuals with age from 20 to 44 are more likely to use sharing systems |
| Age20-44 (R) | 0.80 | 0.04 | 19.99 | |
| isMale (B) | 1.44 | 0.04 | 37.73 | Males are more probable to use bike-sharing & car-sharing systems |
| isMale (C) | 1.25 | 0.04 | 35.96 | |
| hasAnyLicense (R) | -0.23 | 0.04 | -5.24 | Individuals having (any) license are less probable to use ridesharing system |
| hasUnivOrVocational Degree (B & R) | 0.92 | 0.04 | 25.13 | Individuals with a university or a vocational degree are likely to use sharing systems |
| hasUnivOrVocational Degree (C) | 1.50 | 0.05 | 31.11 | |
| PTPassDummy (B) | 1.07 | 0.04 | 24.18 | Owning a public transport pass positively influences the use of bike-sharing & car-sharing systems, especially a stronger influence is found for the former, while negatively influences ridesharing. This could mean that car-sharing and bike-sharing complements PT, while ridesharing does not. |
| PTPassDummy (C) | 0.83 | 0.04 | 20.04 | |
| PTPassDummy (R) | -0.32 | 0.04 | -8.11 | |
| HHCarsNum (B) | -0.68 | 0.03 | -26.82 | A. With an increase in the number of private cars in the household, there is a decrease in the likelihood to use bike-sharing system. B. However, an increase in likelihood is observed for car-sharing system. This could mean that people with higher number of cars might give up their secondary cars and shift to car-sharing. |
| HHCarsNum (C) | 0.43 | 0.02 | 21.95 | |
| TripDistKM≤2 (B) | 1.57 | 0.07 | 21.77 | |
| TripDistKM>2And≤5 (B) | 2.37 | 0.06 | 36.54 | A. Bike-sharing systems are more likely to be used for trips with distances up to 5 km, with significantly higher probability for the range 2 to 5 km. It is to be noted that for distances less than |

MOMENTUM

**Modules: Induced demand | OD | Synthetic population generation | Mode choice |**
**Fleet management | Traffic assignment | Car ownership | Emissions**

| | | | | |
|---|---|---|---|---|
| TripDistKM>2And≤5 (C) TripDistKM>5And≤15 (R) | 1.75 | 0.04 | 44.92 | 2 km, one could walk and distances beyond 5 km could be considered long.<br><br>B. Car-sharing systems are expected to be used for a distance range of 2 to 15 km, with a higher probability for the range 2 to 5 km. |
| TripDistKM>2And≤5 (R) TripDistKM>5And≤15 (C) | 1.67 | 0.04 | 41.12 | C. Similarly, ridesharing systems are also expected to be used for a distance range of 2 to 15 km. However, a higher probability is found for the range 5 to 15 km. The reason could be better savings for longer distances. |
| TravelTimeMins≤15 (C) | 1.85 | 0.06 | 31.04 | |
| TravelTimeMins≤15 (R) TravelTimeMins>15And ≤30 (C) | 1.26 | 0.05 | 27.59 | There is a lower probability to use sharing systems for travel times beyond 30 minutes. |
| TravelTimeMins>15And ≤30 (R) | 0.76 | 0.05 | 15.42 | |
| TravelTimeMins≤30 (B) | 0.79 | 0.07 | 11.61 | |
| numberOfSharingBikesIn Zone (B) | 1.38 | 0.05 | 28.43 | With an increase in the number of sharing bikes in the traffic zone, there is a higher probability to use bike-sharing. Note: the number of bikes is represented in terms of hundreds. |
| ASC (B) | -4.60 | 0.09 | -50.45 | - |
| ASC (C) | -5.54 | 0.08 | -66.17 | - |
| ASC (R) | -2.44 | 0.06 | -39.38 | - |

McFadden $R^2$: 0.22; Log-likelihood: -28261

*Table 7. Estimation result – Disaggregate mode choice model*

Besides the aforementioned variables, in order to consider non-availability of a sharing vehicle, a dummy variable with very high negative coefficient (-100) is added to the utility specification of the sharing systems. Thus, if no sharing vehicle is available to serve a trip request, the utility becomes highly negative, thereby restraining the allocation of a sharing mode for that trip. Similarly, in order to consider the fact that car-sharing cannot be used by individuals without license type B or higher, another highly negative coefficient is added to the utility specification of car-sharing system.

We acknowledge the importance of influence of travel cost on mode choice. Unfortunately, the household survey does not contain any cost related data. To overcome this issue, synthetic travel cost could be estimated using information such as published public transport and shared mobility system fares. However, this involves making several assumptions about the costs of travel, which we do not feel warranted making.

### 4.4.1.5. Application within MOMENTUM

Within MOMENTUM, this model will be implemented in all the four case studies. The split between conventional systems-as-a-whole and the different shared mobility systems will be determined using the model presented in this section and the split between the different conventional systems will be determined using the conventional aggregate mode choice models of the cities.

**Modules: Induced demand | OD | Synthetic population generation | Mode choice | Fleet management | Traffic assignment | Car ownership | Emissions**

### 4.4.2. Data-driven shared mobility demand

The prediction of the expected shared mobility demand is relevant for the correct planning and strategic development of the systems and crucial for the understanding of the city transport system by any urban planning. Having an accurate estimation of the expected trips captured by shared mobility services is therefore relevant for both operators and urban planners to obtain an accurate picture of the mobility in the city.

Each city's mobility is explained in detail through "general mobility OD matrices". Such OD matrices can be approximated using different sources, such as city-wide surveys, traffic counts or new data sources like mobile phone records and simulation models.

The main hypothesis for the development of the current demand estimator is that the trips performed by any shared mobility service is the combination of different levels of trips captured according to a series of segmentations (traveller age, destination purpose, etc.) of general mobility matrices. The proposed demand prediction model takes as input different segmentations of the general mobility OD matrix along with other environmental elements from the specific trip origins and destinations. This translates into an OD pair-based prediction model that takes as input the general mobility OD matrix (e.g., the output from the model presented in Section 4.2), weather observations at each origin zone and land use shares of each zone and predicts the amount of trips captured by a specific shared mobility service by OD pair and unit of time.

The disaggregate mode choice model (Section Disaggregate mode choice model4.4.1) and this model have a substitutional nature, since the use of one negates the need for the other. Mode choice models are the commonly used methods in transport models. However, if one wishes to use shared mobility service data, the data-driven demand model can be used to replace the disaggregate mode choice model. The output of the data-driven demand model is an OD matrix of shared mobility, and the information of this matrix can be fed into the synthetic population module. Since the entry matrix is already mode specific, the output of the synthetic population does not have to pass through the disaggregate mode choice model, rather it can enter directly to the fleet management module. In this case, the framework will be different to the one presented in Figure 2. As a consequence, a feedback between fleet management module/traffic assignment and shared mobility demand estimation is not possible due to the data-driven nature. Similarly, a feedback between induced demand and OD generation step cannot be implemented.

The next sections describe the architecture of the model and the main reasons behind it, the features considered and the results of the development and validation of two prediction models for two shared mobility services: BiciMAD and Muving.

#### *4.4.2.1. Shared mobility and the histogram problem*

An important issue regarding the correspondence between shared mobility and general mobility is the trip volumes of each alternative. At present, shared mobility services have still a low penetration within cities' mobility ecosystems, not even reaching 1% of observed trips as a whole. In fact, the total volume of trips observed at any given shared mobility service is almost negligible when separating in smaller geographical units, such as OD pairs.

As a result, the relation between shared and general mobility is difficult to observe, as the volume of trips in shared mobility is comparable to noise with respect to general mobility trip volumes. Moreover, when shared mobility trips are scattered over different dimensions, such as OD pairs, there is a significant reduction on observed values that complicates the process of any machine learning algorithm to generate a useful model.

Even though the values observed in the target variable suggest that a service shared mobility trip distribution is limited and has not many variations, it may be the case than the underlying distribution (the one to be predicted)

is much more diverse and useful, but the available sample is limited due to trip scarcity. This has been called the histogram problem.

In this light, data augmentation techniques have been explored in an attempt to increase the richness of the observed target variable to facilitate the pattern recognition process carried out by machine learning models. This way, the augmented variables should provide more representative samples for the problem that simplify the learning process. For this model, the proposed methodology for data augmentation consists of summing the observed trips (in shared mobility) at each OD pair for the same days of the week (for instance, all Mondays together, all Tuesdays, etc.) to amplify the target variable and make it comparable to the main input features.

To measure the potential of this approach, an estimation of the richness of the target variable is needed. One way of measuring how informative a dataset is computing its entropy. In this sense entropy indicates whether the observed values of a distribution are homogeneous and not representative of the real distribution (low entropy) or heterogeneous and therefore more representative of the actual distribution (high entropy).

An important remark is that observing a low entropy value in the target variable does not necessarily mean that the variable is easy to predict, rather that the values available for training are not a representative sample of the underlying distribution. Table 8 displays the entropy of each of the datasets along with the observed number of trips:

| Dataset | Total trips | Entropy | Entropy after augmentation |
|---------|-------------|---------|----------------------------|
| BiciMAD | 752,103 | 1.2 | 5.18 |
| Muving | 44,828 | 0.11 | 0.91 |

*Table 8. Entropy of the trip registers per day, hour, and OD pair of each service*

In the table it can be observed that the data augmentation process is able to significantly increase the observed entropy of each variable, making target variables better for better inference of machine learning model.

### 4.4.2.2. Architecture of the data-driven shared mobility demand model

The proposed model consists of a machine learning regressor that takes as input a set of features (described in the feature section below) and returns an estimation of the trips captured by shared mobility for each OD pair and day of study. The general workflow of this model is displayed in Figure 16 below.
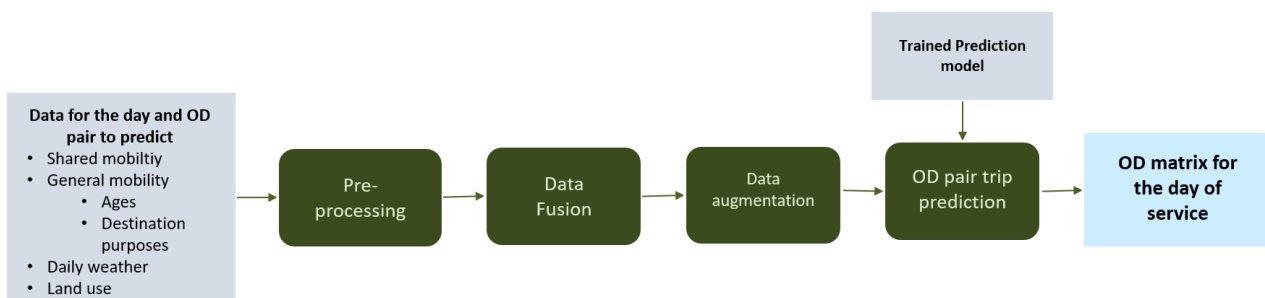


*Figure 16. Workflow of the prediction model.*

The model follows a simple flow where raw data is initially pre-processed into a set of feature tables that contain the variables derived from each data source organised by OD pair, hour, and day (or a subset of them if the data source does not have such a high granularity). Once these feature tables are obtained, they are fed into a data fusion process where they are merged altogether based on the previously defined indexes (OD pair, hour, and day). The result from that block is a complete training set that contains as target variable the number of trips

performed in the given shared mobility service and as input different segmentations of the general OD matrix as well as weather values and land use value, everything for every combination of OD pair, hour and day.

This input is ready for use in a machine learning setting. Nevertheless, as shown in the previous section of the histogram problem, it has been observed that shared mobility trips have a very low volume in contrast to general mobility, which makes the learning process much harder and yields worse performance from the resulting trained model. To alleviate this, the resulting input data is subject to a process of data segmentation and aggregation that increases the volume of observed shared mobility trips and subdivides the model into more specific and targeted models. Concisely, the steps in the data augmentation process are the following:

- **Spatial aggregation**: Both shared and general mobility OD matrices are obtained by assigning the trips of different agents (shared vehicles and mobile phone users) to a specific zoning. For the present model, the selected zoning is a square grid matrix of 1,000 metres side.
- **Daily aggregation of trip counts**: For each day of study, sum all hours by OD pair and day, making the prediction target the daily estimated trips per OD pair.
- **Day of the week aggregation**: Extract the day of the week of each day and aggregate by day of week and OD pair, summing shared mobility trips and averaging general mobility trips. This way, for each day of the week and OD pair there is a register with average values for the general OD matrix segmentations of all the available same days of the week and summed shared mobility trips of these days.
- **Distance segmentations**: Using the inter-quantile range, the model gets segmented into four full models according to OD pair distances, each model for each quantile of distances. After the individual prediction of each sub-model, the predictions are grouped and provided as a single prediction and, therefore, the results presented in this document are presented as a single model in practise. The trip distances are (in kilometres) the following:
    - Bike-sharing: 0-1.256,1.256-1.893,1.893-2.734,2.734-10
    - Moto-sharing: 0-1.343,1.343-2.42,2.42-3.52,3.52-10

Once the data has been augmented, each segmentation can be fed to a machine learning regression algorithm that will train a model to predict the amount of shared mobility trips under the augmentation conditions (aggregated into a daily forecast of summed trips by day of week per OD pair). In order to obtain a daily prediction per OD pair, the output of the model is then divided by the number of weeks used for the training set.

### 4.4.2.3. Shared mobility demand model prediction features

The main hypothesis of the prediction model is that shared mobility trips are influenced by different segmentations of the general mobility OD matrix. Hence, the main data source for trip prediction are general mobility trip registers. Apart from these data, weather information has been included under the premise that the weather at the origin is relevant specially for bike-sharing and moto-sharing services under study. Finally, land use at origin or destination is considered as a proxy of the kind of areas where shared mobility services are more popular.

#### 4.4.2.3.1. General mobility OD matrix

It has been observed that shared mobility trips are more influenced by certain segmentations of the general OD matrix, concisely by those generated from the age of the travellers and the destination purpose of each trip (The reader may refer to Deliverable D3.3 of the MOMENTUM project for further details).

For that purpose, the features derived from the general mobility OD matrix have been derived as the number of trips obtained for the following segmentations of the general matrix in terms of age and destination purpose:

- **E1_H:** Age group 1 (between 20 and 44 years old) and destination purpose home.
- **E1_W:** Age group 1 and destination purpose work.

- **E1_O:** Age group 1 and destination purpose other frequent activities.
- **E1_NF:** Age group 1 and destination purpose non-frequent activities.
- **E2_H:** Age group 2 (between 45 and 64 years old) and destination purpose home.
- **E2_W:** Age group 2 and destination purpose work.
- **E2_O:** Age group 2 and destination purpose other frequent activities.
- **E2_NF:** Age group 2 and destination purpose non-frequent activities.

Even though it is not expected that shared mobility demand is a direct function of general mobility, each service demand could be explained to some extent by a combination of the demand on different population segmentations according to their user's preferences and characteristics.

### 4.4.2.3.2. Weather data

The weather is a very important factor in the modulation of shared mobility demand of a city. In general, bad weather can impact on shared mobility user's willingness to take a shared mode to their destination differently. While for car-sharing services bad weather (rain, low temperatures, etc) might incentive use for being a much more comfortable alternative to almost any other mode (except private car), other services such as bike-sharing or moto-sharing will experience a demand reduction due to potentially uncomfortable and dangerous trip experiences.

In this light, the proposed prediction system takes as input a collection of weather-related variables that capture variations on different dimensions that could affect shared mobility services. Concisely, the proposed features are the following:

- **Precipitation**: the amount of precipitation collected at ground in mm. Values are obtained with an hourly granularity. The use of non-car vehicles during precipitation is dangerous very uncomfortable, so service demand could be severely impacted when observed precipitation is high.
- **Temperature**: the average temperature observed during a unit of time. Values are obtained with an hourly granularity. Low temperatures make the use of non-car vehicles uncomfortable and many users may avoid using these vehicles (and services) when temperature is low.
- **Maximum temperature**: the maximum temperature observed within a pre-determined period of time. This value is computed hourly.
- **Wind speed:** the average wind speed observed within a period of one hour. Strong wind gusts make driving dangerous, especially non-car vehicles.
- **Barometric pressure**: average measured barometric pressure collected hourly. Low pressure is a typical sign of bad weather conditions that would impact the demand of shared modes: car-sharing services may experience a spike on demand whereas the rest of services' demand will drop.
- **Visibility**: A qualitative measurement of the visibility provided by weather services. Bad visibility makes trips more dangerous and can be perceived as a sign of bad weather with consequences explained above.

### 4.4.2.3.3. Land use

In general, every building within a city is built for a specific use like household, offices, sports, etc. Governmental agencies typically provide such data at the building level and could be useful to characterise each zone within the city in terms of the services and facilities available inside each zone. For that purpose, the introduction of land use variables is proposed to capture such information on the origin and destination zone of each OD pair.

The process to derive land use variables consists of intersecting the zoning file with a building-wise spatial file that has associated the main use of each building. This way, it is possible to sum together the area of each usage type available for a given zone and divide it by the total area of each zone. The result of this process consists of the proportion that each land use type represents for every given zone. Concisely, the land uses are the following:

- Amount of total area dedicated to parking and warehouse facilities.
- Amount of total area dedicated to households in the zone.
- Amount of total area dedicated to industrial uses.
- Amount of the total zone area dedicated to office buildings.
- Amount of the total zone area dedicated to shops and commercial use.
- Amount of the total zone area dedicated to sports uses.
- Amount of the total zone area dedicated to shows and performances.
- Amount of total area in the zone dedicated to restaurants and leisure.
- Amount of area within the zone dedicated to health and charity.
- Amount of area within the zone dedicated to culture.
- Amount of area in the zone dedicated to religious uses.
- Amount of area in the zone of construction sites and gardens.
- Amount of area dedicated to singular buildings (such as monuments, stadiums, or remarkable governmental buildings).

Each of these variables is introduced into the prediction system for both the origin zone and destination zone at each OD pair. For each use two values are reported: the amount of space dedicated to that use in the origin and destination zone.

### 4.4.2.3.4. Alignment of model data

In order to generate the data described above, each of the required data sources is initially pre-processed to generate tabular format data sources that contain the feature values associated to a specific zone or OD pair, date and time that come from that data source. Concisely, the level of aggregation is the following:

- **General OD matrices:** general mobility OD matrices are ordered by OD pair, date and time.
- **Weather data**: weather data is associated to date and time and to a meteorological station that has a well-known spatial position. When assigning weather values to each of the OD pairs in the matrix, the closest station to the origin zone of each pair is selected.
- **Land use**: land use data is organised by zone and gets associated to both the origin and destination zones of each OD pair.

Once the data is arranged in this way, the data fusion process consists in aligning the features from each source according to a subset of time, date and origin and destination zones with the target data (shared mobility trips for a given date, time and origin and destination zones). The result of this step will consist of a tabular dataset that contains for each day, time and OD pair the number of trips observed in shared mobility along with each of the features described above. Then, the data augmentation process described before is in charge of aggregating and segmenting the data for the model training step.

### 4.4.2.4. Shared mobility demand model training

Previously, it has been defined that each model is sub-divided into four different model by separating OD pairs according to their distance. As a result, in terms of machine learning, the system trains and uses four different models which results get aggregated for result presentation and performance analysis.

Each of the models is a regression model based on the random forest algorithm. Random forest algorithm is a machine learning model that trains a set of decision tree regressors from different random sub-samples of the input data points and features. Once trained, such an ensemble performs a prediction of each tree for a given data point and averages all of them into a single prediction.

In order to optimise the outcome of the random forest algorithm hyper-parameter tuning, that consists of the optimisation of certain free model parameters, is performed over the training set. Concisely, the set of hyper-

parameters to be updated are decision tree depth and number of samples per tree leaf and the number of trees the random forest trains.

To ensure the correct characterisation of these sets of parameters, 3-fold cross-validation is used. 3-fold cross-validation consists in randomly splitting data into 3 uniform chunks and perform 3 training iterations for each set of parameters, using a different chunk as testing data each time. This way, the performance score metrics obtained for each set of parameters are robust and the best performing set of parameters can be safely selected. Each model is trained and evaluated over three datasets that are derived from the available data:

- **Validation set**: In order to ensure the correct generalisation abilities of the model, the last two days of each dataset are kept aside for final validation.
- **Training set**: It accounts for 80% of the remaining data and is used in for training the model through cross-validation.
- **Test set**: It accounts for the remaining 20% of data and is used as an initial test of the developed model generalisation abilities.

After training, the system computes the performance metrics of each model evaluated at each one of these sets. This enables to ensure that the resulting model is capable of generalising and also enables early detection of potential model problems, such as over-fitting. The metrics computed over each dataset are the following:

- **Coefficient of determination ($R^2$)**: The coefficient of determination is a statistical score that measures dispersion between target variable variance and model residuals variance. Model residuals are defined as the errors the model incurs in when making predictions. Typically, it is interpreted as the measurement of the amount of variance from an observed variable a model is capable of predicting.
- **Root Mean Squared Error (RMSE)**: Root mean squared error is the square root of mean squared error (MSE). MSE measures the average squared differences between target variable and model predictions.
- **Mean Absolute Error (MAE)**: The mean absolute error measures the average of the absolute differences between target variable values and predictions performed by the model.
- **Predicted trip volumes**: Compare the total number of trips predicted with respect to the total number of trips observed in the service.
- **Trip volume variation**: Difference in percentage between predicted and observed trip values.

### 4.4.2.5. Experiment setup

This model has been developed for the city of Madrid using data from official sources and two shared mobility operators: the public bike-sharing operator (BiciMAD) and a private moto-sharing company operating in the city (Muving). General mobility matrices are obtained from mobile phone network data by Nommon and provide mobility estimations within the city for the required age and destination purpose segmentations. Weather data is collected from the national meteorology agency (AEMET) and land use is obtained from the national treasury agency (Catastro).

Each of the shared mobility services is used independently to train a service-based model that takes as input all the features defined and provides a prediction of expected trips in such service for each OD pair and day of week. In all cases, the data available corresponds to the month of October 2019 and the three first weeks of February 2020. The last week of February 2020 has been removed to avoid the potential impacts that COVID-19 measures carried out by companies may have on general mobility.

Despite the model segmentation, its validation reports are provided as a whole, joining the predictions from all sub-models together into single model metrics. In the case of the models for BiciMAD and Muving services, the validation set is composed by the daily data from February 23rd and 24th 2020. The training and test sets consist of a random sampling (80% train, 20% test) of the augmented data of all days used except from those in the validation set.

### 4.4.2.6. Shared mobility demand model results

In this section we provide the modelling results and performance analysis of the implementations of the demand prediction models for the shared mobility services of BiciMAD (bike-sharing) and Muving (moto-sharing).

### 4.4.2.6.1. BiciMAD

The BiciMAD service is a station-based shared bicycle service that is deployed mainly in Madrid city centre, as shown in Figure 17. The service has an average trip volume of 8,000-10,000 trips a day, for approximately 2,500 bicycles deployed.
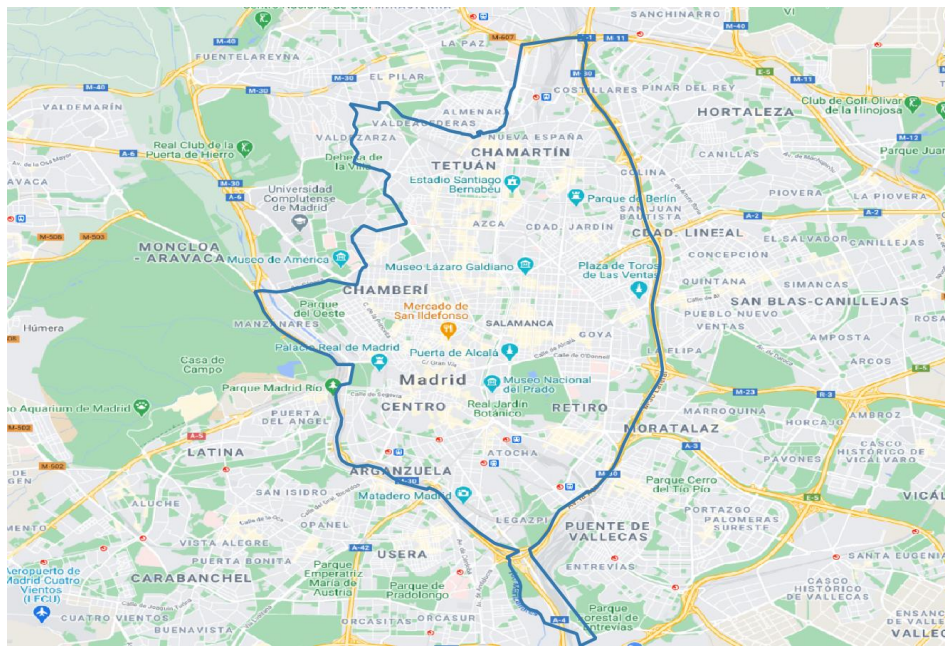


*Figure 17. Domain covered by BiciMAD stations*

The results for the demand model of BiciMAD service and the metrics of each set are presented in Table 9.

| Metric | Train | Test | Validation |
|---|---|---|---|
| Coefficient of determination ($R^2$) | 0.94 | 0.88 | 0.73 |
| RMSE | 21.94 | 29.65 | 4.51 |
| MAE | 14.3 | 18.75 | 3.05 |
| Target entropy | 5.13 | 8.75 | 7.39 |
| Aggregated trips (predicted/actual) | 448,048/447,825 | 111,875/112,005 | 8,095/7,407 |
| Trip variation (%) | 0.04 | -0.11 | 8.5 |

*Table 9. Test, training, and validation results from BiciMAD model. Validation values correspond to disaggregated predictions*

As observed in the matrix, the model has very good performance, with a very high $R^2$ value at train and test data sets. Similarly, the observed error is reasonable, taking into account that the reported values in train and test correspond to an 8-week data aggregation. In addition, Figure 18 displays the regression graph of each dataset.
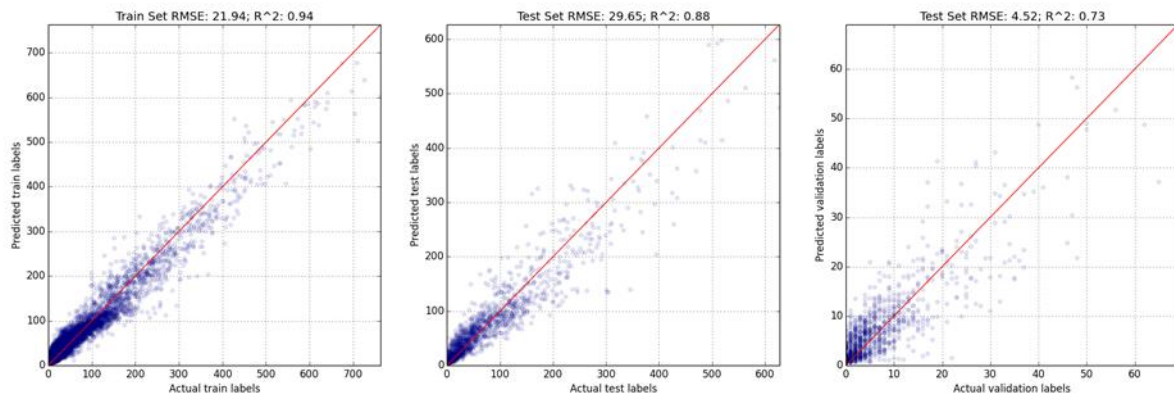
*Figure 18. Performance plot of the regression system. Each plot represents a single data set (train, test and validation respectively)*

The figure displays for each dataset a scatter plot that contrasts trips observed in the service on the x axis to their equivalent model predictions on the y-axis. Thus, the closer the scatter is to the red diagonal line, the better performance the model will have. In this case, we can observe that all three cases are correlated with the red line, suggesting that the model has good generalisation capabilities in spite of the deterioration observed at the validation set.

### 4.4.2.6.2.    Muving

The Muving service is a free-float motorcycle-sharing service that operated within a geofence in the central area of Madrid (typically called "Almendra Central" and some whereabouts). The geofence of this service is shown in Figure 19. The service had approximately 1,000 vehicles deployed in the city and a volume of nearly 500-1,000 trips a day. It is worth noting that shortly after the time periods selected for this experiment the service stopped their operations in Madrid.
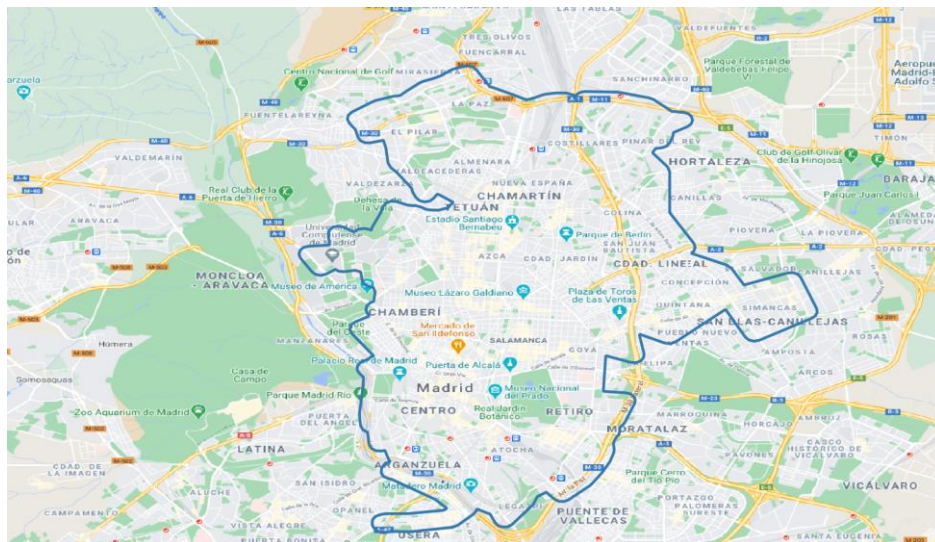


*Figure 19. Geofence of the Muving moto-sharing service*

Results for Muving service prediction model are presented in Table 10.

| Metric | Train | Test | Validation |
|---|---|---|---|

| | | | |
|---|---|---|---|
| Coefficient of determination ($R^2$) | 0.75 | 0.67 | 0.14 |
| RMSE | 0.94 | 1.04 | 0.22 |
| MAE | 0.48 | 0.52 | 0.08 |
| Target entropy | 0.94 | 10.44 | 9.22 |
| Aggregated trips (predicted/actual) | 28,968/29,066 | 7,060/7,140 | 538/353 |
| Trip variation (%) | -0.33 | -1.13 | 34.5 |

*Table 10. Test, training, and validation results from Muving model. Validation values correspond to disaggregated predictions*

The table clearly shows that the model reaches a fair performance, especially in the train and test sets but shows very bad results in the validation set. This is probably related to the shutdown of the service shortly after February 2020, which together with the low volume of trips observed indicates that the modelling phase has been carried out using data from the final time period of the service in the city. As a result, it is possible that the low performance obtained in the validation phase is motivated due to a decreasing trip trend that cannot be captured by the model. Figure 20 displays the performance plots of the model for each of the available data sets.
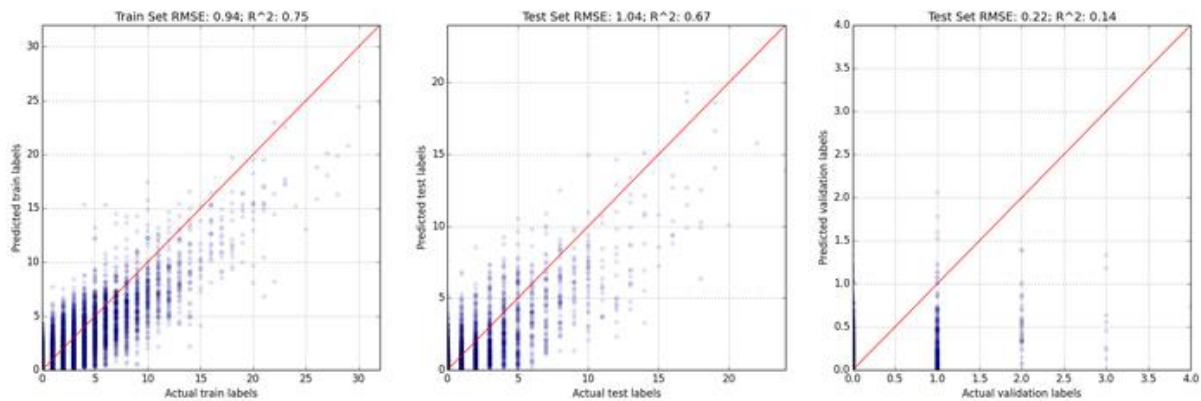


*Figure 20. Performance plot of the demand prediction model for Muving service*

While the performance shown by train and test datasets is reasonable, showing a model capable of accurately predicting demand, it is clear that the sample from the validation set is small and much smaller than the actual prediction carried out by the model. Hence, even though the Muving case has particular problems at validation, it can be concluded that, in general, the proposed modelling scheme is capable of capturing the demand of a given service and perform valid predictions for established services.

# 5. Fleet management

This chapter presents the fleet management modelling approach as part of strategic transport models, integrated with a shared mobility service simulation platform. The following sections will provide more detailed explanation of the fleet management planning and operational models and the Aimsun Ride traffic simulation platform. Furthermore, the fleet management objectives, methods, and KPIs vary depending on the shared mobility service that is being modelled and evaluated. Thus, each section revisits the aforementioned three topics to give more specific details about the implementation. The current deliverable considers four discrete case studies of on-demand transport shared mobility services: 1) Demand Responsive Transport (DRT), 2) Ridesharing (RS), 3) Car-sharing (CS), 4) Bike-sharing (BS). These shared mobility services have similarities as well as differences with respect to the objectives of the shared-service, service specifications and fleet resources. All shared mobility services share similar features that lie in the general on-demand framework. For example, all the services receive online requests. Additionally, they aim to maximize the number of accepted requests, while utilizing as few resources as possible. Lastly, all modes care about sharing economy, environmental footprint, and user's trip duration. Nevertheless, because of the differences, some of the objectives and KPIs need to be adjusted based on the service specifications.

## 5.1. Motivation and background

This section presents the overall modelling framework on how the fleet management module and transport simulation platform communicate and cooperate. Mainly, the Aimsun Ride shared mobility service simulation platform, implemented within the Aimsun Next (Aimsun, 2020) transport modelling simulation software, is used to get precise and accurate information about transport network behaviour, while fleet management algorithms are used to handle both planning and operational components in the simulation experiments. The fleet management term used in this document refers to both the operational aspect of the problem and the planning procedure. In general, there are two concrete categories of problems in transport service design:

1) Planning - Planning models are responsible of generating the strategic characteristics of the service, such as the desired fleet size, the number of stops and the whole network it covers (in case of service with stops or docks), the human resources, and the area to operate. However, it is usually difficult to create exact mathematical models capable of capturing all the uncertainties involved as well as the large number of decision variables that need to be considered. Thus, it needs to make use of transport simulation along with demand generation based on various probability distributions, so that the proposed design is robust and efficient; and

2) Operational - Operational algorithms are used to expand the available search space, as better approaches produce lower optimal bounds and make use of fewer resources. More precisely, the integration of efficient and high-performance optimization algorithms allows lower bounds on optimal solution, and less available resources.

With the use of the shared mobility service simulation platform, Aimsun Ride, this study also aims to examine and develop algorithms that could be applicable in real world cases, as the study incorporates the simulation results, which can reveal interesting real-life cases and dynamic events like congestion, accidents, and urban mobility demand trends. Consequently, the transport modelling, planning, and operation must take place under the same framework which involves the optimization strategies, Key Performance Indicators (KPIs), and the stochastically distributed demand scenarios.

The general workflow illustrated in Figure 21 describes how fleet management, simulation platform, metrics and generated demand interact with each other. At first, the disaggregated demand is inserted into the simulation platform to generate the OD matrices and demand requests. Additionally, this demand data feed the fleet management planning module, which is responsible for decisions like the size of the fleet, the capacity of each

vehicle, the area to be served or the location of the stops (or docks) and depots. Given those resources and demand, the fleet management operational module is used to handle the requests that are created dynamically inside the simulation. Therefore, the whole process can be described as two major loops that have direct interaction. The planning loop (big and slower) takes as an input the disaggregated demand and the KPIs (for both users and the fleet) produced by a batch of simulation experiments and use them to compute the new system parameters (planning features) via optimization techniques. In contrast, the operational loop (small and frequent) interacts immediately with the simulation environment, in the role of service manager, using operational research algorithms that allocate resources or assign requests to routes. The operational fleet management problem uses the actual operational costs including energy, customer satisfaction and fixed costs; while planning optimization aims to optimize strategic features, related with macroscopic econometric parameters of the system.
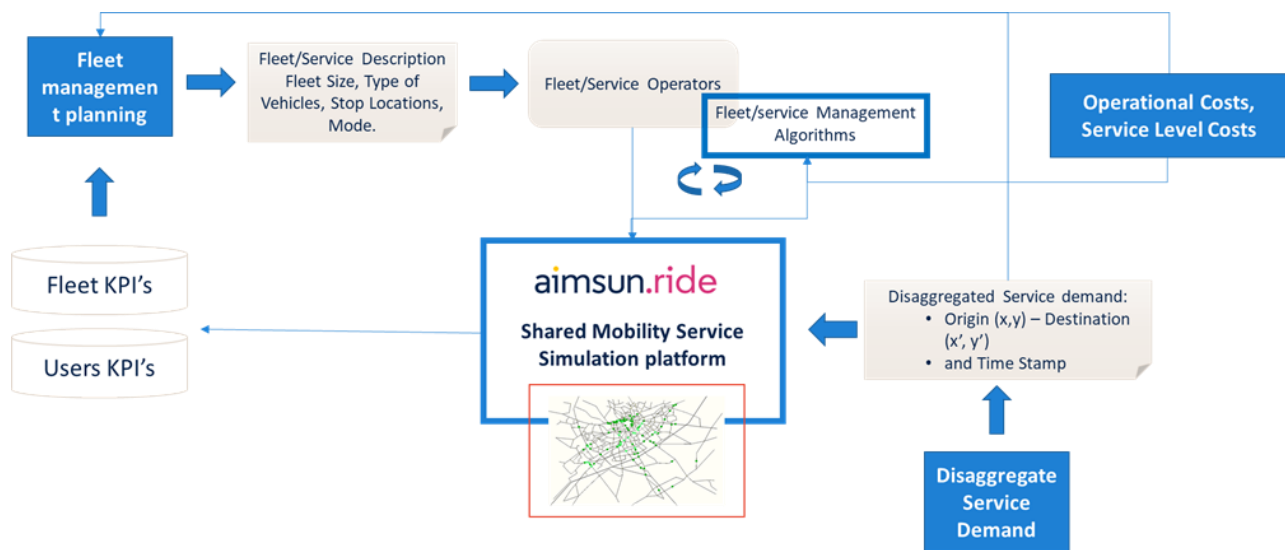


*Figure 21. Workflow between planning and operation fleet management*

## 5.2. Input data required for fleet management modelling and simulation

As presented in Figure 21, the input data must have the form of disaggregated demand that contain, at least, the origin, destination, and the timestamp of each request. Those data can be produced from various data sources. The most common ones are the household surveys, which can produce a reliable and representative sample. In other cases, floating car data, produced either by taxi fleets and public transport services or by individuals via GPS devices and smartphone applications, can be processed to create a dataset of trips with origin and destination features. Moreover, smart ticketing of modern transport services can be used to collect and analyse the pattern to generate the appropriate data.

Data sources are summarized in Table 11, along with comments about the easiness of collection, the quality and the ability to retrieve a representative view of mobility patterns, and the services for which details can be extracted. For instance, survey data collection can provide high quality data, but it is expensive to collect adequate sample size, which can be reliable. On the other hand, Floating Car Data (FCD) can be collected relatively easier and in a more affordable way. However, they need detailed pre-processing as they include significant number of outliers. Lastly, user data from micro-mobility and car-sharing related services can approximate origin and destination observations, however the information is restricted across the service network – a fact that also exists in public transport generated data.

| Source | Service | Quality | Cost of collection | Representative |
|---|---|---|---|---|
| Survey - Household | All transport modes | High | High | High (require decent sample) |
| FCD | Taxi | Medium | Low | Medium |
| FCD | Individuals (Smartphone app GPS) | Medium | Low | High |
| Smart ticket | Bus, Metro | High | Medium | Medium |
| User profile Monitoring | Bike-sharing, car-sharing, e-scooter sharing | High | Low | Medium |

*Table 11. Data sources for disaggregated data collection*

## 5.3. Traffic simulation tool required for fleet management: Aimsun Ride

This section introduces the simulation platform Aimsun Ride designed for the deployment and evaluation of the shared-mobility services. The platform was designed as a plug-in inside the Aimsun Next software (Aimsun, 2020) and has been improved and extended for the scope of the MOMENTUM project.

Traffic simulation is an important means with which to evaluate and optimize the design of complex transport applications in a timely and efficient manner. Within this project, a simulation platform is implemented to model and analyse system performance due to the introduction of new shared mobility applications. The Aimsun Ride simulation platform for shared-services is an advanced tool aiming to enable cities to deploy and test various scenarios related to new shared mobility applications (such as Demand Responsive Transport (DRT), car-sharing, bike-sharing and car-pooling). Scenarios can be defined and evaluated in order to explore different aspects of the provision of a mobility service. The investigated aspects can be related to both the fleet operators as well as the users of the system. For example, at the fleet operator level the platform provides the possibility for assessing alternative trip plans. At the user level different preferences and expectations on the system´s level of service can be investigated.

### 5.3.1. Methodology

The simulation platform Aimsun Ride executes the requests for new services (which have been estimated by the mode choice model) according to the optimised trip plans provided by the fleet management planning algorithms. The trip plans consist of a list of steps to arrive from an origin to a destination. Moreover, the fleet management operator feeds the service demand simulator with information related to the supply representation of the operator´s fleet that will be used to serve the requests. For instance, the number of vehicles in the fleet, number and locations of stations for bike-sharing and station-based car-sharing, etc.

A request is made by an individual to be transferred from point A to point B. Every request can include constraints based on the individual´s needs and preferences (e.g., accessibility, departure and/or arrival time windows, walking distance thresholds, etc.). These constraints are taken into consideration by the fleet management operator algorithms. Subsequently, the optimised trip plan by the operator is passed into the simulator for execution. Following, the simulator provides travel information to the fleet management operator to calculate the best routes of its vehicles. After each scenario execution, the simulator communicates with the fleet management algorithm in order to provide the operator with adequate KPIs so as to evaluate and re-optimise the process.

In the following subsections, the input and output files related to the developed service simulator are briefly described. More details regarding the format and structure of the input and output files will be provided in WP5, where the proposed framework will be implemented. The developed service simulation framework considers path costs (e.g., path travel times) which can be obtained either from a simulation or provided externally. The different path costs possibilities are summarised later in this document. Finally, in the last section the main KPIs that provided by the simulator are presented.

## 5.3.2.  Input files

The main input files for the service simulation platform are related to the service requests and operator's information. The files should be provided in JSON format.

In particular, the requests file has a collection of fields related to the requests to be executed during the simulation. Besides the information with respect to each trip (i.e., origin, destination, departure time, etc.), each request can include several user-defined fields that are, in turn, provided to the operator as additional attributes (e.g., accessibility constraints for specific individuals, walking time constraints, etc.). However, they are not considered by the simulator. The operator file includes information about the specific service operator that is being evaluated (e.g., car-sharing, DRT, etc.) as well as the fleet specifications. These specifications can be, among others, the vehicle type (e.g., bus, taxi, bike, etc.), origin position of the vehicles, number of seats in each vehicle, etc.

## 5.3.3.  Output files

After an execution, the simulation platform will produce a file with all the events executed as well as an optional recording file to visualize the simulation. The events file is a binary file that can be exported to JSON format, which will contain a list of events (see Figure 22) with information for the different event types that have been executed (either for a request or a vehicle in the fleet). This information is related to the state of a request or a vehicle executing it, the position and used capacity of vehicles, the path chosen.

| Event | Icon |
|---|---|
| Request | |
| Request accepted | |
| Request rejected | |
| Request dropped | |
| Request completed | |
| Vehicle starting a request service | |
| Vehicle going to origin | |
| Vehicle doing a pickup | |
| Vehicle going to destination | |
| Vehicle doing a delivery | |
| Vehicle going to repositioning | |
| Vehicle stopped after a repositioning | |
| Vehicle idle | |

*Figure 22. List of event types characterised by a unique icon*

### 5.3.4. Path cost calculation

The developed simulation framework provides a path calculation interface that can be used by the fleet management operator to calculate the optimal routes of its vehicles aiming to minimize the costs. The interface provides the flexibility to calculate the most efficient routes for executing the requests, in terms of the prevailing travel times inside the traffic network, based on three possible sources:

1. Free flow conditions
2. Simulated travel times obtained from a traffic assignment model
3. Historical travel times

The selection of the approach for obtaining the path costs depends on the assumptions made about the effect of the demand for new services on the network traffic conditions. Specifically, travel times based on free-flow conditions may be assumed for modes and services that do not interact with traffic (e.g., walking or to some extent bike-sharing systems). Hence, this approach does not require a network loading.

The low demand penetration scenario, which is one of the two demand scenarios considered in the project, assumes negligible or no change in travel times due to the introduction of demand for the new mobility services. In that case, historical travel times obtained from a previous static assignment model or based on the available travel time observations, can be used and considered fixed in all fleet management scenarios. Also, in this case no simulation of the network demand is required in order to obtain the travel times.

On the other hand, in the high demand penetration scenario, the network traffic conditions are assumed to be affected due to the increase in demand for the new services. For this scenario it may be necessary to update the travel times by performing a new traffic assignment. The simulated travel times can be obtained by performing a traffic assignment using multiple traffic flow resolutions, namely, microscopic, mesoscopic, or macroscopic. The

simulator will then pass the updated travel information obtained from the simulation to the operator. Several iterations between the simulator and operator might be needed in order to converge to an optimal solution. Different functions are implemented to obtain the travel times between an origin and a destination point using a specific mode. Moreover, travel times for the fleet can be also calculated from the position of each vehicle to the destination point.

Furthermore, the path costs calculation interface can be used to calculate routes for other existing modes, such as walking and Public Transport.

## 5.4. Modelling and simulation of fleet management for shared mobility services

As mentioned above, the Fleet Management module is separated into two sub problems: the planning and the operational. That discretization is necessary as the methods to handle each one significantly differ. Indeed, planning methods can be solved with the use of multi-objective optimization and/or station-based heuristics, while operational problems can be treated with online Traveling salesman problem (TSP), Approximate Dynamic Programming (ADP), and Reinforcement Learning on Markov Decision Processes (MDP -RL). That categorization is illustrated in Figure 23**,** along with the mostly used solution methods to handle the aforementioned problems.
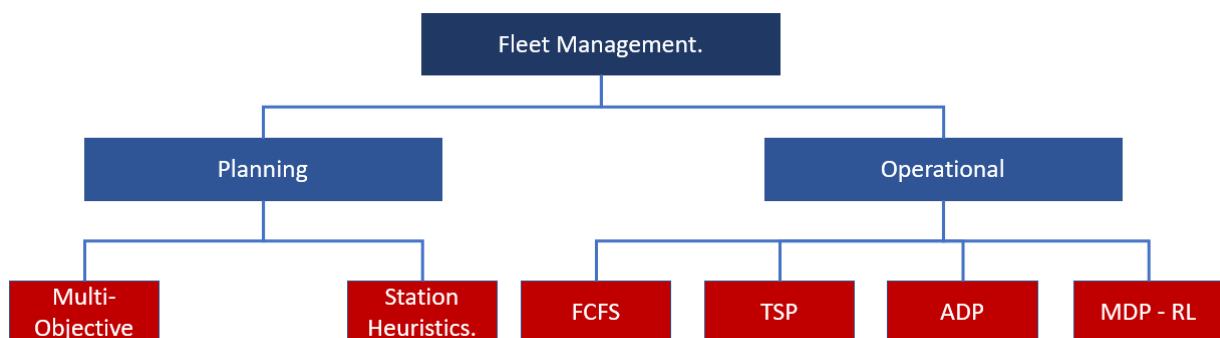


*Figure 23. Fleet Management Methods*

### 5.4.1. Algorithms for fleet management planning

The scope of planning on-demand transport services is to design flexible, affordable and responsive infrastructure for a user, in parallel with a profitable and sustainable business model. Especially, planning studies aim to find the econometric equilibrium that try to fill the gap between demand and supply in an optimal way. Thus, the most important stage is to design an objective function that contains all the revenue flows involved in the systems. As presented in Table 12**,** there are two types of costs, which are related to the performance of the service; the customer cost in terms of time, and the operators' costs which mostly related to salaries, vehicle and system maintenance (vehicles, software, etc.) costs. The customers' time related costs encapsulate the waiting time, the access time, the trip duration, and the acceptance probability. Therefore, poorer transport networks or insufficient fleet impose negative effect on the objective function as the waiting time, access time or acceptance probability will be high. In contrast, operator's cost embodies vehicle costs such as 1) purchase and maintenance of vehicles and the service software, 2) operation costs involving fuel consumption, renting public space or cloud computing expenses, and 3) utilization costs. While large networks and surplus fleet can result in higher service levels (low customer costs), the operational costs can start to rise, due to the resource expenditure. To conclude, the optimal network parameters must consist of both customers' and operator's point of view during the econometric equilibrium estimation process, to achieve a global optimum solution that makes the service prosperous for both the society and the service provider (Salanova and Estrada, 2015, Estrada et al. 2011).

| Cost Feature | Description | Unit. |
|---|---|---|
| Access Duration | The time each customer needs to get access to service | Minute |
| Waiting Duration | The time a customer needs to reach a stop | Minute |
| Trip Duration Service | The trip duration using the service | Minute |
| Total Trip Duration | The total trip duration with the use of the service | Minute |
| Accepted/Total | The ratio of requests accepted from total request | - |
| Vehicle Fixed Cost | The fixed cost of each vehicle (Purchase, maintenance, driver) | € |
| Vehicle Operational Cost | The costs of the operational prosses | € |
| Vehicle Utilization | The average occupancy of each vehicle | - |

Table 12. Cost features of planning module

There are two approaches that could handle such problems and there is a need to combine them:

- Formulating the problem as Multi-Objective optimization problem and approximating a solution with heuristics-like evolutionary algorithms.
- Generating an initial solution with many available resources and a large network, and during simulation episodes, eliminating them by taking a subset of the primal solution.

The first approach uses the costs detailed in Table 12 in the objective function, Equation (20), which relates to those with environment parameters. For instance, larger number of stops in a demand responsive transport must be negatively correlated with the walking, access and in-vehicle times. However, it needs to take as an input, a set of parameters like the candidate stops or the estimated walking distance and duration for a passenger to reach a stop. The second approach will also help by using object (stops, vehicles, docks) values in order to support the optimization algorithm to better converge on the optimal solution. In that setup, the sets of Requests and Trips refer to passengers, while Routes refer to vehicles.

$$
\begin{aligned}
min\, f(system) = &\left( \sum_{\forall i \in Trip} Access\ Duration_i\ +\ \sum_{\forall i \in Trip} Waiting\ Duration_i \right. \\
&\left. +\ \sum_{\forall i \in Trip} Trip\ Duration_i \right) \times Value\ Of\ Time \\
&+ \sum_{\forall i \in Requests} Rejected\ Request_i \times Revenue_i \\
&+ \sum_{\forall j \in Route} Maintenance_j \times Distance_j \div Utilization_j \\
&+ \sum_{\forall j \in Route} Fixed\ Cost_j \times Driver_j \times Duration_j \div Utilization_j \\
&+ \sum_{\forall j \in Route} f(Distance_j, Duration_j) \times fuel\ Price
\end{aligned}
\qquad (20)
$$

The starting supply parameters are defined by the disaggregated demand of origin and destination samples. As described in D3.3, those data can be processed with spatial clustering techniques like K-Means or DBSCAN. For instance, in the K-Means algorithm, the number of clusters can correspond to the stops (or the candidate stops)

of the DRT/Bike-sharing/Ridesharing/ Carsharing service. In fact, small customer cost flows require large number of clusters along with large fleet. Instead, restricted fleet and infrastructure expenses assume fewer number of stops, and shorter trip durations. To conclude, the process to define the initial system resources follows the workflow in Figure 24 and include 1) the desired parameters definition, 2) the algorithmic processing that depends on the transport mode, and 3) the output which has all the parameters needed for the simulation.

**Disaggregated Demand:**
(Origin – Destination)/Trip

**Parameters :** Maximum Distance, Maximum Mean Distance, Maximum Trip Duration, Number of Vehicles, Number of Bikes/cars,

K-Means + Penalty : → Stops.
VRP + Maximum Duration : → Cluster Routes.
Facility Location MIP : → Docks.
Shortest Path : → Ridesharing Routes.

**Planning Parameters.**
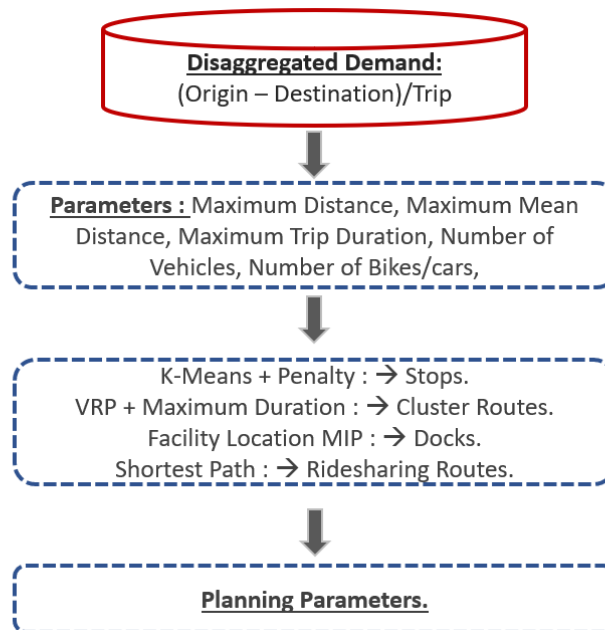
*Figure 24. System parameters initialization*

The last step is to design a heuristic optimization process which uses the objective function, Equation (20), and an object-based function to compute the next planning parameters to be simulated. Explicitly, the object-based function must provide metrics for all parametrized variables of the simulation, such as stops, docks, vehicles, and bikes. That function must aggregate performance related metrics similar to those in Equation (20). For instance, in DRT each stop would have a value that measures the average walking distance or the proportion of customers it serves. Therefore, it can be used as a criterion to evaluate if that stop must be eliminated or aggregated with another one. More details about the planning optimization procedure will be provided in the following chapters.

## 5.4.2. Algorithms for fleet management operations

The main problem of on-demand services is that they must handle dynamic and usually stochastic vehicle routing problems. Dynamic stands for the fact that the information about new requests is usually revealed as the vehicle is already on the move (online). Stochastic terms are caused by uncertain factors, such as congestion events or requests that are eventually rejected. Additionally, these services require both pick-up and delivery operation, either for the resources (bikes) or the customers (in case of ridesharing). There are many aspects of the problem that may have to be optimized via an operational model, but the most common aspects are the waiting time and the number of customers that will be served. Particularly, on-demand routing focuses on minimizing the waiting time, as well as maximizing the number of accepted requests. Moreover, the mathematical models must include the vehicle capacity constraints, time-windows constraints, and the vehicle availability (to reject a request, in case of non-availability). Lastly, there can be multiple depots and many vehicles, and the problem is called multi-depot and vehicle routing problem, rather than traveling salesman problem (Psaraftis, 2016). The most promising solutions for those problems are:

- **The Waiting Strategies.** This strategy focuses on the decision whether to start a route or wait for more requests to occur. For instance, if a there are few requests the route would have low utilization (e.g., passengers/km), so the route would be less profitable. In contrast, if the dispatching process waits too long, it may induce some customers to reject their trips. Thus, the critical decision that needs to be made is the period that the vehicle must stay immobile to maximize the number of served requests and minimize the waiting time. Those strategies are combined with TSP solutions and heuristics to create the optimal routes.
- **The First Come First Served Strategies.** These strategies are usually named also as queueing-pooling strategies. In fact, the system is described as multiple queues and one or more vehicles that serve requests on those queues.
- **The Markov Decision Processes (MDP) and Approximate Dynamic Programming (ADP) Strategies.** The last two strategies have a lot of similarities and methods in common. Modelling the problem as MDP is a useful formulation to apply ADP or neuro-DP algorithms. Especially, those methods provide powerful and efficient techniques to handle dynamical problem, as the Dynamic vehicle route problem or the dynamic resource allocation problem. Moreover, there are also solutions that combine MIPs with algorithms to approximate the value function with the use of the dual values of MIPs. In parallel, modern methods for those formulations are called Reinforcement Learning (RL), and these methods provide a very powerful framework to get optimal decisions in those problem instances (Sutton, 1998). With the rise of AI and Deep Learning methods, Deep-RL algorithms face a lot of popularity due to their ability to generalize and learn efficiently complex demand distribution. To give a brief illustration, the process of on-demand transport is modelled with the State-Action-Reward functions. More precisely, State contains all the information about the systems state, such as the position of open requests, the time each customer waits, and the vehicle position and capacity. A Neural Network (NN) can process that state and return as an output the best Action. That Action is passed into the simulation system and the simulation system returns the Reward and the next State. Therefore, the goal of simulation runs is to approximate the value function $V(S_t)$ which evaluates the value of each state, and guide policy improvement algorithms to maximize the expected profit (refer Figure 25). Finally, in the case of transport problems it is useful to form the input requests as graph related entities and make use of Graph NNs to process the state and produce actions. The interaction with shared mobility simulation platform, Aimsun Ride, is illustrated in Figure 26.

The Waiting Strategies (WS) and FCFS (First Come First Served) are easier to integrate and implement into a micro-simulation while RL methods require a lot of iterations to train a reliable agent which is computationally expensive in case of large network instances. Thereby, during MOMENTUM fleet management operational task uses the WS and FCFS strategies as it can overcome computational complexity issues. However, the RL framework could be tested in a macro or meso simulation set up to see how it performs.
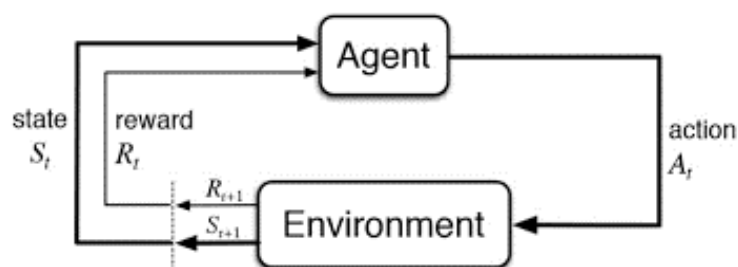


*Figure 25. Reinforcement Learning State Action Reward flow*
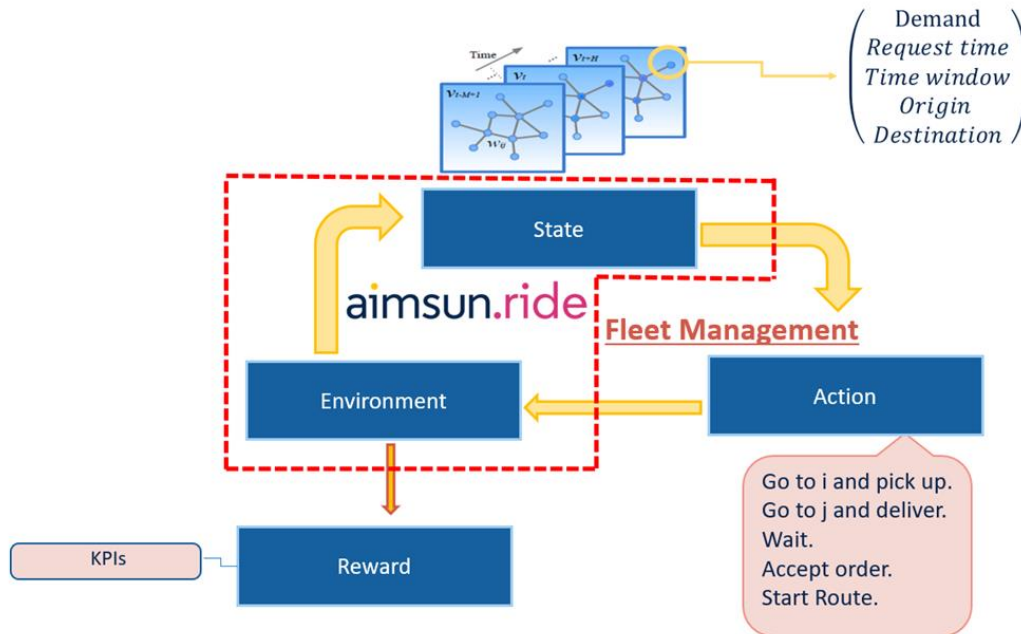
*Figure 26. State-Action-Reward flow between Fleet Management and Aimsun Ride*

### 5.4.3. Fleet management KPIs estimation using shared mobility service simulation

The Key Performance Indicators (KPIs) are important and need to represent the overall service performance as good as possible. Most of them already were presented in the previous section, as they play key roles in both planning and operational optimization processes. Nevertheless, when the optimization task is over it needs to extract some KPIs that reflect the expected system performance and compare them with the results that were generated in the real-life testing. Moreover, those KPIs used in the objective are more user-centric, and hence, they need to be aggregated in a more general form. Table 13 presents those KPIs.

| KPI | Description. | Unit. |
|---|---|---|
| Average Vehicle Utilization | It measures the ratio of passengers in each vehicle to the vehicle capacity. The goal is to maximize that ratio. The service needs to utilize resources as much as possible. | $\dfrac{Passengers}{Capacity \times Route}$ |
| Average Waiting Time | Represents the average waiting time for a user. More specifically, the metric does not include the access time. It measures only the time during which the customer has reached the point (stop or dock) and the resource is not available. The goal is to minimize this KPI. | $\dfrac{Minutes}{Passenger \times Route}$ |

**Deliverable 4.1**

New transport modelling approaches
for emerging mobility solutions

Page **78** of **137**

Copyright © 2021 by MOMENTUM

Version: Issue 1 Draft 2

| | | |
|---|---|---|
| Average Service Duration | Represents the average trip duration for a user. More specifically, the metric includes the duration of actual service usage. It measures only the time that customer is in-vehicle or use it. The goal is to minimize that KPI while maximizing the $\frac{Average\ Service\ Duration}{Average\ trip\ Duration}$. | $\frac{Minutes}{Passenger \times Route}$ |
| Average Access Duration | Represents the average time for a user to reach the service. More specifically, the metric includes the walking time and the time spent using other means of transport. The goal is to minimize this KPI. | $\frac{Minutes}{Passenger \times Route}$ |
| $\frac{Average\ Service\ Duration}{Average\ trip\ Duration}$ | The proportion of duration the passenger spends, using the current service. | - |
| Number of accepted requests. | Indicates the estimated proportion of accepted requests. The goal is to maximize this KPI. | - |
| CO2 emissions | Evaluates the average CO2 emission for a trip. The goal is to minimize this KPI. | $\frac{CO_2\ kg}{Passenger \times Route}$ |
| Area | Represents the area ($km^2$), in which the service operates. | $km^2$ |
| Population | Indicates the population of the served area. | Citizens |
| User cost | Indicates the average cost for a user. | $\frac{Euro}{Passenger \times Route}$ |
| Operator cost | Indicates the average cost per passenger for the operator. | $\frac{Euro}{Passenger \times Route}$ |

*Table 13. List of KPIs for fleet management planning and operational applications*

### 5.4.4. Algorithms for planning and operation of Demand Responsive Transport – DRT

Demand Responsive Transport (DRT) is referred to describe a service, usually governed by public authorities, that aims to provide affordable and on-demand trips using medium size vehicles. Specifically, DRT vehicles are between taxi, which is a fully on-demand service, and a public bus or metro line, which operates according to a schedule. In fact, DRT adopts the stop-based model of public bus system and the on-demand request features of the taxi services. In that way, DRT can be more flexible, as it relies on people's needs in parallel with the scalability derived from the large capacity of the vehicles. The requests can be booked either in advance or during the time when the vehicle is on the move. Each request includes the origin, destination, and time-window information. The operator

needs to manage those requests along with the online dispatching of the vehicle. Especially, such services fit better in ex-urban, sparsely populated and poorly supported by public transport areas, or even in disruption management, which usually occurs in case of traditional fixed bus or metro lines due to technical failures. Thus, DRT mainly focus on connecting areas (where traditional transport is not efficient) or emergency situations within the core urban areas and is relatively quicker than public transport and more affordable than taxi services (see Figure 27).
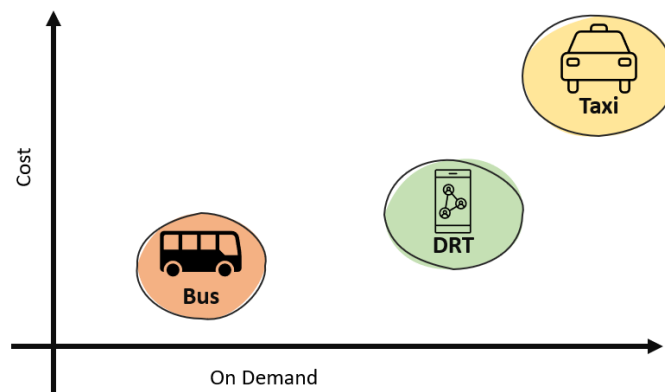


*Figure 27. Demand Responsive Transport role in transport services*

As discussed extensively in D3.3, the first step of designing a DRT service is to analyse mobility and public transport network data to detect the areas that are more suitable to implement it. Once those areas are specified, the planning procedure starts. The DRT service must provide an online booking platform that allows users to post their trip requests. The operator collects those requests and use them to generate the trips. While vehicle is on move, the operator can decide whether a re-routing is needed or not according to the online requests it receives. The main decision that must be taken is when to start a route or how long the vehicle must wait. In other words, there is a trade-off between the waiting time and the route efficiency, considering that more reactive routes will lead to less occupied vehicles with decreased capacity and energy utilization per km, as presented in Figure 28. Moreover, since the service could possibly have a lot of stops (>60), VRP (Vehicle Routing Problem) solvers could be set to pre-assign stops to mini-busses and the online optimization algorithms could be used for each route separately. Lastly, the system must assure that those passengers can use the same service to return where their first route started as most of the trips usually start from users' houses.
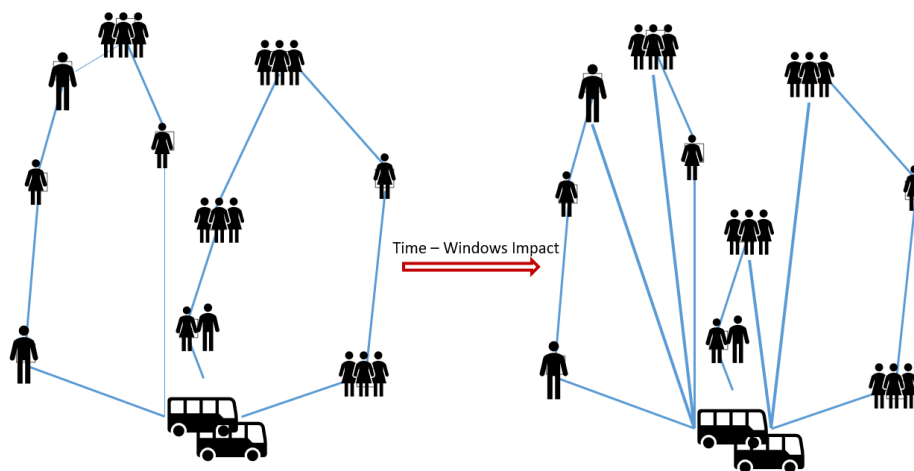


*Figure 28. Impact of online and time constrained requests*

### 5.4.4.1. Planning

As previously discussed, Demand Responsive Transport adopts the station-based system of the bus transit system. In fact, DRT aims to develop a bus network in areas with poor transit network support and fill the gap between on-demand responses and affordable pricing. Hence, DRT stops locations is one of the most important factors as the system try to serve as many users as possible, even those in solitary neighbourhoods. The second important system resource is the vehicles that perform the operations. The following methodologies will provide a detailed illustration of how the fleet management tool and shared mobility service simulation platform, Aimsun Ride, will cooperate to help operators decide which resources are needed to achieve the given service levels, which need to be defined first. Namely, the transport planner needs to define some constraints on the system, such as the maximum walking distance/duration of a candidate passenger or the maximum route duration. The objective function in Equation (20) remains the same, while all elements are held for the DRT case. In that setup, the sets of *Requests* and *Trips* refer to passengers, while *Routes* refer to vehicles.

| | Access Duration | Waiting Duration | Trip Duration | Route Distance | Utilization |
|---|---|---|---|---|---|
| Number of Stops | + | - | - | | + |
| Vehicles. | No impact. | + | + | + | - |

*Table 14. Impact of Decision variables to Objective function.*

The decisions the transport planner has to make are the desired maximum distance, the distance of the DRT stops from each customer and the maximum route duration for each vehicle. In Table 14, the impact of increasing the value of those decision variables is presented. For example, larger number of stops lead to a more accessible and efficient network, while the waiting time and trip duration increase. Thus, the maximum distance criterion could be used as a good starting point for searching the optimal combination of stops rather than the final solution. The Algorithm 1 (Figure 29a) is used to compute the initial number of clusters in the initial setting. In brief, the algorithm increases the number of stops (clusters) until all the stops have walking distances smaller than the decision parameter. To evaluate the number of stops that satisfy the maximum distance criterion the Equations (21) and (22) are used. The output contains the DRT stops coordinates that will be inserted in the first round of simulation experiments.

$$P(S, MaximumDistance) = \sum_{\forall s_i \in S} M \times Dist(s_i) \tag{21}$$

$$Dist(s) = \begin{cases} max(dist_j) \ \forall \ dist_j \in Requests \ \textbf{\textit{if}} \ max(dist_j) > MaximumDistance \\ 1/M \qquad\qquad\qquad\qquad\qquad\qquad\qquad\qquad\qquad\quad \textbf{\textit{else}} \end{cases} \tag{22}$$

Given that set of stops, the next step is the initialization of the number of vehicles that need to operate in order to satisfy the maximum route duration criterion. That task is performed via Algorithm 2 (Figure 29b) which takes as input those stops along with the desired route duration and returns both the number of vehicles and the set of stops assigned to each vehicle. The evaluation-2 function in Figure 29b is a trivial method that evaluates if each vehicle satisfies the maximum duration criterion. Given the setup of the first round of simulations, those system parameters must be tuned and optimized as experiments proceed. The mechanism must be based on merging or division of stops according to their performance.

**Deliverable 4.1**

New transport modelling approaches
for emerging mobility solutions

Page **81** of **137**

Copyright © 2021 by MOMENTUM

Version: Issue 1 Draft 2
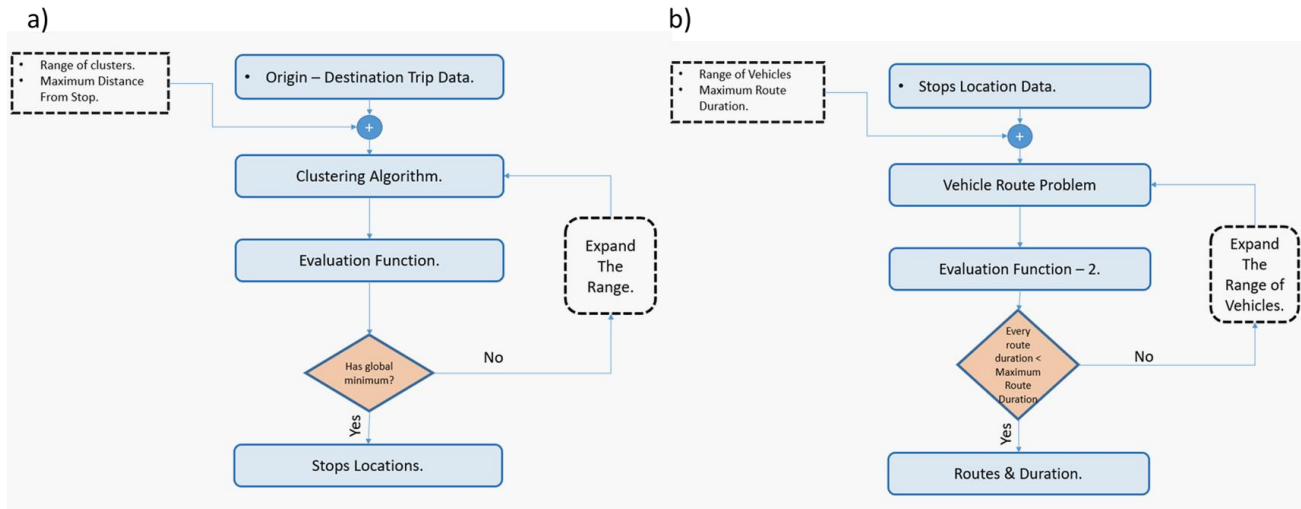
*Figure 29. DRT a) stops location (Algorithm 1)  b) route duration (Algorithm 2)*

The evaluation of the impact of the stops and the arcs connecting them are based on Equations (23) and (24) respectively. Equation (23) calculates the average access and waiting duration of each stop based on the trips that used that stop as an origin point. Hence, lower values indicate higher levels of service. In parallel, Equation (24) evaluates the frequency of using the arc between stops $i$ $and$ $j$. In fact, lower usage of one arc could be used as a proxy to evaluate if those two stops could be merged into one. The rule goes as follows: if two stops have relatively high service level and the arc that connects them has relatively low frequency, those two stops could be merged into one. The new stop can be located at the centre of those two previous stops.

$$C(stop_i) = \frac{\sum_{\forall i \in TripS} \text{Access Duration}_i + \sum_{\forall i \in TripS} \text{Waiting Duration}_i}{3\,|TripS|} \ \forall \text{ TripS} \qquad (23)$$

$$\in \{ \text{Trip}|\text{Trip} \in \text{Stops}_i\}$$

$$A(stop_{ij}) = \frac{\sum_{\forall i \in E} 1}{|Trips|}, E \in \{Trip \mid stop_{ij} \subseteq Trip\} \qquad (24)$$

In case a stop has large queues or a large value of Equation (23) and so the arcs which destinate in that stop, it can be divided into two smaller stops based on the spatial distribution this stop has. The actual number of stops that will be merged or divided in each iteration depends on the threshold 'n' which can be defined by the software user. For instance, if n = 1, at each simulation experiment the algorithm will choose the arc that is ranked as better for merging, according to the equations mentioned above. Similarly, for the case of division, the most popular stop will be divided into two smaller stops. Once the new set of stops is ready, the Algorithm 2 (Figure 29b) takes place to compute the new set of vehicles and the assignment of station for each one. As this process moves on, the objective function, Equation (20), evaluates each setting. At the time it finds a minimum, the simulation experiments break, and the set-up, along with the KPIs of the Table 13, are presented to the transport planner. The diagram in Figure 30 illustrates that optimization workflow.

MOMENTUM

Modules: **Induced demand | OD | Synthetic population generation | Mode choice | Fleet management | Traffic assignment | Car ownership | Emissions**
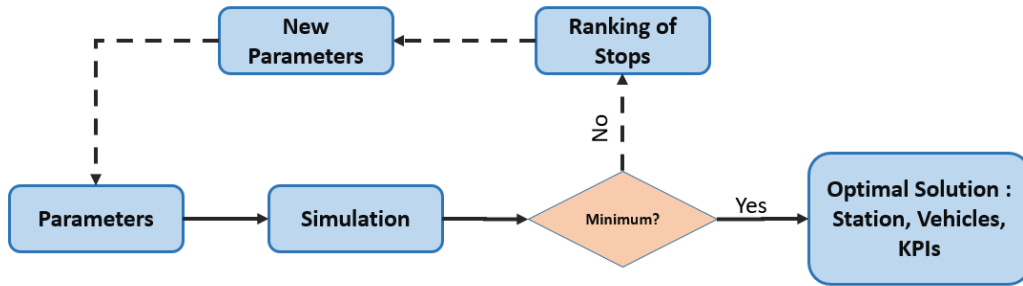
*Figure 30. DRT planning optimization workflow.*

### 5.4.4.2. Operational

DRT services fall in the routing category of the Dial-a-Ride problem (DARP). In fact, DARP is a special case of Pickup and Delivery Vehicle Route Problem (PDVRP). The core difference lies on the pickup and delivery locations, that in case of DARP are predefined from the passenger, while classical PDVRP has a set of stops that vehicle can pick up units and a set of delivery points, so there are no constraints of which origin must serve one destination (Häll, 2009). Additionally, the system assumes that each request will arrive before the trip starts a route. Therefore, if route duration is 20 minutes, the waiting time of each customer is 20 minutes at most. The following model consists as a general solution in PDTSP problem, which could be used both for DARP and rebalancing purposes. Indeed, the same algorithm will be used in the case of bike-sharing and car-sharing rebalancing in the BS section. However, the final experiments will also consider and evaluate a more straightforward formulation of DARP, such as the one proposed by Cordeau (2007), which is closely related with the current solution. The model formulation consists of the following variables:

- $G = \{V, A\}$, Graph with the set of stops V and the set of Arcs (connecting the stops) A.

- $x_{ij} = \begin{cases} 1, & \text{If vehicle moves from stop } i \text{ to } j \\ 0, & el \end{cases}$

- $f_{ij} \geq 0$, the flow of users from $i$ to $j$

- $q_i = \begin{cases} > 0, & \text{if station } i \text{ has a demand of pickup of } q \text{ passengers,} \\ < 0, & \text{else.} \end{cases}$

- Q = Vehicle Capacity.

Thus, that MIP of PDVRP problem is formulated as follows:

**_Model 1: MIP – PDTSP_**

$$\min \sum_{i \in V} \sum_{j \in V} c_{ij} * x_{ij} \qquad (25)$$

s.t.: $\qquad \sum_{i \in V} x_{ij} = 1 \ , \forall j \in V \qquad (26)$

MOMENTUM

**Modules: Induced demand | OD | Synthetic population generation | Mode choice | Fleet management | Traffic assignment | Car ownership | Emissions**

$$\sum_{i \in V} x_{ji} = 1 \ , \forall j \in V \tag{27}$$

$$\sum_{j \in V} x_{0j} < \mathrm{m} \tag{28}$$

$$\sum_{j \in V} x_{0j} = \sum_{j \in V} x_{j0} \tag{29}$$

$$\sum_{j \in V} f_{ij} - \sum_{j \in V} f_{ji} = -q_i \ , \ \forall j \in V \tag{30}$$

$$\max 0, -q_i, q_j * x_{ij} \leq f_{ij} \leq \min Q, Q - q_i, Q + q_j * x_{ij} , \forall (i,j) \in A \tag{31}$$

$$\sum_{i \in S} \sum_{j \in S} x_{ij} \leq |S| - \max 1, \left\lceil \frac{\sum_{i \in S} q_{ij}}{Q} \right\rceil , \forall S \subseteq V / \{0\} \tag{32}$$

In that formulation, *Model 1*, the objective is to minimize the travel time for each route. In parallel, constraints in Equations (26)-(29) are typical for TSP models and ensure that vehicle will leave each station visited and it will finally return to the depot. Moreover, constraints in Equations (30) and (31) are the flow conservation constraints and ensure that the maximum capacity of the vehicle will not be exceeded. Finally, constraint in Equation (32) prevents the program from reaching a solution with subtours. The output provides the simulation with the final optimal path that must be followed to serve the trip requests.

In summary, designing a DRT system requires the cooperation and communication among different techniques, such as transport simulation, clustering algorithms, and routing algorithms. In general, DARP is a well-studied problem in literature, while the planning schema does not face the same popularity. However, the present section shows that, given a sequence of requests with origin-destination and the time-windows, the proposed process can be used along with the shared mobility service simulation platform, Aimsun Ride, to search in a more systematic way for the optimal DRT resources. In addition, the methods developed are already well studied across different scientific fields. Thus, these methods can be easily extended and enriched with other instances of those algorithms. To conclude, this section illustrates a framework that interacts with the Aimsun Ride, shared mobility service simulation platform in a 2-stage analysis and supports rational decision-making processes for planning DRT services.

## 5.4.5. Algorithms for planning and operations of ridesharing service

The first on-demand service introduced in the urban mobility environment involves the taxi service, further indicating its long-term existence and thus, attracting the interest of the academic community. While the initial research efforts on taxi services focused mainly on their design, planning and control under profitability maximization objectives, new research efforts moved further into the development of multi-objective optimization methodologies that considered additional parameters, such as passengers waiting time, cost of trip, demand, trip distance and duration, value of time and willingness to pay. However, as modern cities tend to get overcrowded, problems, such as congestion or high levels of carbon dioxides, arise. Thus, the sharing economy in transit sector is emerging as it could help to encounter those challenges efficiently. Especially, ridesharing forms one of the best practices in sharing economy due to low cost and trip duration features that it offers. In that sense,

MOMENTUM

**Modules: Induced demand | OD | Synthetic population generation | Mode choice | Fleet management | Traffic assignment | Car ownership | Emissions**

RS refers to the service wherein car owners or professional taxi drivers can provide shared trips to commuters, whose desired origin, destination, and time-window preferences are relatively close. In fact, RS is preferred in densely populated areas where citizens perform a vast number of trips, so there are a lot of cars and/or taxis trips that ensure the appropriate supply levels for the passengers. In contrast to DRT services, which focus on sparsely populated ex-urban areas, RS try to take advantage of the rich trip activity of urban areas. Moreover, RS service business models can be discretized in 3 categories, as Table 15 presents: 1) Matching agent, 2) Service provider, and 3) Hybrid.

| Business Model | Resources | Scope | Optimization Task |
|---|---|---|---|
| Matching Agent | Private cars | The role of the operator is to match car owners with passenger requests. | Maximize the accepted requests. Utilize as much private cars as possible. Balanced routes. |
| Service provider | Taxi fleet | Assign passengers to trips with respect to sharing objectives. | Maximize the accepted requests. Utilize the taxi fleets. |
| Hybrid | Private Cars + Taxi fleets | Matching operator with outsourcing choice of taxi fleets. | Maximize accepted requests. Use private car at most and minimize the outsourcing requirements. |

*Table 15. Ridesharing models*

The hybrid model is the most general one; hence, this study will focus on it as it is also the most realistic one. Indeed, matching model has the problem of demand and supply. More precisely, higher demand requires significant levels of supply (private cars) and vice versa. Thus, it is difficult to design a system that is based on private cars only. On the other hand, service provider model needs either large investments on fleet or increased operational expenses in renting the taxi drivers. Therefore, the hybrid model fills the gap as it tries to exploit the private cars as much as possible, ensuring that there is a fleet that could always serve the demand in case of supply shortage.

Another major issue in RS services is the ridesharing pattern the system follows. Those patterns can be summarized in four main categories according to Furuhata (2013). Those differences can have a significant impact on the overall system performance and each pattern require different algorithmic approach. Inspired by that categorization, this study generalizes those patterns into four new clusters that fit better the objectives of the MOMENTUM project. Those four categories are presented in Figure 31 and can be summarized as ::

- **Pattern-1 (identical ridesharing)**: In that pattern, both origin and destination of all trip participants in a shared route join and leave the car at the same point. Thus, the trip contains commuters that have the close origins and destinations.
- **Pattetn-2 (Inclusive ridesharing):** In that case, the passenger's origin and destination are on the driver's way. Therefore, the driver must have, at least, two stops during the trip (in case of one passenger, one pickup stop and one drop off).
- **Pattern-3 (partial ridesharing):** In that category, either pick-up or drop-off are same for all participants. That problem is also referred as one-to-many or many-to-one RS.
- **Pattern-4 (detour ridesharing):** The final pattern stands for the case in which the driver makes a detour to find the path that best serves all passengers assigned to that trip.

All those patterns have some advantages and weaknesses. For instance, if the service operates according to Pattern-1, it significantly limits the set of possible candidate passengers. Consequently, the service will need to withhold larger fleets of taxi via outsourcing. However, drivers avoid pick-up or drop-off stops, so then the route

duration reduces, and the trip becomes more convenient for drivers. In contrast, pattern 2 can lead to reduced taxi outsourcing costs, but higher trip durations with pick-up and drop-offs between drives origin and destination. Figure 31 provides a quick summary of that trade-off.

| Pattern | Driver – Trip duration | Passenger Trip Duration | Passenger Walking Distance | Matching Efficiency | Driver's Convenience. (less stops, detours) |
|---|---|---|---|---|---|
| 1 | +++ | +++ | +++ | | +++ |
| 2 | + | +++ | ++ | ++ | ++ |
| 3 | + | +++ | ++ | +++ | + |
| 4 | - | +++ | +++ | +++ | - |

*Table 16. Impact of RS patterns along different system variables (Very Positive: +++, Positive: ++, Medium: +, Negative: -)*
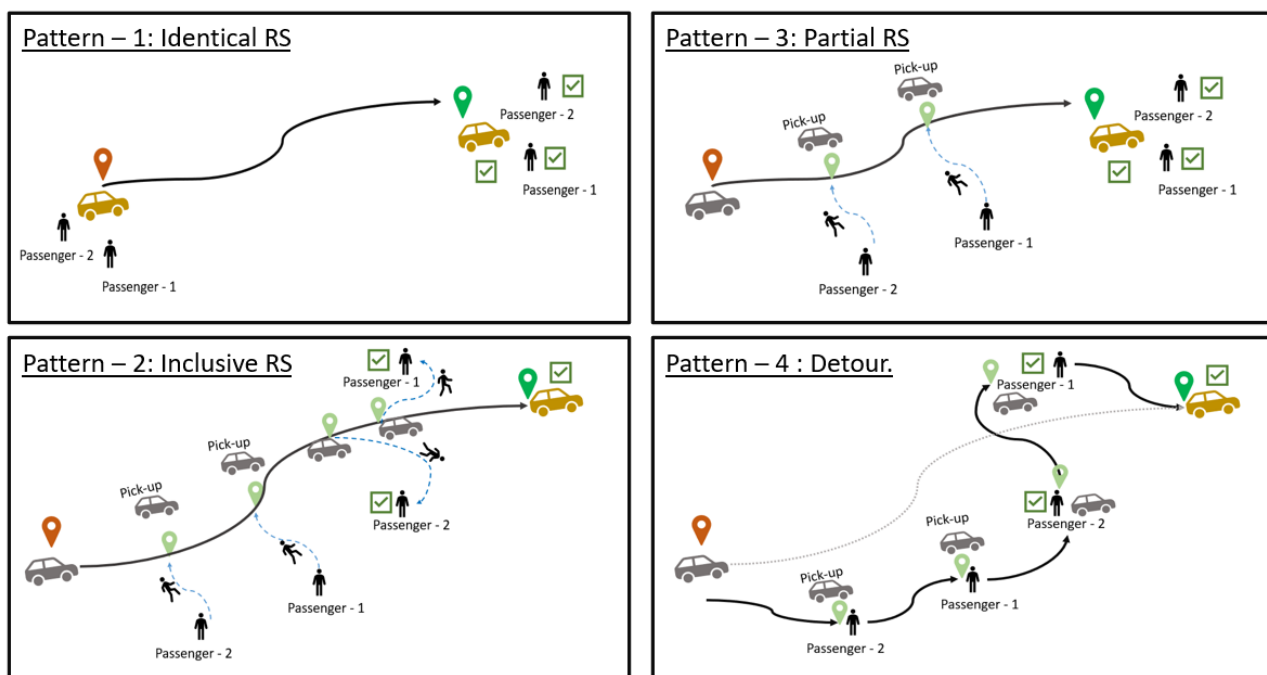


*Figure 31. RS patterns*

### 5.4.5.1. Planning

The planning process of RS service is not a trivial task. In fact, the first problem arises in the fleet size and the maximum number of customers that could share a trip. In case of private cars and taxis, that boundary is limited to 4 people. However, the main difficulty is to estimate that number of vehicles that must be available. In reality, those services start to operate with a specific number of vehicles and, as time passes, more driver (supply) enter the system. Thus, in the early stages of the service, it could be assumed that most of the vehicles will come from rental taxi fleets. In the course of time, as more drivers join the service, the increment of supply drives the demand. This is a closed loop dynamical phenomenon though, so as the demand increases the supply also follows that trend (positive loop). Consequently, the service starts the operation with minimum earnings (possibly with losses), but as the time passes and the proportion of private cars increases the profits also increase.

In that case, the simulation could be used in order to see how different mixtures of private cars and fleets could serve several demand scenarios. Especially, the simulation and planning iterations will be used to estimate the

**Deliverable 4.1**   New transport modelling approaches   Page **86** of **137**
for emerging mobility solutions

Copyright © 2021 by MOMENTUM   Version: Issue 1 Draft 2

optimal fleet size that is needed to serve the demand of each scenario. Additionally, the RS pattern will vary along the scenarios to evaluate each strategy and make sure that the system performs in a convenient way both for the driver and the passengers. Finally, the simulation uses two different setups:

- The first one considers that the fleet size is predefined, and hence, the objective is to define the optimal size.
- The second considers that it has a specific supply of private cars, so it tries to find the optimal RS strategy via taxi outsourcing.

The objective for that task differs from objective in Equation (20) as more stakeholders are involved in the system. There is a set of Drivers' Routes (DR), Passengers' Routes (PR) and Outsourcing taxi fleet (OTF) routes. The RS objective function in Annex A3, contains time relate costs of both drivers and passengers, vehicle maintenance costs, outsourcing costs, fuel costs and private car payments.

The next step is to define the fleet size that is needed to serve the demand. Similar to DRT, the fleet size is an estimation, so during experiments it will be adjusted according to optimization techniques. The first round of experiments assume that all the requests will be accepted. The assignment step is performed via the algorithm presented in the Operational section. Moreover, the assignment uses a 3-step procedure which firstly assign passengers to trips based on Pattern-1. Then, the subset of unserved demand uses the Pattern-2 and, finally, those who do not match with any driver are assigned to shared taxi trips. While all costumers are assigned to trips, the hourly supply need to be extracted. Finally, the fleet size of the most popular hour of day (the hour that needs the more vehicles) is considered as the initial available fleet.
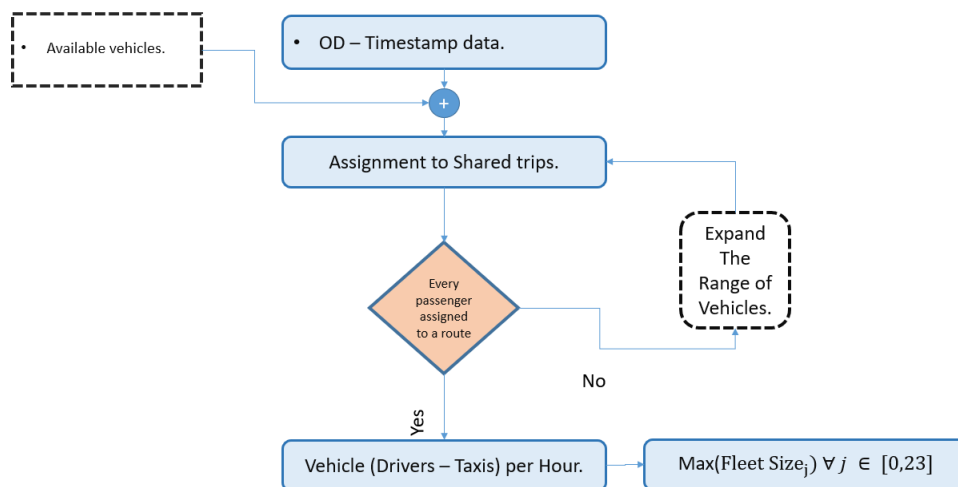


*Figure 32. RS fleet size (Algorithm 3)*

In that sense, the only resource of the system is the available vehicles. Given that the starting fleet size is overestimated, the following planning optimization starts eliminating vehicles. When the algorithm (Figure 32) finds a size for which the losses from unserved customers are equal to the vehicle expenses, the process stops and returns the fleet size. In parallel, planning routine searches for the optimal Pattern to maximize the profits with respect to predefined service levels.

### 5.4.5.2. Operational

Ridesharing problem (RSP) exists as a special case of the Dial-a-Ride problem (DARP), which in general falls into a bigger category of Pickup and Delivery Vehicle Route Problem (PDVRP).  A typical PDVRP considers a graph, $G =$

$(V, E)$, where $V$ is the set of nodes (all the possible pickup and delivery places) and $E$ stands for the set of edges that connects those nodes. In that general case, vehicles can perform pickup or deliveries actions at every node. Hence, the problem faces a large state space due to many degrees of freedom. Carpool stands as a relaxation of PDVRP in terms of each vehicle has a specific origin and destination node and each client must arrive at the same destination node. In that way, there are not too many states which the algorithm must take into account. Therefore, RSP is computationally intensive even for medium size problems and classical approaches cannot handle it. This app further reduces the dimensions and complexity of the problem by reducing the form in an assignment problem.

As a consequence, that relaxation creates a lower bound of the optimal solution. To prevent a lower bound far from the true optimal a new feature is added in the feasible solution space. Each driver can pick one among three paths. Hence, the variables that decide for that are:

$$x_{ij}^k = \begin{cases} 1 \text{ if driver } i \text{ take the path } k \text{ and pickup the passeger } j, \\ 0 \text{ else} \end{cases}$$ (33)

$$y_i^k = \begin{cases} 1 \text{ if driver } i \text{ take the path } k, \\ 0 \text{ else} \end{cases}$$ (34)

The distance for each passenger to the closet point on the trajectory of each driver and each path are denoted as $d_{ij}^k$. Other parameters are:

$Cap_i$ : The capacity of each vehicle.

$T_i^k$ : The total time that vehicle I needs from origin point to destination.

$P_{ij}$ : Penalty factor in case that passenger j did not assigned on driver i.

$PT_{ij}^k$ : The time that driver i from path k needs to reach the passenger j.

$l_i$ : The latest time that passenger or driver have to be on destination.

$e_i$: The earliest time it can start the route.

The mixed- integer model that used to make the assignment is the following:

$$\min \sum_{i,k} T_i^k - \sum_{i,j} P_{ij} \sum_k x_{ij}^k$$ (35)

s.t. $\qquad \sum_j x_{ij}^k \leq Cap_i \, y_i^k \qquad \forall \, i, k$ (36)

$$\sum_k y_i^k = 1 \qquad \forall\, i \tag{37}$$

$$\sum_{i,k} x_{ij}^k \leq 1 \qquad \forall\, j \tag{38}$$

$$\sum_{i,k} x_{ij}^k\, d_{ij} \leq minDistanceToWalk \qquad \forall\, j \tag{39}$$

$$T_i^k x_{ij}^k \leq \left| \min[(\max(e_i, e_j - PT_{ij}^k + 1) - \min(l_i, l_j)), 0] \right| \quad \forall\, i,\, j,\, k \tag{40}$$

The objective function of the model, Equation (35), tries to minimize the total time for the driver. In parallel, the penalty vector tends to help that minimization goal by forcing the model to activate as many variables as it can. Constraints in Equations (36)-(38) ensure that each vehicle chooses only one path and each passenger is assigned to one vehicle at most. Constraint in Equation (39) defines the minimum distance that each passenger walks to reach the trajectory of the driver. Finally, constraint in Equation (40) is a compact and lightweight formulation of time windows limits that both passenger and driver should satisfy.

Additionally, the penalty vector can be used as a learnable vector, which the service provider could optimize dynamically. For instance, the penalty vector can contain the age, gender, commitment to service, or purpose, so that passengers with the same profile are more likely to match. In case of dynamic requests, the algorithm searches for the vehicles with available seats and assign them into the most suitable vehicles, according to similar criteria used in the matching MIP. Lastly, those passengers who are assigned to those routes create a shared taxi trip. The same algorithm is also used for the case of taxi shared trips. Especially some of the passengers are considered as drivers (when the trip starts) and the rest of the process remains the same.

## 5.4.6. Algorithms for planning and operations of bike-sharing service

During the last decades, most city authorities started to adopt policies that encourage citizens –especially in urban areas– to shift a significant proportion of their trips into more sustainable and green transit modes. The bicycles are one of the most comfort modes that anyone could use for small trips (up to 6km) in urban environments. In parallel, sharing economy trends start to leverage the rapid growth of bike road networks. Moreover, long and more dynamic tourist periods, seasonality trends, and similar patterns, lead some people to avoid investments in private vehicles. Therefore, the sharing economy and, especially, bike-sharing, stands as an excellent transit alternative. Among the advantages of the service, the affordability of trips, zero carbon footprint, healthy lifestyle, and congestion reduction are the most important. However, the planning, facility location and resource estimation of such a system it is not a trivial problem. Firstly, the planner must decide if the service will be using docks or not. A free-floating service is more convenient for users, but it is more difficult to redistribute the bikes to be available for the future users. On the other hand, a system with docks must be sufficiently dense so every user can have easy access to the system. Additionally, dock-based systems are easier to manage in term of demand prediction, redistribution, and monitoring.

In general, the bike-sharing systems can be summarized (Figure 33) in three major categories:

- **Dock-based system:** In that category, all trips must start and end in one of the available docks. Thus, each user needs to walk up to the nearest dock. Additionally, each customer needs to walk to the destination

after dropping the bike into the nearest node. The dock based system is useful to predict demand and flows in the network more accurately. Moreover, it is easier to design rebalancing strategies.

- **Free-floating system:** In that case, no docks are included in the service network. In fact, usually the passenger can track the nearest bike via a smartphone app. Moreover, there are no restrictions on where the drop-off location of the bike could be, so it can go up to the destination point. However, most of these services have a restricted area in which the bike trip can take place. The demand forecasting and rebalancing operations are more difficult due to continuous search space.
- **Hybrid:** In reality, dock less system is impractical. The most common operation model is a mixture of dockless and dock-based. In practice, most systems are dock-based, but the user has the option to drop the bike wherever it is convenient. In parallel, that schema uses pricing policies to encourage customers to make use of docks.

In summary, the system design procedure involves both operational and planning decisions. The operational decision is related with category and pricing policy preferences. The planning decisions deal with the location of the docks, the capacity of each one and the size of available vehicles in the system. Then, the design process must provide guidelines about the redistribution strategy, for example when the operator must perform redistribution and the according routing methods. Lastly, system design requires data analysis that reveals the most suitable area for that service considering factors, such as the available bike network, origin-destination data analysis, weather, and topological conditions.
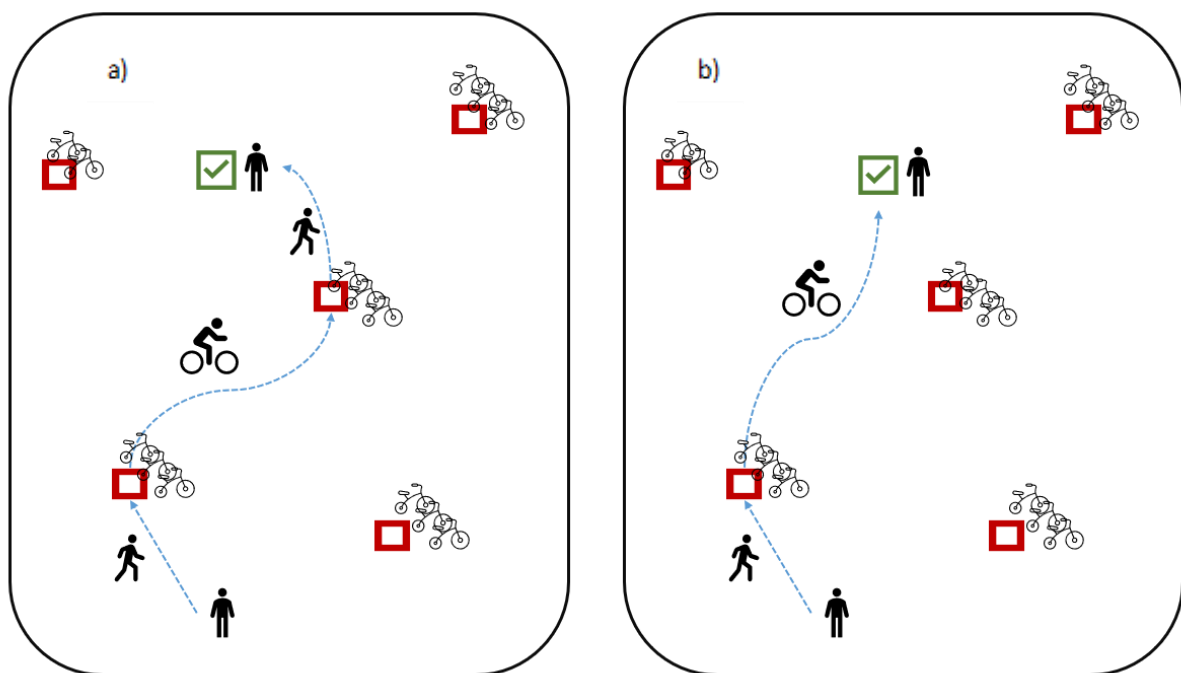


*Figure 33. a) Fully dock-based system, b) Hybrid system*

### 5.4.6.1. Planning

The planning process is similar to the one described in previous sections. At first, the objective of the system must be defined. In that case, the systems costs can be split into two sets: 1) Passengers 2) Operations. The passengers' costs involve access time, trip duration and waiting time. However, in case of hybrid model the waiting time can be eliminated as the customer has the choice to drop the bike outside the dock.

The objective function in Annex A3A4 contains   both the user costs and system management costs. Thus, that function is used to define the optimal design. Additionally, the planning stage should involve decisions on the actual location of the stations and the capacity of each one. Lastly, during experiments the rebalancing strategy varies in terms of interarrival time or inventory control parameters.

At first, the process described in Figure 29 is used similarly to the DRT case, to define the candidate docks. However, the final set up depends on some service level parameters. . In fact, most literature studies propose some facility location models (in which they try to select the optimal subset of station candidates) with respect to specific service level constraints (Nikiforiadis, 2021; Junming, 2015). More precisely, those models also involve sets of decision variables related to demand coverage, area coverage and unbalanced stations (Frade, 2015). Consequently, in BS planning the goal is to find the optimal value of those decision variables that optimizes the overall performance of the system. After that, the methodology and workflow of Figure 30 is used to define a better location candidate for the next round of experiments until the optimal design found. Finally, simulation experiments are repeated for both dock-less and hybrid systems to distinguish which is more suitable for the target area.

### 5.4.6.2. Operational

The operational scale of BS is closely related with the pick-up and delivery vehicle route problem (PDVRP). In fact, during the day, the system is usually unbalanced, as some docks have shortage of bikes, while others have surplus. Thus, the operator must choose the optimal sequence, wherein drivers should follow and perform the pick-up and delivery actions, to bring docks into a balanced state (Dell'Amico, 2014). The surplus or shortage classification of each dock is based on the demand prediction (Xiao, 2020), optimal inventory estimation (Raviv, 2013) and remain inventory monitoring. In case of static rebalancing, those tasks are computed separately. However, dynamic models can relate those problems with time dimension. More precisely, dynamic-PDVRP uses the state-action-reward formulation of RL-MDP. For instance, the inventory of each stop, the vehicle location and capacity, and the historical demand could represent the state of the system, while the action produces the vehicle's next location to be visited and the size of items to pick-up or deliver. Additionally, the reward can depict the waiting time of customers, the total revenue, and the operational expenses for rebalancing routing.
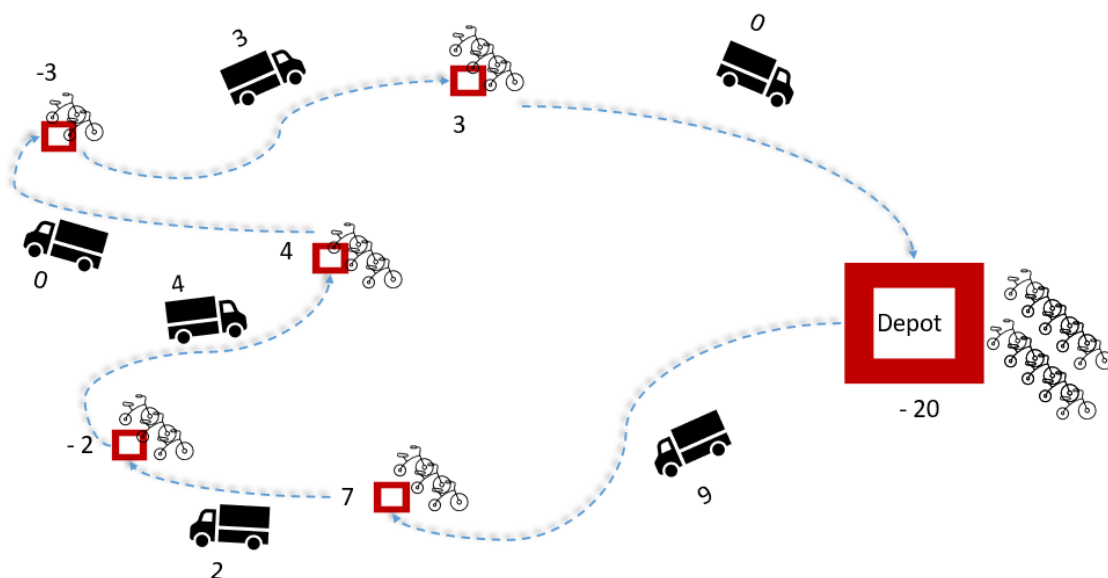


*Figure 34. Rebalancing without subtour*
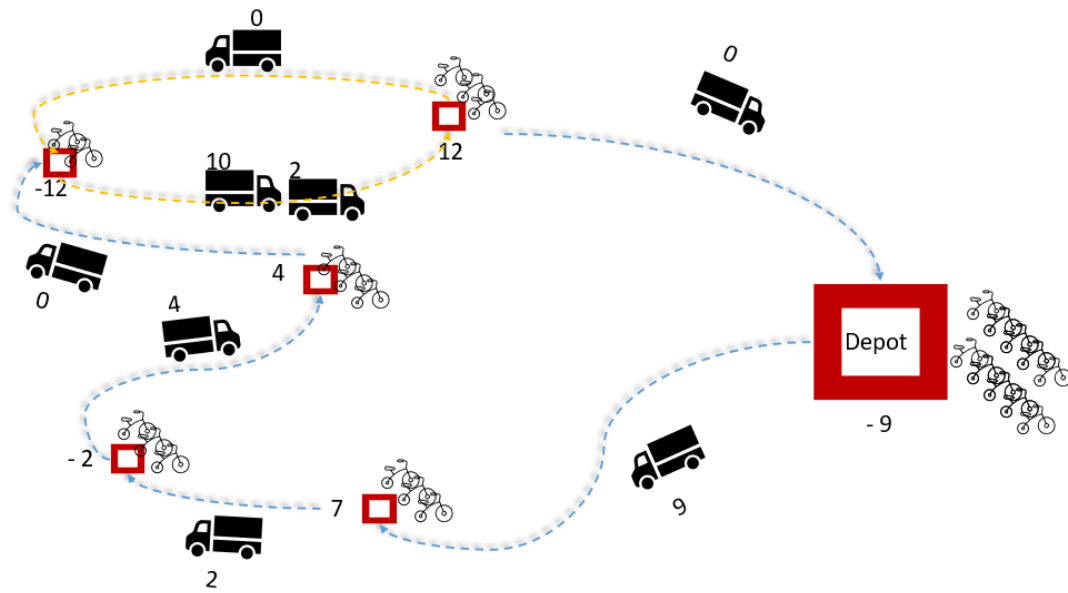
*Figure 35. Rebalancing with subtour*

Moreover, the vehicle used for redistribution is subject to capacity constraints which necessitates the use of subtours in order to efficiently cover a station demand that exceeds capacity. For instance, in the example of Figure 34 the demand in every station is not higher than the vehicle capacity so it needs to visit each station only once. On the other hand, in the example of Figure 35**,** there is a station in which the demand exceeds the vehicle's capacity and therefore a subtour is necessary. Thus, the subtour elimination constraints of Model 1, Equation (32), must be replaced to allow the correct amount of subtours. Additionally, the constraints which allow only one time visit on each station, must also change to follow the sub-tour paradigm. Lastly, the new model must be able to handle even unbalanced demands, meaning that the surplus could be greater than the shortage and vice versa.

Nevertheless, the classical MIP approaches usually struggle to achieve computationally efficient solutions. Hence, the exact PDVRP with medium size problems use cutting plane techniques mostly for the subtour elimination and connectivity constraints. However, larger instances could be solved via 2 stage process of assigning pick-up as origin points and drop-off locations as the destinations, and then using classical VRP formulation, which are easier to compute the final path. Therefore, the ridesharing assignment program without the time-windows and maximum distance constraints, produces the origin-destination pairs that will be used subsequently in the VRP algorithm to generate the final PD route.

According to those new real-life needs, the formulation considers the following decision variable:

$$x_{ij} = \begin{cases} \in \mathbb{Z}^+, \text{if vehicle goes from } i \text{ to } j \\ 0, else \end{cases} \tag{41}$$

The constraints in Equations (26) – (29) of Model 1 are replaced with constraints in Equation (42), which allows more than one visit in each station. Additionally, constraints in Equation (30) remain the same, while Equation (32) is eliminated and Equation (31) is replaced by Equation (43). Finally, constraints in Equation (46) are the new constraints for subtour elimination according to existing subtour needs and Equations (44)-(45) assure that the demand will be served.

$$\sum_{i \in V} x_{ij} = \sum_{i \in V} x_{ji} \,, \; \forall \, j \, \in V \tag{42}$$

$$0 \leq f_{ij} \; \leq \; Q * x_{ij} \,, \forall \, (i,j) \in A \tag{43}$$

$$\sum_{j \in V} f_{ij} - \sum_{j \in V} f_{ji} = -q_i \;\;, \; \forall \, j \in V^+ \tag{44}$$

$$\sum_{j \in V} f_{ij} - \sum_{j \in V} f_{ji} \leq -q_i \;\;, \; \forall \, j \in V^- \tag{45}$$

$$x(\delta^-(S)) \; \leq \; r(S), \forall \, S \subseteq V \tag{46}$$

The case, of the free-floating unbalanced system handled in a similar way. In particular, the dock-less bikes clustered into small groups and treated as they are virtually in stations. Hence, the rebalancing techniques remain the same as the fully dock-based system.

## 5.4.7. Car-sharing

The car-sharing (CS) services fall into the same category as BS services in terms of resource sharing, relocation management strategies, and station versus free-floating dilemmas. Namely, sharing transport modes is the major category while bikes, cars, or scooters can be the mode alternatives. However, CS systems have some practical limitations compared to BS systems that mostly depends on the cost of the resources (bikes, cars, scooters), on the environmental impact, relocation easiness, and parking/station locations availability. In contrast, the road networks are much larger than bike networks, so that they can cover large distance trips more effectively, while micro mobility services are restricted to urban areas, where the network infrastructure allows operations. The Table 17 summarizes the advantages and disadvantages of each mode, which are closely related to the costs of each system.

|  | Bike-sharing | Car-sharing |
|---|---|---|
| Advantages | Low cost of bikes and depreciation costs<br>Easier rebalancing<br>Minimum stations and parking requirements<br>Environmentally friendly<br>Fewer labour costs for rebalancing<br>Cost effective for users<br>Minimum maintenance costs<br>Healthy habit | Large operational area<br>Environmentally friendly (EVs)<br>Do not depend on weather conditions<br>Efficient for non-flat cities<br>Every modern city has an extensive road network<br>Convenient and restful |
| Disadvantages | Short trip range<br>Most cities do not have the appropriate bike network<br>Requires good weather conditions<br>Hard to use in cities that are not flat | High depreciation, purchase, and maintenance costs<br>A lot of parking requirements<br>Expensive rebalancing/relocation operations |

Table 17. Comparison of Bike-sharing and Car-sharing

Based on those special issues, the CS system with the objective function in Annex A5 needs some additional terms. In particular, the objective must also contain the depreciation, purchase and maintenance costs of shared cars,

which are important. Moreover, considering the high cost of fleet relocation, there will be a set of experiments that test the case of system without rebalancing. Lastly, the rest of the process remains the same while free-floating/dock-based and fleet size are still decisions need to be made.

The operational plan does not differ a lot from the one for BS. In fact, there are some practical differences. For instance, there is no vehicle that can load the cars, instead the system can have a car that relocates the staff that perform the relocation. Therefore, at each step the maximum capacity of car transactions is one vehicle per move. Thus, the system has two parallel routing processes, the one that carries the rebalance drivers to car and the one that performs the actual relocation of the fleet. To conclude, the whole operation is relevant to BS but the time between relocation and the relocation process itself remains an open issue, which needs to be determined via the simulation.

### 5.4.8. Micro-mobility (Scooter sharing)

The last part refers to scooter sharing systems, which during last decades have faced a lot of popularity as an urban mobility alternative. However, the methods for planning and operational design are similar to the bike-sharing system ones. Especially, the scooter sharing system usually operates only in free floating mode. Hence, the planning module must decide only the fleet size and the service area. Table 18 presents some of those properties along with some constraints the scooter sharing systems have.

| | Advantages | Disadvantages |
|---|---|---|
| Scooter sharing | Low cost of scooters and depreciation costs<br>Minimum stations and parking requirements<br>Environmentally friendly<br>Cost effective for users<br>Minimum maintenance cost<br>Do not require dock fees<br>Do not require bodywork | Restricted in urban areas<br>Free-floating system requires a lot of effort in rebalancing/relocation<br>Depends on weather conditions<br>Efficient for non-flat cities<br>Charging requirements<br>Safety issues. |

*Table 18. Scooter sharing system advantages and disadvantage*

Lastly, one major difference, compared to dock-based bike system, is that scooter sharing relies on the prediction and redistribution modules of the operational system. To handle this task, the algorithm uses a pre-process step that defines zones of scooters. These zones are based on density criteria across the spatial and temporal features of the scooter trips. The rebalancing algorithm uses them to perform the calculations. However, the algorithm must also contain pick-up and delivery delay as the station is a large area and so the process need some time to perform the actions. In summary, scooter sharing, and bike-sharing are roughly similar, although some practical changes need to be implemented, to make the models more realistic.

**Deliverable 4.1**

New transport modelling approaches
for emerging mobility solutions

Page **94** of **137**

Copyright © 2021 by MOMENTUM

Version: Issue 1 Draft 2

# 6. Supply

This section consists of models related to traffic assignment and car-ownership. Usually, a static assignment model is employed within the traditional 4-step approach. To build over this model, an improved static assignment method has been developed. Subsequently, a dynamic assignment approach is also elucidated, which offers the flexibility to model the new mobility services at a strategic level and at the same time enables more detailed evaluation on specific study areas at a disaggregate level. With regards to car-ownership, there is a growing concern for private car ownership and use, and hence, a module for it is added. Both a simple aggregate and a complex disaggregate models are proposed. Depending on the data availability and the requirements, one could choose a model between the two.

## 6.1. Traffic assignment

### 6.1.1. Assignment methods for urban environments

#### 6.1.1.1. Motivation and objective

For many years, traffic network models have been used to aid in the planning of large-scale infrastructure projects. Typically, the network models for macroscopic analysis are focused on the main roads used by traffic. Recent developments and the continuous evolution in our transport system intervene at a much lower network level. The introduction of shared mobility and Mobility As A Service (MaaS) systems requires the adaptation of the traditional transport planning tools to this new context. MaaS systems provide a door-to-door solution for urban trips and, as a result, this requires the full network to be considered in urban analyses. On top of this, there is an evolution towards a mixture of modes on local roads. Urban infrastructure is redesigned to accommodate slow modes, public transport, traditional cars, and logistic services. Urban planners are required to forecast what the impact will be of introducing such systems. They need to answer questions about shifting mobility patterns and future usage of road infrastructure.

In most existing traffic assignment models, centroids and connectors are used to distribute traffic over the network. For each zone that generates and attracts demand, a centroid is considered as a hypothetical point that acts as a source/sink of traffic for that zone. Next, connectors are used to connect each centroid to the actual roads in the network.

It is well known that there are two main sources of errors that are introduced by considering centroids and connectors (Manout et al., 2020; Jafari et al., 2015). Firstly, intrazonal traffic on local roads is completely missing. Intrazonal traffic starts to become more important if large zones are considered. Many trips remain local and consider only a short route through the network. If this trip is completely within a zone, it is considered an intrazonal trip and it cannot simply be modelled by assignment models with centroids and connectors. Secondly, the positioning of connectors leads to unrealistic route choice near its attachment points. If connectors are attached too far away from the centroid, local roads are hardly used because traffic will leave the network too soon. Attaching connectors close to the centroid on the other hand will overload local roads. On top of this, the attachment problem must be reconsidered each time a zone is changed or when the demand pattern evolves. These sources of error make it hard to use traffic counts on local roads efficiently in the calibration process, and can introduce errors due to overfitting.

Decreasing the size of zones to address the above problems introduces additional problems related to computational burden and memory efficiency, as the number of routes increases quadratically with the number of zones. In this work, we develop a traffic assignment method in which all roads act as a potential origin or destination by users, without overloading the computational burden of the assignment problem.

*6.1.1.2. Methodology*

To avoid the problems related to the discrete nature of connectors, we suggest refraining from the use of connectors, but instead treat every link within a zone as an origin and destination. However, applying this strategy naively can render the assignment infeasible, as the number of routes increases quadratically with the number of zones.

We suggest applying an implicit routing algorithm within a stochastic assignment framework to substantially decrease the computational effort. In the following sections we specify the details of this approach.

### 6.1.1.2.1.    Destination-based implicit routing

Many user equilibrium solvers require the storage of every used path in the network. It is known that most of these paths share multiple segments or sub-routes (Bar-Gera, 2010). Therefore, similar sub-route switches are made by users of different OD-pairs and even multiple OD-pairs reach an equilibrium state over a mutual sub-route set. The destination-based (DB) approach exploits this and efficiently manipulates/stores route flows in an implicit fashion (Ziliaskopoulos et al., 2004). Here, it is assumed that traffic from any origin towards the same destination behaves identically once merged at a specific node.

The implicit routing data structure is composed of link-destination specific proportions $\phi_{ad}$, which form the splitting rates at each node of the node set $n \in N$, for its corresponding outgoing links $a \in FS_n$ (forward star). These proportions guide the traffic at node $n$ into each of the outgoing links of that node towards their respective destination. By definition $\sum_{a \in FS_n} \phi_{ad} = 1$ must hold for each node in the network. In Figure 36b, link-destination proportions are given for every link in the network formed by the directed graph G$(N, A)$ of Figure 36a. In a network with more than one destination, such a split proportion map must be constructed for each destination.

Reconstructing the possible paths in Figure 36b, an infinite cyclic path is formed by consecutively visiting link $a_3$ or link $a_4$. This path cannot easily be excluded from the path set, herewith allowing some vehicles to run around that circle and to accumulate. Therefore, techniques to avoid cyclic flows will need to be applied. The solution stems from Bar-Gera (2002), Dial (2006), and Gentile (2014a). In that case, the problem has been solved by considering only acyclic bushes as valid data structures for implicitly storing destination-based routing information. A split rate graph is an acyclic bush if the set of edges with strictly positive split rates form a (reverse spanning) bush rooted at the destination for which no sequence of edges loops back onto itself. The graph of link proportions in Figure 36b can be transformed into an acyclic bush by setting $\phi_{a_3d}$ or $\phi_{a_4d}$ to zero and removing that edge from the graph. Note that, in this case, only a subset of three of the four non-cyclic paths in the network is feasible in the data structure.
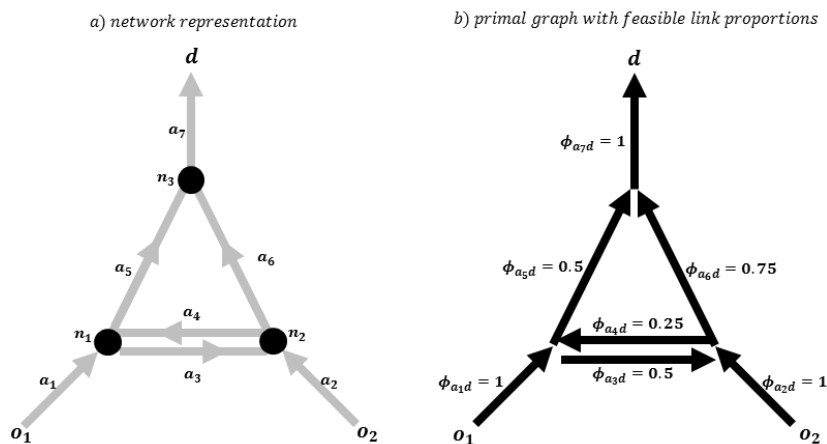


*Figure 36. Simple single destination network (a) with the primal link-node splitting rate map (b)*

### 6.1.1.2.2. Stochastic assignment

The destination-based implicit routing algorithm above is combined with a stochastic assignment approach. We choose a stochastic instead of a deterministic assignment because this can result in a more realistic distribution of traffic over the network.

In the stochastic route choice model of (Bellei et al., 2005) the proportions $\phi_{ad}$ represent the probability of choosing link $a$ conditional on being at node $n$ when traveling to destination $d$. Cyclic routes are avoided by only considering links with end nodes being closer to the destination than the current node. This is referred to as exploiting the topological order in the graph (like in Dial's algorithm proposed in Dial and Voorhees (1971)).

The destination-based link probabilities are computed in two phases. First node and link weights are computed. This is done in an upstream way starting at the destination, visiting nodes in ascending order according to distance towards the destination. The node weight $w(n)$ of the destination is initialized as 1. The other node weights are computed by summing the link weights $a(l)$ of all links in the forward star that are closer to the destination:

$$w(n) = \sum_{l \in FS_n} a(l)$$

*(47)*

Link weights are computed based on the downstream node weight and the travel time $tt_l$ on the link:

$$a(l) = w(n) \cdot \exp\left(-\theta \cdot tt_l\right)$$

*(48)*

with $n$ being the downstream node of $l$ and $\theta$ being the scaling parameter of the logit formula.

Pseudo code for computing node and link weights:

```
For (all sorted nodes in shortest path three)
    For (all links in the backward star of the selected node)
        update link weight
        add link weight to upstream node weight
```

Next, destination-based link probabilities are found for every node in the network by relating the node weights to link weights of the forward star. As such flows can be easily propagated through the network by initializing demand on origin links and propagating it downstream according to descending node distance towards the destination:

```
For (all sorted nodes in shortest path three in reverse order)
    For (all links in the forward star of the selected node)
        update link flows
        add link flows to downstream node flow
```

### 6.1.1.2.3.   Access points

The algorithm above propagates the flows on each link, and this for each destination. It can easily be extended to a network where every link is a potential source of traffic because most links are already covered when propagating the demand over the network. Therefore, the computational effort does not substantially increase.

The fact that every link is a potential destination is harder to deal with, as the algorithm needs to propagate traffic for each destination separately. Increasing the number of destinations therefore increases the number computational effort proportionally.

To avoid this, we propose the concept of access points. These access points are hypothetical connections at the boundary of each zone (see Figure 37). The number of access points of a zone is typically substantially lower than the number of links within a zone.
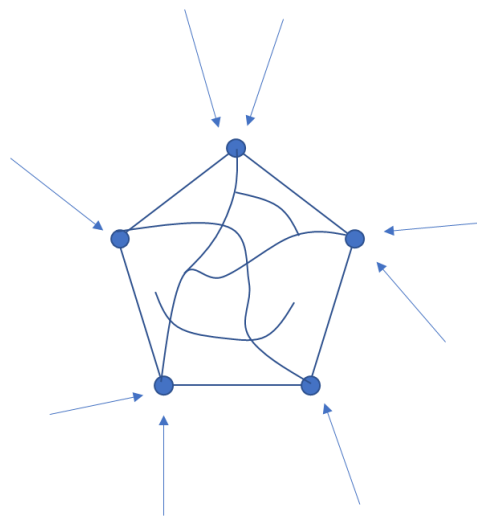
*Figure 37. Access points towards a zone*

These access points will determine the attraction towards that zone and are used to initialize the shortest path search upstream from that zone. In a final step, the flows arriving at the access points are propagated to each of the destination links:

**For** (each destination layer)
   Find access points to the destination zone
   Calculate shortest path tree initialized with access points weights
   Compute node and link weights
   Initialize node and link flows in each origin zone
   Propagate flows towards the access points
   Distribute flows from access points to links within the destination zone

The access points of a zone can be determined exhaustively, but they can also be determined based on available data (e.g., Floating Car Data) or based on the network hierarchy.

The model can be calibrated by setting the initial cost of the access points. For each access point we initialize this value to the average distance towards each link within the zone. Alternative approaches are also possible, for example, based on available data.

### 6.1.1.3. Proof of concept

We apply the methodology above on the Leuven network. Figure 38 shows a comparison between the traditional connector-based approach and the access-points method. As discussed before, all links in the origin zone are potential sources of traffic that produce trips and all links in the destination zone are considered sinks that attract trips. In the connector-based approach a single connector per zone is used. The differences between both approaches can of course be minimized if every node within the zone is connected to the centroid by a connector.
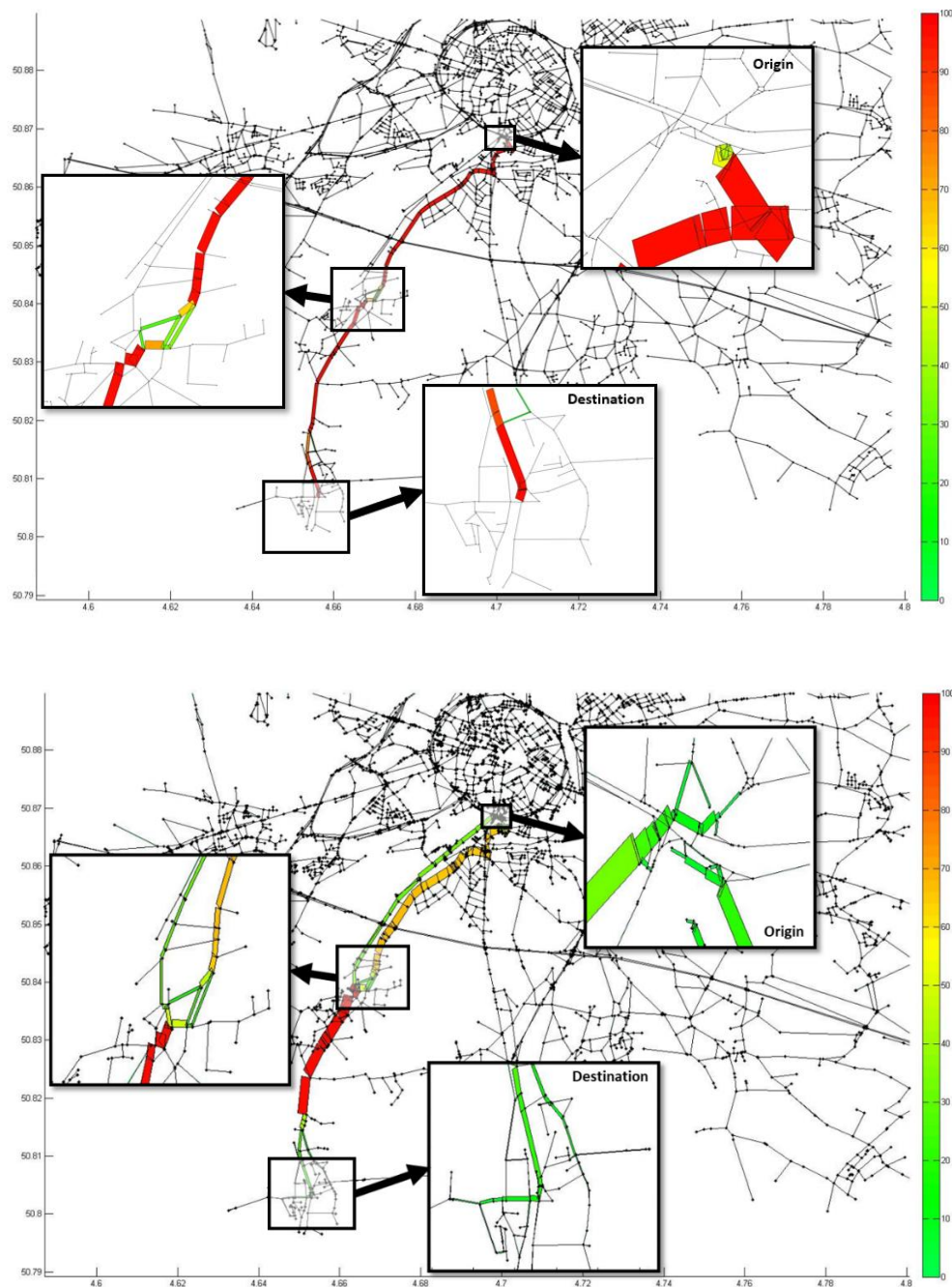


*Figure 38. Distribution of traffic expressed in percentage of the total volume between a selected origin and destination in Leuven area. Top graph: traditional assignment. Bottom graph: assignment with access points*

The difference between both methods is clearly visible when zooming in on the origin and destination zone. Traffic distributes more evenly within a zone in the suggested approach.

Furthermore, the example illustrates that the effect is not limited to the distribution of traffic within the zone; by considering multiple access points, different approach routes towards the zone are taken into account. This can have an important effect on the calibration and the resulting validity of the traffic model on major roads.

### 6.1.1.4. Application within MOMENTUM

The traffic assignment model will be demonstrated in the case study of Leuven, as in this case study the traffic flows on a substantial part of the network are monitored, particularly on local roads. This makes it possible to calibrate the traffic model more accurately, specifically on the local roads.

## 6.1.2.  Dynamic traffic assignment

### 6.1.2.1. Motivation and objective

This section introduces the hybrid Dynamic Traffic Assignment (DTA). The model is developed within the MOMENTUM project and has been implemented as part of the traffic simulation software, Aimsun Next (Aimsun, 2021).

Traditional strategic models are widely used by transport planners to support decision makers regarding investments in infrastructure and transport services. Traffic assignment is one of the key components of strategic transport models, which maps traffic demand to traffic network supply, by simulating route choices and network conditions, resulting in traffic flows, congestion, travel times, and emissions. Nevertheless, these models are not capable of modelling the transport supply and traffic behaviour in detail, often generating problematic and unrealistic traffic conditions and travel times. Therefore, they may not be the most suitable tool for decision making in some transport planning applications such as the modelling and assessment of new mobility services. Such services (e.g., car-sharing, on-demand ride services, etc.) are more complex in the sense that they would require running the model at the individual, agent-based, level in order to support the policymakers in their decision-making process for introducing any mobility policy.

Moreover, the modelling of shared mobility services involves, besides the assignment of the trips into the network, algorithms for planning and allocation of the fleet of vehicles to serve the demand requests. Optimisation of these operations requires accurate information with respect to the network traffic conditions, such as travel times. Hence, for a realistic modelling of the shared service operations it may be necessary to iterate between the DTA and fleet management and/or mode choice models. In particular, the optimisation of the planning and operations of the fleet to serve the demand requests depends highly on the updated travel times obtained from the traffic assignment. Furthermore, a significant increase in demand for new services may result in variations of travel times that can, in turn, affect the modal split.

To address these issues and needs within MOMENTUM, a hybrid DTA modelling framework is developed in which the route choice set is determined by dynamic path assignment for the whole large-scale network, while traffic supply is simulated with dynamic mesoscopic model in specific area of interest and the static macroscopic model in the remainder network. The developed framework is beneficial for the large-scale networks used in strategic transport planning where infrastructure changes or new mobility services require realistic knowledge of traffic conditions and travel times but may have a wider influence in terms of rerouting in the network. The use of the static macroscopic model outside of the areas where mesoscopic is strictly needed for realistic estimation of traffic conditions allows the transport modeller to increase the network size in the model without impacting too heavily on the runtime. Hence, an important contribution of the hybrid model is the improved run times when simulation of large-scale networks is needed, however, the analysis focuses on a smaller study area.

*6.1.2.2. Methodology*

This section provides a description of the proposed hybrid DTA modelling framework with dynamic path assignment and hybrid network loading, namely a combination of static macroscopic and dynamic mesoscopic network loading, for large scale strategic transport models.

The first subsection briefly presents the scope of traffic simulation software Aimsun Next, where the proposed framework on DTA is implemented. The second and third subsections describe the network loading and the path assignment models.

### 6.1.2.2.1.   Aimsun Next

Aimsun Next is a traffic simulation software that integrates a set of demand and supply models, using a single, unified transport network infrastructure representation for simulation and assignment of all transport modes, such as car, public transport, bike, and pedestrian mode. The main advantage of an integrated modelling platform, like Aimsun Next, is that information used by models can be seamlessly and conveniently shared across different modelling granularity levels.

The scope of the hybrid DTA modelling framework proposed in this chapter is to adopt an innovative approach which combines a static macroscopic and mesoscopic network loading with path assignment in a single network model. In Figure 39, the area to be simulated with mesoscopic network loading is defined by a polygon which is then converted to a simulation area. The area outside of the polygon is simulated at the same time, however, with static macroscopic network loading in which travel time depends on a function (e.g., volume delay functions), instead of depending on behavioural models (e.g., car-following).



*Figure 39. Example of macroscopic and mesoscopic simulation areas*

Individual vehicles are generated and assigned on the transport network, instead of path flows traditionally used in strategic transport models. Individual vehicles are assigned to a path using either a stochastic (Stochastic User

Equilibrium, SUE) route choice path-assignment algorithm or a dynamic user equilibrium (DUE) path-assignment. The path choice set generation considers all the links in the transport network. Figure 40 depicts the interaction scheme between network loading and path assignment, as part of the hybrid DTA framework. The network loading in the macro and meso areas, as well as the path assignment, are described in the following subsections.
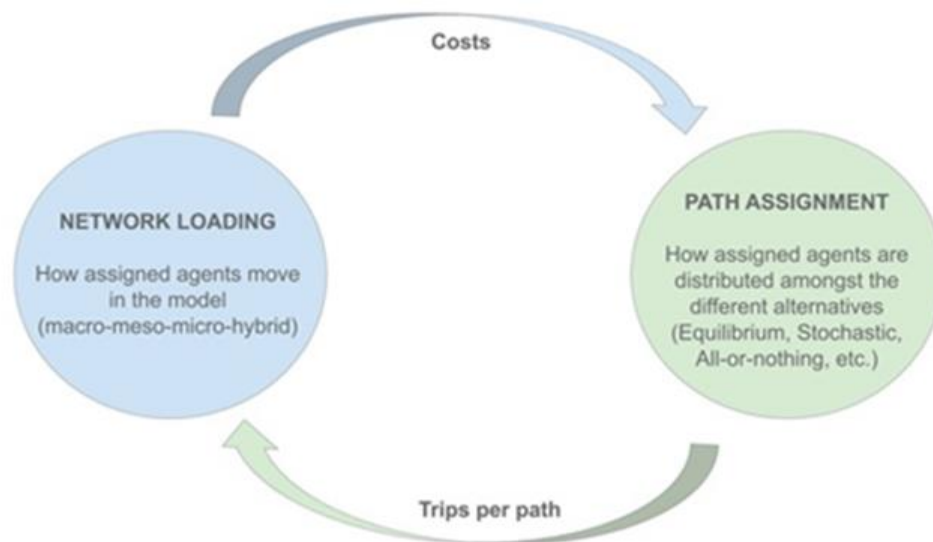


*Figure 40. Interaction between network loading and path assignment*

### 6.1.2.2.2. Network loading: hybrid static macroscopic and dynamic mesoscopic solution

Network loading describes how a vehicle moves in each element of a network (sections, turn, nodes). Consequently, it determines how travel time is calculated and therefore it has a direct impact on the costs obtained.

**Network loading with hybrid static macroscopic and dynamic mesoscopic solution consist of three main functionalities/steps:**

**Function 1: Individual vehicle generation**

Instead of traffic flow, individual vehicles are generated at intervals according to a constant distribution at their origin centroid.

The generation of individual vehicles enables the following functionalities:

- Individual tracking of vehicles/trips
- Realistic congestion in the meso boundaries
- Consider time dependent generation of traffic following traffic demand profile
- Dynamic path calculations in the macro area

**Function 2: Static macroscopic network loading**

In the macro area, vehicles are treated as individual vehicles rather than using a flow as in traditional strategic transport modelling. The differences compared to meso areas are that individual lanes are not considered, and travel time is the same for all vehicles passing through a section or turn during the same time period. Vehicles which begin their trip within the macro network, before being generated, they are assigned a path from the path assignment calculation. They are then generated either instantaneously or with a delay onto the first section with

the meso area following the generated path. The delay on vehicle generation can be specified using either a volume delay cost function or a pre-selected cost-function component. The travel time and cost are retained by the vehicle for the macro sections defined by the volume delay functions (VDFs), turn penalty functions (TPFs) and junction delay functions (JDFs). A virtual queue is generated at the boundary, where a turn goes from a macro section to a meso section. In this type of turn, a vertical queue is created where vehicles coming from the macro area wait to enter the meso area as soon as possible. The delay incurred in the virtual queue is considered in the next meso link.

As explained above, vehicles are generated individually at the centroid level, however, the model aggregates the number of trips for each path and assigns flows of vehicles to each section and turn of the macro area. The value of the flows assigned depends on the changes in the time-dependent demand as well as changes in routing at every route choice cycle, due to congestion in specific paths at a given time interval. Hence, the sections and turns of the macro area have time-dependent outputs, namely, dynamic flows as well as dynamic costs for each route-choice interval.

**Function 3: Mesoscopic network loading**

In the meso area, vehicles move as individual vehicles and the average experienced travel time within a section and turn is reported. Hence, the meso area needs to have detailed representation of the network geometry. In contrast to the macro areas, the travel time is different for each vehicle and is obtained by applying the mesoscopic behavioural models (a simplified car-following model and the gap acceptance model).

For vehicles which begin their trip within the meso network, they are generated within the network and start their trip along the path defined by the path assignment process. The number of vehicles generated depends on the input OD matrix and the time between two generated vehicles is determined by the arrivals model. When a vehicle exits the meso area, it is assigned to all downstream macro sections taking into consideration the following two cases:

1. The vehicle completes its path in the macro area.
2. The vehicle leaves the macro area and re-enters a meso area.

In the second case, where the vehicle re-enters a meso area, the vehicle enters through the virtual turn, being the boundary between macro and meso areas. The travel time when moving from meso to meso through a macro area cannot be instantaneous but it is evaluated using the macro functions or function components.

### 6.1.2.2.3.    The hybrid path assignment

The path assignment computes a set of candidate paths for each origin and destination and assigns a number of trips to each path based on the generalised cost and traffic assignment algorithm. For instance, a DUE assignment algorithm can be used. This is an iterative procedure aiming to minimise, for each OD pair, the travel costs experienced by vehicles departing at the same time. In other words, no driver can reduce his travel time by switching to another path. The convergence to an equilibrium is measured using the relative gap (RGap), which is the relative difference between the total cost actually experienced and the total cost that would have been experienced if all the vehicles had a travel time equal to that of the current shortest path. Finally, the route choice cycle of the path assignment model can be defined to indicate how frequently the path choice set will be recomputed throughout the simulation period.

### 6.1.2.2.4.    Hybrid macro-meso example

The hybrid DTA framework is illustrated with a simple example on Figure 41 and consists of the following main steps:

1. A vehicle is generated according to the arrivals process at the origin centroid.

2. The simulation considers the next vehicle to enter the network and then calculates a path for the vehicle according to the generalised cost equation.
3. If the start is within the macro area, it is generated either instantaneously or with a delay to the first meso section and the volume on all sections that have been traversed is increased by one.
4. If it is safe to enter the meso section, the vehicle enters and then moves according to mesoscopic network loading.
5. If the destination is in the macro area, once the vehicle traverses all meso sections, the vehicle is instantaneously or with a delay moved to the destination centroid with the volume updated accordingly.

As described above, the final costs for the trip will be the sum of the costs (e.g., travel times) derived by macroscopic and mesoscopic network loading models. Those are derived by the macro cost functions (VDFs, TPFs, JDFs) and the dynamic cost functions (experienced travel time), respectively. DUE evaluates new paths, assigning vehicles to them every route choice cycle (e.g., 15 mins) and iteratively performs equilibrium assignments until the convergence criteria are met.
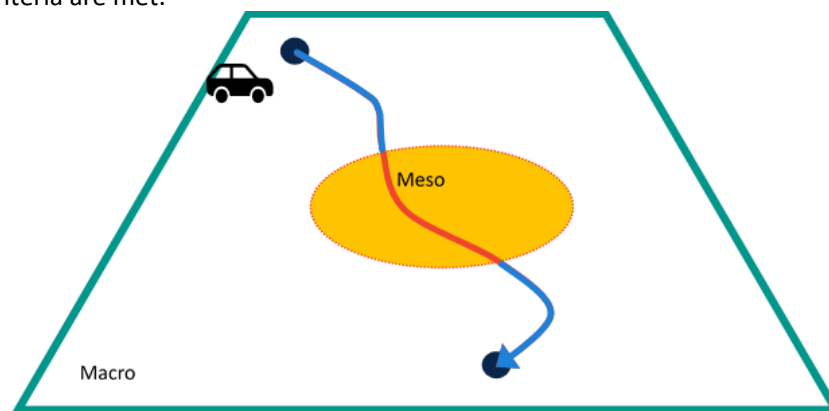


*Figure 41. Hybrid macro-meso approach*

### 6.1.2.3. Application within MOMENTUM

The proposed hybrid DTA framework offers the flexibility to model the new mobility services at a strategic level and at the same time enables more detailed evaluation of their impacts on specific study areas, which can be modelled at a disaggregate level. The area where key strategic decisions will be implemented is modelled as a meso area, while the rest of the urban network will be modelled as macro area to capture the propagation of traffic flow dynamics (delays, queues, etc). ). Nevertheless, the application of the hybrid DTA model within the MOMENTUM project would require modelling and calibration of the area where specific services will be tested and implemented at a mesoscopic level, to accurately capture the real traffic dynamics across those network areas, which need to be modelled with a mesoscopic traffic flow resolution. Calibration and validation of the mesoscopic areas depend on the data availability for each city involved in the project. It is anticipated that the hybrid DTA model will be used for strategic modelling of the new mobility services in the future and therefore would need to integrate with the general scheme for modelling shared mobility services, which is presented in this deliverable.

## 6.2. Car-ownership module

### 6.2.1. Aggregate car-ownership model

#### 6.2.1.1. Motivation and objective

With an increasing interest towards sustainable transport in cities, there is a growing concern for private car ownership and use. Hence, one of the objectives within MOMENTUM is to build a model for estimating car-

ownership. Existing car ownership models from the pertinent literature are usually based on indicators such as vehicle sales. However, to the best of our knowledge, an aggregate car-ownership model suitable for integration with the traditional four-step transport model is still not seen in the pertinent literature. Such a model should be based on the aggregate socio-demographic characteristics of city districts or traffic zones (e.g., population density). Furthermore, given the ability of shared mobility systems to reduce car-ownership, supply of such systems should also be considered. Therefore, within this section, the development of an aggregate car-ownership model based on socio-demographic variables and sharing system supply is presented.

### 6.2.1.2. Data sources used for model estimation

This analysis is based on the data from the statistical yearbooks 2017 and 2018 from the city of Regensburg. The yearbook provides data such as the household characteristics and car-ownership aggregated at the level of the (18) districts of Regensburg city. The data is compiled by Statistics Department from the Office for Urban Development and is available at http://www.statistik.regensburg.de.

### 6.2.1.3. Estimation methodology

The aggregate car-ownership model presented in this section is based on linear regression and two different variants of car-ownership are explored. As shown in Figure 43, initially, a model is estimated with total number of cars as the dependent variable, followed by another model with average number of cars per individual as the dependent variable (which is total number of cars/total population) . The estimation is carried out in R.

Given that the statistical yearbook provides data in the former format, it was naturally the first choice to be considered as the dependent variable. It is to be noted that a major issue with the estimation is the correlation between the independent variables (as shown in Figure 42), which is a common issue when modelling at an aggregate level. Hence, several transformations of and interactions between the variables have been carried out, before arriving at the final best model specification.
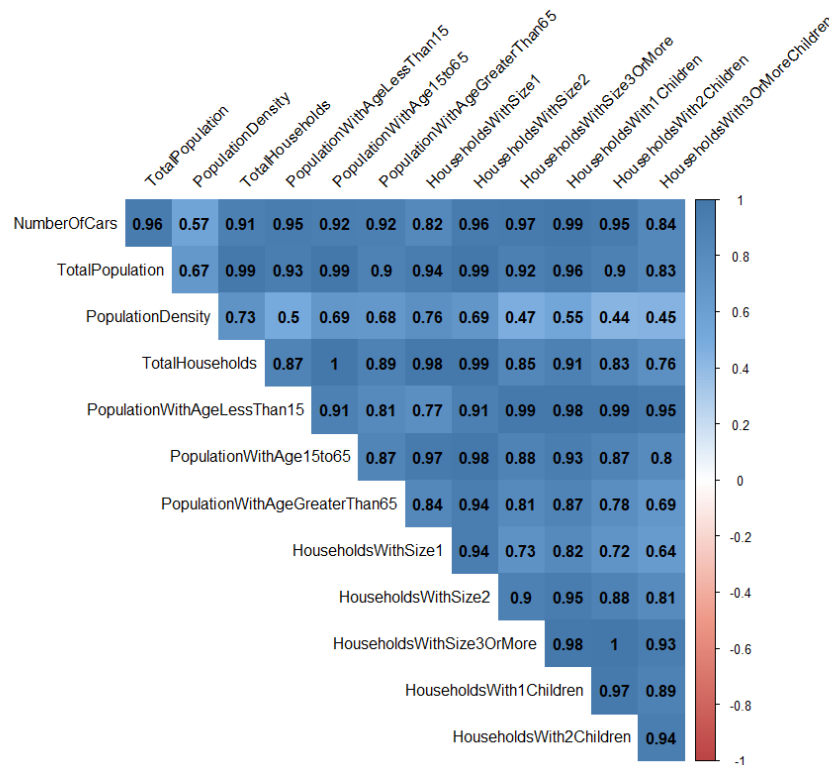


*Figure 42. Aggregate car ownership model – correlation between the variables available for model estimation*

The estimation result showed that the population density is an insignificant factor, which is unforeseen, as it is expected to be a significant factor (i.e., with an increase in population density, total number of cars is expected to decrease). Following this result, k-means clustering is used to cluster the districts according to population density and the algorithm distinguished the districts into three categories, which can be named as low, medium, and high density districts.

Inclusion of the cluster variables in the model showed that the medium density districts have a higher number of cars, when compared to low and high density districts. This is counter-intuitive as low density districts are expected to have a higher number of cars. A deeper look into the data shows that the low density districts are the locations of large commercial areas or weekend spots. Hence, they are mostly destination zones and therefore, low number of cars in such zones, thereby resulting in a positive coefficient for medium density districts. It is to be noted that the higher number of cars in the medium density districts is the reason for the insignificance of the original population density variable (i.e., the relationship is not linear and continuous).

A second model, with average number of cars per individual as the dependent variable, is estimated to further explore the influence of population density. The estimation results show a clear pattern of the influence of population density, i.e., a decrease in average number of cars per individual, with an increase in population density. Thus, different variants of a dependent variable could show different influence of independent variables.

As mentioned in Section 6.2.1.1, shared mobility systems can reduce car-ownership, and hence, their influence has to be considered in the model specification. However, the car-sharing system in Regensburg is still a small service and hence, it is not possible to quantify its impact on car-ownership. Hence, existing pertinent literature is explored, which showed a magnitude of car-ownership reduction of 2-5 per sharing vehicle in European cities (Fromm et al., 2019). Leaving the extreme values, a coefficient of 3 and 4 could be used. To be conservative, a value of 3 is selected for inclusion in the regression model.



*Figure 43. Methodology – Aggregate car ownership model*

### 6.2.1.4. Estimated coefficients and insights

The estimated coefficients for the models (1 & 2) are shown in Table 19. Based on the estimated coefficients, there is an increase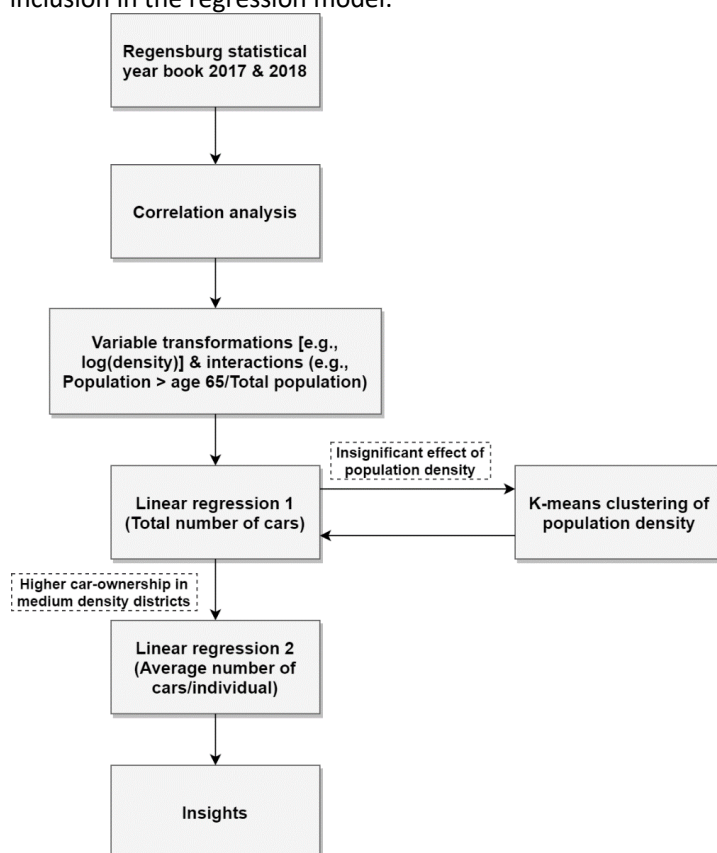 in the total number of cars in a district (or average number of cars per individual in a district, in case of Model 2), when the percentage of households with "size 3 and above" increases. This implies that larger households have a higher number of cars. Similarly, there is an increase in the value of the dependent variable, when the percentage of population with "age 65 and above" increases, suggesting that older people are more probable to own a car. On the one hand, when considering Model 1, the total number of cars is higher in the medium density districts. On the other hand, when considering Model 2, there exists a linear relationship (in log scale) between average number of cars per individual in a district and population density, which is not true in the case of Model 1, as medium density districts are found to have a higher value.

| Model 1 (Total no. of cars in thousands) | | | | Model 2 (Average no. of cars per individual) | | | |
|---|---|---|---|---|---|---|---|
| **Variable** | **Estim.** | **S.E.** | **t-stat** | **Variable** | **Estim.** | **S.E.** | **t-stat** |
| Intercept | -3.94 | 0.55 | -7.17 | Intercept | 0.21 | 0.05 | 4.40 |
| % of households with size ≥ 3 | 0.10 | 0.01 | 7.50 | % (in decimal format) of households with size ≥ 3 | 0.69 | 0.10 | 6.91 |
| % of population with age ≥ 65 | 0.08 | 0.02 | 4.74 | % (in decimal format) of population with age ≥ 65 | 0.81 | 0.12 | 6.96 |
| Medium density districts (dummy) | 0.73 | 0.23 | 3.20 | Population density (log) | -0.03 | 0.01 | -2.96 |
| Population in thousands | 0.42 | 0.01 | 28.62 | | | | |
| Adj. $R^2$: 0.97 | | | | Adj. $R^2$: 0.84 | | | |

*Table 19. Estimation result – Aggregate car ownership model*

The final model specification, along with the addition of coefficient for sharing system supply, is as follows:

$$Total\ no.of\ cars\ in\ thousand\ = -3.94 + 0.10\ (\%\ of\ households\ with\ size \geq 3) + 0.08\ (\%\ of\ population\ with\ age \geq 65) + 0.73\ (Dummy\ for\ medium\ density\ districts) + 0.42\ (population\ in\ thousands) - 0.003\ (number\ of\ sharing\ vehicles$$

(49)

### 6.2.1.5. Application within MOMENTUM

Model 1 will be demonstrated in the case study of Regensburg, as it has a better fit (when compared to Model 2) and the impact of sharing vehicles on car ownership is explored in terms of reduction in total number of cars in the pertinent literature.

## 6.2.2. Disaggregate car-ownership model

### 6.2.2.1. Motivation and objective

Analysing the impacts of sociodemographic and mobility variables on car-ownership can generate relevant results for both the development of public policies and the estimation of transport models. This section presents the main methodology and results of estimation of a disaggregate car-ownership model, developed using a combination of mobility survey data and supply data of car-sharing services.

In the scientific literature, car-ownership has been modelled from many different perspectives such as aggregate time series models, aggregate cohort models, pseudo-panel models, and static disaggregate models (de Jong et al., 2004). The latter group has gained relevance in the past couple of decades, particularly the so-called *unordered-response* models, which have been proved to be more appropriate for modelling car-ownership than the *ordered-choice* models (Bhat and Pulugurta, 1998). The Multinomial Logit Model (MNL) presented in this section belongs to the class of *unordered-response* models, based on random utility theory.

In the existing literature, multinomial logit models for car-ownership modelling have typically been limited to the use of sociodemographic variables such as age, income, occupation, number of household members, etc. The proposed model, however, incorporates the effects of other transport alternatives; for instance, cargo bike (availability) and emerging mobility solutions (both existing car-sharing subscriptions and willingness to use car-sharing in the future). Furthermore, the model integrates the effects of car-sharing supply, by means of the number of car-sharing vehicles in the city districts.

### 6.2.2.2. Data sources used for the model estimation

Two main data sources from the city of Leuven have been employed to develop the model. The Stadsmonitor survey (City Monitor) provided disaggregated sociodemographic information and transport demand data for a sample of 2669 individuals. This survey was carried out in Spring 2017 in the region of Flanders and the dataset contains details such as sociodemographic characteristics and mobility habits. The survey description and dataset are available at https://gemeente-stadsmonitor.vlaanderen.be/.

The second dataset is the car-sharing supply data for the year 2019. This dataset included the number of available car-sharing vehicles in the 8 districts of Leuven. Unfortunately, no district-level data was available for 2017 (the year in which the City Monitor survey was conducted), but only the aggregate number of car-sharing vehicles for the city. Hence, considering the spatial distributions of vehicles in 2019, i.e., the number of car-sharing vehicles per district in relation to the total number of car-sharing vehicles in Leuven, the number of car-sharing vehicles per district in 2017 was estimated.

Both the data sources were combined to assign the car-sharing-supply to the samples in the City Monitor survey. Besides, the City Monitor dataset was analysed and filtered for possible errors (e.g., inconsistencies between variables) and outliers.

### 6.2.2.3. Estimation methodology

The data processing and the model estimation were carried out using *R Statistical software* and the open-access package *Mlogit* (Croissant, 2020). A preliminary analysis of the dataset indicated that the number of households in the dataset with three or more cars was too small to provide statistically relevant results. Consequently, as indicated in Figure 44, the multinomial logit model was developed considering four possible alternatives for every household: no car, one car, two cars, three or more cars.
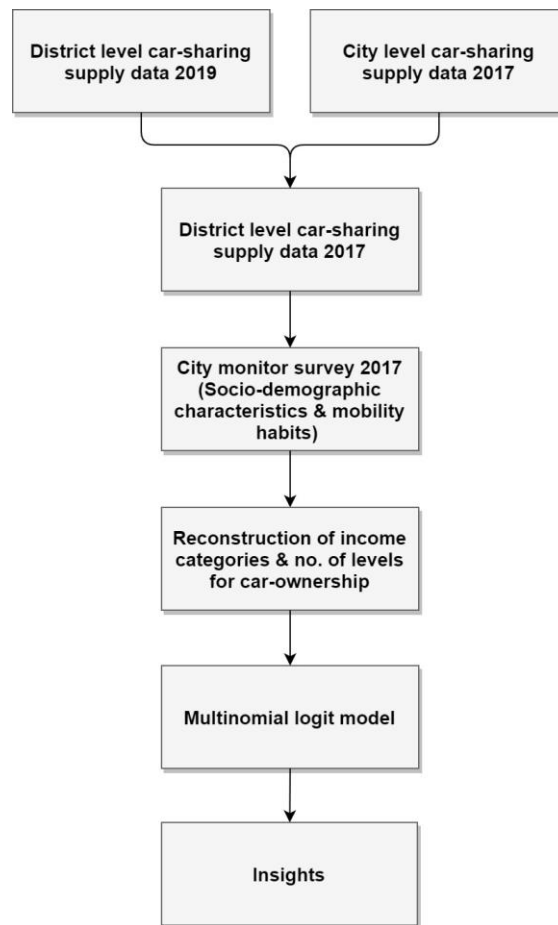
*Figure 44. Methodology – Disaggregate car ownership model*

Household income data was provided in the City Monitor survey by means of an ordinal variable with eleven levels. Considering numerous levels is likely to produce insignificant estimates for the coefficients, especially as some levels have a small number of observations. Therefore, several transformations and aggregations into a reduced number of categories were explored, before arriving at the following final categories: Low Income, <1750 €/month; Medium Income, 1750-3250€; and High Income, >3250€/month. Similarly, transformations were tried out for age. However, inclusion of the variable in the ordinal form with numeric coding from 1 to 8 resulted in better estimation.

Models are developed in a stepwise fashion. The decision to keep an independent variable is based on the p-value of the corresponding coefficient (threshold level of 0.10), the log-likelihood test, and the plausibility of the coefficient sign according to the existing literature.

### 6.2.2.4. Estimated coefficients and insights

The final model specification, which is selected based on the p-value of the independent variables and the likelihood ratio test, is as follows:

$$
\begin{aligned}
No\ car\ (0) &= 0\ (base\ category) \\
One\ car\ (1) &= isBelgian + hasLowIncome + hasMediumIncome + Age3 + Age \\
&\quad + HHSize + hasCargoBike + hasPTPass + isUnwillingToUseCS \\
&\quad + CSSupplySubscriptionInteraction + CommuteSpeed
\end{aligned}
\tag{50}
$$

Version: Issue 1 Draft 2

$$Two\ cars\ (2) = Intercept + isBelgian + hasLowIncome + hasMediumIncome$$
$$+ Age3 + Age + HHSize + hasCargoBike + hasPTPass$$
$$+ isUnwillingToUseCS + CSSupplySubscriptionInteraction + CSSupply$$
$$+ CommuteSpeed$$
$$Three\ or\ more\ cars\ (3)$$
$$= Intercept + isBelgian + hasLowIncome + hasMediumIncome$$
$$+ Age3 + Age + HHSize + hasCargoBike + hasPTPass$$
$$+ isUnwillingToUseCS + CSSupplySubscriptionInteraction + CSSupply$$
$$+ CommuteSpeed$$

The estimation result is shown in Table 20.

| Variable | Estim. | S.E. | z-val | Interpretation |
|---|---|---|---|---|
| isBelgian (1) | 1.88 | 0.28 | 6.78 | Belgian citizens are relatively more likely to own a higher number of cars than non-Belgians. |
| isBelgian (2 & 3) | 2.10 | 0.38 | 5.47 | |
| hasLowIncome (1) | -1.53 | 0.29 | -5.28 | With an increase in income there is a higher, probability to own cars (note: high income is kept as the reference category). |
| hasLowIncome (2 & 3) | -3.60 | 0.45 | -8.01 | |
| hasMediumIncome (1) | -0.70 | 0.28 | -2.51 | |
| hasMediumIncome (2 & 3) | -1.46 | 0.30 | -4.79 | |
| Age (1 & 2) | -0.66 | 0.17 | -4.01 | Age (ordinal variable with levels 1 to 8, as provided by the City Monitor survey) is found to positively influence the car-ownership. However, there exists a polynomial relationship, i.e., a changing slope rather than a constant one (e.g., the differences between older age groups are greater than for middle age groups). |
| Age (3) | -1.18 | 0.35 | -3.38 | |
| Age$^3$ (1 & 2) | 0.02 | 3.64 e-3 | 4.79 | |
| Age$^3$ (3) | 0.03 | 6.28 e-3 | 4.50 | |
| HHSize (1) | 0.50 | 0.09 | 5.55 | Larger households are more likely to have a higher number of cars. |
| HHSize (2) | 0.85 | 0.10 | 8.19 | |
| HHSize (3) | 1.13 | 0.15 | 7.59 | |
| hasCargoBike (1) | -0.72 | 0.40 | -1.78 | The availability of a cargo bike in the household decreases the likelihood of having a car (especially, in the case of two or more cars). This could be due to the distinctive features of cargo bikes, which turn them into effective car-substitutes for activities such as shopping, transport of mid-size/weight cargo, etc. |
| hasCargoBike (2) | -2.19 | 0.48 | -4.52 | |
| hasCargoBike (3) | -3.10 | 1.13 | -2.74 | |
| hasPTPass (1) | -0.85 | 0.22 | -3.88 | Possession of a PT pass negatively influence car-ownership. |
| hasPTPass (2 & 3) | -1.22 | 0.25 | -4.85 | |
| isUnwillingToUseCS (1) | 0.61 | 0.22 | 2.75 | With respect to the attitude of citizens towards car-sharing services, the |
| isUnwillingToUseCS (2) | 1.04 | 0.26 | 4.03 | |

| | | | | |
|---|---|---|---|---|
| isUnwillingToUseCS (3) | 1.38 | 0.45 | 3.10 | unwillingness to use car-sharing in the future, as stated by the survey participants, is shown to be related with higher car-ownership levels. |
| CSSupplySubscription Interaction (1, 2 & 3) | -0.12 | 0.02 | -5.27 | When a car-sharing subscription is available, an increase in car-sharing supply results in lower probability to own cars. Besides the interaction effect, there is generally a decrease in utility to own two or more cars, with an increase in the number of car-sharing vehicles in the district. |
| CSSupply (2) | -0.05 | 0.02 | -2.28 | |
| CSSupply (3) | -0.09 | 0.04 | -1.96 | |
| CommuteSpeed (1) | 0.03 | 0.01 | 4.47 | Higher commuting speeds are found to be associated with higher car-ownership levels. A model with coefficient for travel distance suggested an increase in car-ownership for higher distances. These two indicate that existing alternatives to car-ownership are not competitive enough for longer distances. |
| CommuteSpeed (2 & 3) | 0.04 | 0.01 | 4.70 | |
| Intercept (2) | -1.00 | 0.51 | -1.98 | - |
| Intercept (3) | -2.66 | 1.22 | -2.18 | - |

Log-Likelihood: - 937.65; Note: CS – Car-sharing

*Table 20. Estimation result – Disaggregate car ownership model*

### 6.2.2.5. Application within MOMENTUM

This model can help to understand the factors influencing car-ownership, and consequently, contribute to foster measures that reduce dependency on motorized private vehicles. Furthermore, the model can be integrated into traffic simulation models to account car-ownership levels. In the context of the MOMENTUM project, this model will be implemented in the case study of Leuven.

# 7.  Sustainability

Given the increasing interest in environmental performance measures from cities, emission models are developed. Static traffic assignment models are the usual methods employed in the traditional strategic 4-step approach. Nevertheless, there is also a growing interest in dynamic traffic assignment. Hence, both static and dynamic emission models are developed.

## 7.1.  Emission module – Static emission model

### 7.1.1.  Motivation and objective

Road transport emission calculations are rarely included in traffic modelling, for the simple reason that the scope of traffic models is primarily to understand traffic flows in the context of traffic management or for strategic assessment of adaptations to the road network.

Emission calculations typically require an indicator for traffic volumes (i.e., vehicle-kilometre or vkm) and emission factors for key pollutants. Emission factors vary substantially related to properties of the vehicle (fuel, emission standard, age, etc.) or vehicle use (speed, acceleration, etc.). As accurate emission calculations tend to become complex, specific purpose-built emission models are used (e.g., COPERT for the EMEP emission reporting[2]), focusing mostly on the variation of the emission facto (to get an accurate estimate of the total emission), however, making full abstraction of the road network, thereby losing the geo-spatial dimension of traffic emissions.

In some cases, emission calculations are added to a traffic model. Mostly heavily simplified emission factors are used (e.g., the CAR-model[3] or OSPM[4]), which is fine to give a rough idea, but insufficient as input for, for example, air quality models.

In this section, we attempt to merge the benefits of a detailed emission model with the spatial-detail benefits of a traffic model to produce a better estimate of traffic emissions. New mobility forms such as shared mobility are expected to have an important impact on emissions, as they can shift people away from private car use. This impact is expected to increase in the future. A more detailed emission model therefore allows for a better assessment of scenario's in which these new mobility forms are analysed. We use a generic, future-proof approach and also solve issues related to data-granularity to improve beyond the use of single-value emission factors.

### 7.1.2.  Methodology

We focus in particular on the additional features to produce emission estimates and make full abstraction of the traffic modelling side. The input required from the traffic model is quite simple: 1) the amount of vehicles, 2) the speed of the vehicles and 3) the length of the road segment. Temporal granularity can vary from single hour up to a full year, only constrained by data volume and computation time.

The tailoring of emission factors for traffic models in our approach includes:

---

[2] https://www.eea.europa.eu/publications/emep-eea-guidebook-2019
[3] https://www.infomil.nl/onderwerpen/lucht-water/luchtkwaliteit/slag/nsl-rekentool/handleiding/algemeen/stroomschema/rekenvoorbeeld-carii/
[4] https://envs.au.dk/en/research-areas/air-pollution-emissions-and-effects/the-monitoring-program/air-pollution-models/ospm/

- Detailed vehicle fleet data and a one-off fleet projection (using TML's fleet-model[5]), at EU-member state level, to produce an emission factor per year, per EU member state, for the pollutants CO, CO2, NOx, PM and VOC, using the COPERT 5 emission model[6].
- Account for the variation of the emission factor associated with the speed, at link level.

We elaborate on both these elements.

### 7.1.2.1. Fleet-estimate

As indicated, emission factors differ strongly among vehicle types. Large vehicles emit more CO2, diesel vehicles emit more NOx compared to gasoline vehicles, and older cars emit substantially more emissions due to historically less stringent emission standards.

The fleet composition differs between members states, so it is not possible to have a single emission factor for all countries. Moreover, the vehicle fleet constantly changes, so average emission factors are quickly outdated as new, cleaner vehicles replace older vehicles.

For the purpose of maintaining simplicity in the calculation, we use the TML fleet-model[7] and link it to COPERT 5 to construct a date-set of fleet-average emission factors per pollutant, per EU member state and per year from 2016-2050.

The main goal of the fleet module is to convert aggregate estimations of transport demand, in terms of passenger-km, tonne-km and/or vehicle-km, into a more detailed vehicle classification and generation (cohort), which directly relates to technology in terms of vehicle performance and characteristics, fuel use and emissions. The fleet inertia is included in the fleet model with a year-on-year estimate of natural scrappage of older cars, retention of the bulk of the fleet with decreasing use as cars grow older, and an estimation of new vehicles entering the active fleet, driven by traffic demand. The fleet dynamics are schematically shown in Figure 45.
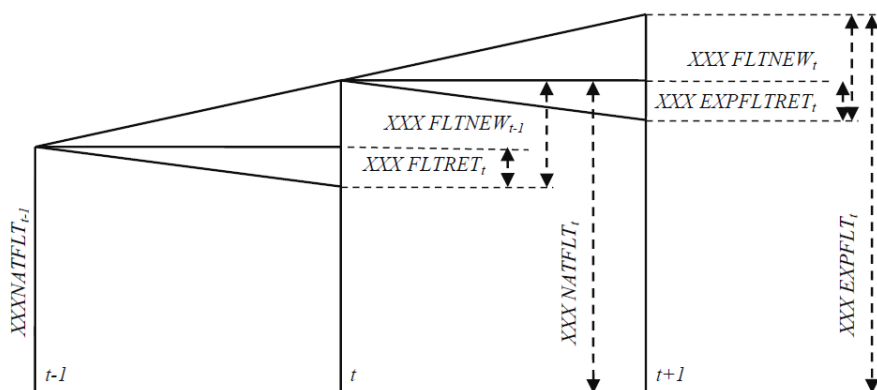


*Figure 45. Fleet capacity planning mechanism in TML Fleet-model*

---

[5] https://www.tmleuven.be/en/navigation/Fleet-Model
[6] https://www.emisia.com/utilities/copert/
[7] https://www.tmleuven.be/en/navigation/Fleet-Model

We align the Fleet-model baseline projections on the common PRIMES-TREMOVE 2015[8] baseline and added changes to fuel efficiency improvements in line with recent policy developments.

For the fleet projection, we make an assumption on the future market share of the different technologies. The largest uncertainty lies in the speed of uptake of electric vehicles (EV) and the duration of the transition period where plug-in hybrid electric vehicles (PHEV) will take a substantial market share.

We use a conservative assumption on the EV-uptake, in line with the (current) targets of a 35% market share for EV by 2030. Figure 46 summarizes the market share of the different technologies at an EU-level.

| | 2015 | 2020 | 2025 | 2030 | 2035 | 2040 | 2045 | 2050 |
|---|---|---|---|---|---|---|---|---|
| Gasoline | 40.40% | 38.92% | 33.57% | 24.79% | 18.92% | 13.05% | 6.52% | 0.00% |
| Diesel | 43.20% | 41.62% | 35.90% | 26.51% | 20.23% | 13.95% | 6.98% | 0.00% |
| HEV gasoline | 5.60% | 5.40% | 4.65% | 3.44% | 2.62% | 1.81% | 0.90% | 0.00% |
| HEV diesel | 3.70% | 3.56% | 3.07% | 2.27% | 1.73% | 1.19% | 0.60% | 0.00% |
| PHEV gasoline | 0.80% | 2.00% | 6.00% | 15.00% | 22.50% | 30.00% | 37.50% | 45.00% |
| PHEV diesel | 0.70% | 1.50% | 3.00% | 5.00% | 5.00% | 5.00% | 2.50% | 0.00% |
| EV | 0.50% | 2.00% | 8.00% | 15.00% | 20.00% | 25.00% | 32.50% | 40.00% |
| FCEV | 0.00% | 0.10% | 2.00% | 5.00% | 7.50% | 10.00% | 12.50% | 15.00% |
| LPG | 3.30% | 2.80% | 1.90% | 1.00% | 0.50% | 0.00% | 0.00% | 0.00% |
| CNG | 1.70% | 2.10% | 1.90% | 2.00% | 1.00% | 0.00% | 0.00% | 0.00% |
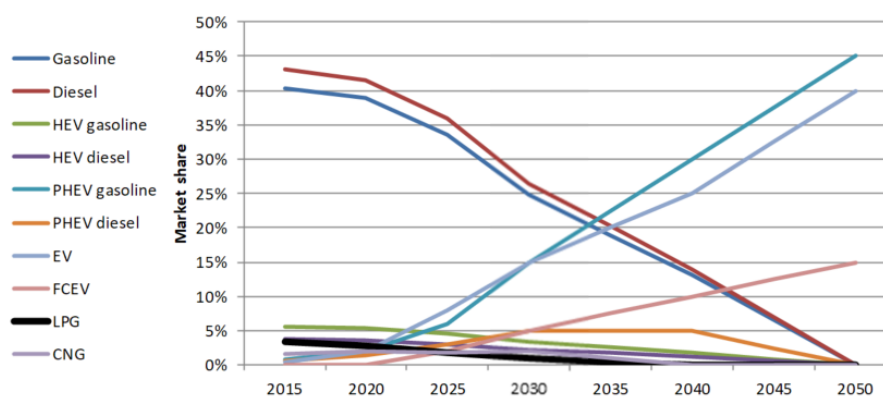


*Figure 46. Central market share assumption of newly sold vehicles per technology type 2016-2050*

In a second step in the fleet model, this central assumption is adapted to member state level to account for:

1. The member state's diesel/gasoline/LPG share
2. The position of the member state as a frontrunner or laggard of EV-adoption
3. The lag or acceleration of the uptake of new vehicle as a result of cross-border trade in used vehicles. Typically, Eastern-EU countries lag due to a large influx of (young) used cars from Western Europe. Western EU countries will see a more accelerated pace of fleet renewal.

Gradual fleet renewal will lead to the fleet composition per technology, as shown in Figure 47:

---

[8] https://ec.europa.eu/clima/policies/strategies/analysis/models_en
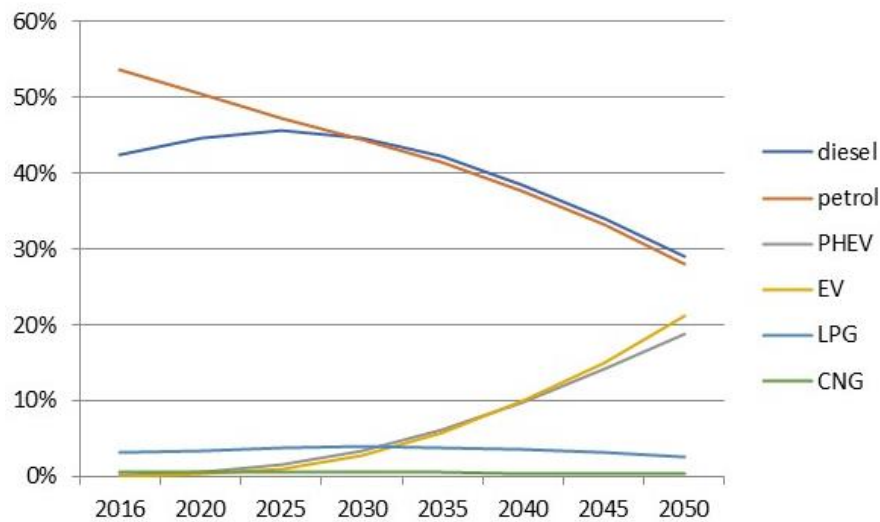
*Figure 47. Fleet composition per technology 2016-2050*

The resulting fleet composition is then fed to the COPERT 5 for an emission estimate. A COPERT 5 standalone software tool exist, however, we opt to use the mathematical formulations of the emission calculation directly to produce aggregate emission factors. The equations are available via the EMEP guidebook.[9]

The final result is a single table with aggregate emission factors with the following sets and dimensions:

1. Country: EU member states + CH, TR, UK, IS, NO (32 countries)
2. Pollutants: CO, CO2, NOx, PM, VOC
3. Year: 2016-2050

Figure 48 below summarizes the trend of the fleet-aggregate emission factor for four pollutants: CO2, NOx, PM and VOC, per member state. The large variation between members states is immediately apparent, especially up to 2030.

---

[9] https://www.eea.europa.eu/publications/emep-eea-guidebook-2019/part-b-sectoral-guidance-chapters/1-energy/1-a-combustion/1-a-3-b-i/view
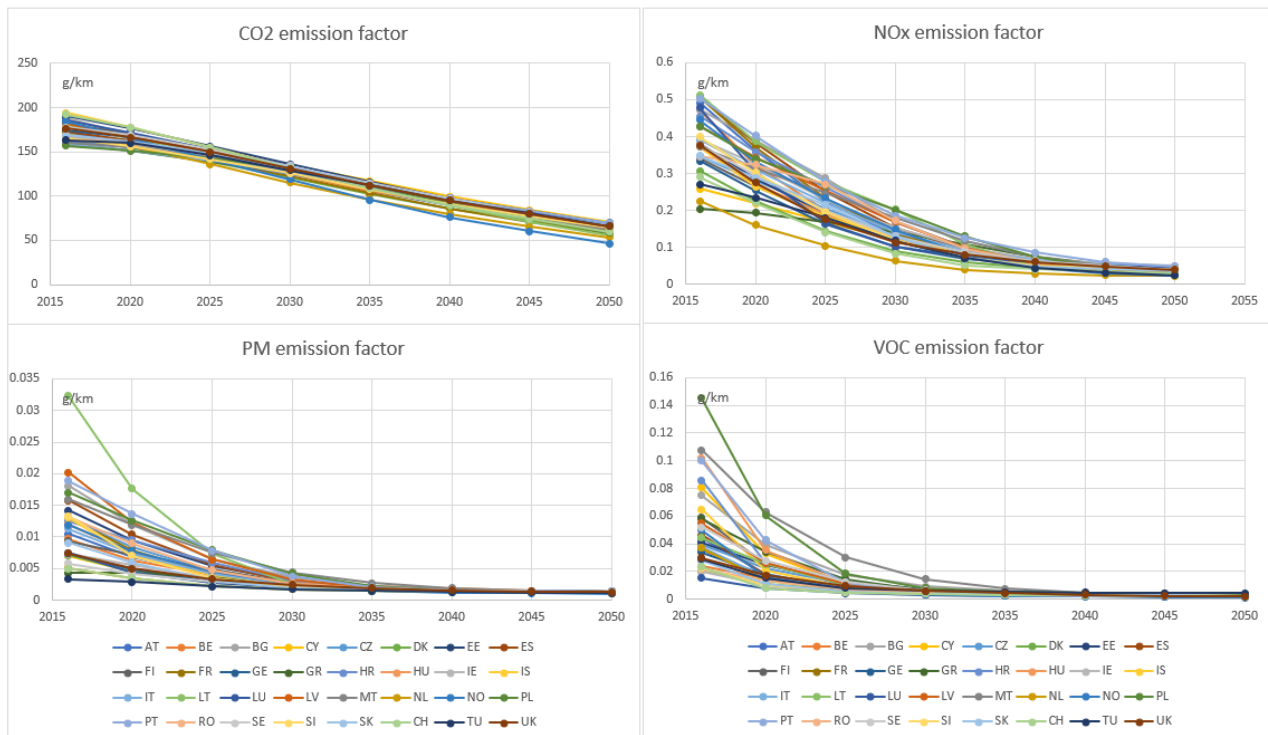
*Figure 48. Trend of fleet average emission factors for CO2 (top left), NOx (top right), PM (bottom left), VOC (bottom right)*

This set of emission factors allows for quick emission estimates at link level, provided total traffic volume and segment length are available from the traffic model. With a distinction of fleet composition per member state and a fleet projection up to 2050 (and associated reduction in emission factor) implicit in the values, this set of emission factors allows for a more detailed and future proof emission estimates in traffic models compared to, for example, CAR or OSPM.

### 7.1.2.2. Account for speed variation

Aggregate emission models do not capture the dependency of emission factors on vehicle speed. In a microscopic approach, emissions of cars are higher when accelerating to increase momentum and at higher speeds to overcome friction and aerodynamic resistance. As such, theoretically, the emission factor should increase with speed.

Macroscopic emission models, such as COPERT and HBEFA[10], make abstraction of these microscopic characteristics and rather empirically estimate emission under different aggregated speed regimes. These speed regimes reflect an average driving pattern, a drive cycle, which includes accelerating, braking, etc. Start-stop traffic and urban traffic requires more acceleration and braking compared to a free-flow rural road or highway, and yet leads to lower average speeds. Because of the high frequency of accelerations, emission at these low speeds (e.g., congestion) are in fact higher compared to a free-flow traffic situation at, for example, 60-70km/h. As such, the typical relation of the emission factor versus the speed is not increasing with speed, yet U-shaped in nature. In macroscopic emission models such as COPERT, we expect high (average) emission factors at low (average) speeds,

[10] https://www.hbefa.net/e/index.html

low (average) emission factors at medium (average) speeds and again high (average) emission factors at high (average) speeds as the energy to overcome friction and aerodynamic resistance increases at higher speeds.

We aim to account for this effect by applying a speed correction factor to the aggregate emission factor discussed in the previous section, under the premise that speed and flow at link level is computed by the traffic model.

We explored both HBEFA and COPERT as a source to incorporate the speed-effect on the emission factors:

- HBEFA does not include speed explicitly as a determinant for the emission factor, but rather uses a set of traffic conditions the reflect a specific driving pattern: free-flow, heavy traffic, light congestion, heavy congestion, start-stop.
- COPERT holds continuous emission functions with speed as a variable. The function is typically a second order polynomial in speed with vehicle type-dependent coefficients.

The benefit of HBEFA is that the driving patterns are easily identifiable traffic situations, however the speed is not clearly known. COPERT on the other hand has the benefit of directly using traffic model output (speed) as an input for emission factor estimation. In neither case it is clear whether the granularity is directly applicable to the microscopic level of the traffic model. The limitation of using macroscopic emission models in microscopic traffic models are further highlighted in De Nunzio (2021).

For simplicity, we opt for COPERT to estimate the speed correction factor. We make abstraction of the difference in coefficient values of the emission functions per vehicle type and use the vehicle fleet average to simulate the emission factors with 10 km/h intervals. We then compare the resulting value versus an "average" regime. The output is then a simple correction factor to the fleet average emission factor, discussed in the previous section. Figure 49 below shows the correction factor in 10km/h intervals for the 5 pollutants.
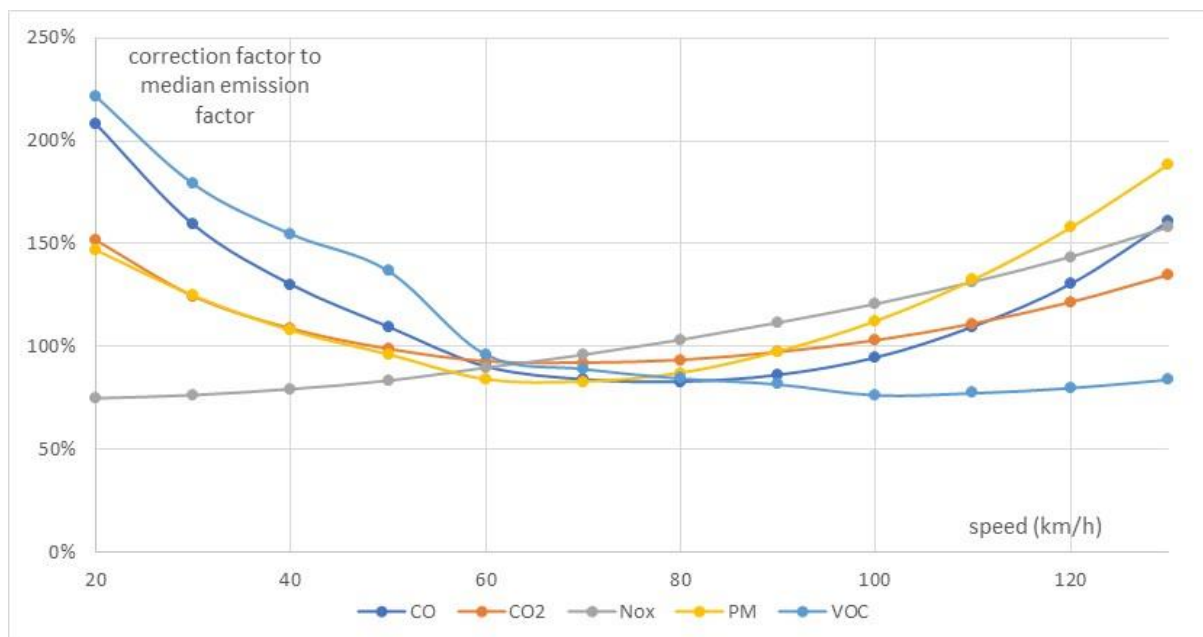


*Figure 49. Correction factor to the fleet-average emission factor, in 10km/h intervals*

As indicated, at lower speeds the correction factor is high, for some pollutants over 2, while in the optimal area of 60-80km/h, the correction factor is below 1. Note that pollutants behave differently.

There are some evident limitations with this approach:

MOMENTUM

Modules: **Induced demand | OD | Synthetic population generation | Mode choice | Fleet management | Traffic assignment | Car ownership | Emissions**

- The speed-dependency can be different per vehicle type, so the approach of an aggregation at fleet-level is not correct. Ideally the speed-correction should be done at the vehicle level and only aggregated after the correction to produce a speed-corrected fleet-average emission factor. For simplicity we opted to stick to a single, per pollutant, speed correction factor function.
- Speed variation within a single link is not accounted for in this approach. In principle, the speed at link level, as output from the traffic model, can be further segmented in sub-segments with more continuous speed regimes (e.g., a segment of 500m at an average of 45 km/h can be split in a 450m section free-flow at an average speed of 50km/h and 50m stop/go at an average speed of 25km/h ).

### 7.1.3. Application within MOMENTUM

The emission model will be demonstrated in the case study of Leuven, as in this case study the traffic flows on a substantial part of the network are monitored. Because of this, there is less uncertainty about the input of the emission mode, namely the vehicle kilometres, and the emissions can be calculated more accurately. Similarly, the model will also be demonstrated in the case study of Regensburg.

## 7.2. Emission module – Dynamic emission model

### 7.2.1. Motivation and objective

One of the objectives of the MOMENTUM project is to develop transferable methodologies to enable cities in assessing various policies oriented towards sustainable mobility solutions, which could avoid or mitigate negative environmental effects. For this purpose, emission models are needed to estimate adequate emission indicators in order to evaluate the implementation of new mobility services in the area of interest. The focus of this project is on macroscopic emissions models, which can be used on relatively large-scale networks.

The emission modelling approach presented in this section is referred to as a dynamic emission model to distinguish it from the static emission model presented in Section 6.1. Hence, the main difference between the macroscopic dynamic emission model and the static emission model is that the dynamic model considers average speed time series (i.e., varying speeds over time), while the static model uses constant speed over time. The motivation behind the selection of the dynamic approach is the limitation of macroscopic emission models based on constant average-speed that was mentioned above. These models are not able to predict accurate emissions at low speeds as well, as the uncertainty from averaging the link speeds increases for short links. Hence, an improved approach for deriving the emissions is to use average speeds over time from a set of vehicle trajectories.

In this section, a macroscopic dynamic emission model is presented for calculating the traffic emissions and their potential reduction due to the introduction of the new shared mobility services that are investigated within the MOMENTUM project. The proposed model aims to enable cities to perform environmental assessments of road emissions for the area of interest. Moreover, the contribution to those emissions can be evaluated depending on the characteristics of the vehicle fleet. This distinction is important as vehicle emissions are strongly associated with the vehicle category (passenger cars, buses, trucks, etc.) and sub-categories representing the fuel type, and vehicle emission standard (Lejri et al., 2018). Analysis of emissions can be used to identify the adequate intervention areas to deploy exhaust pollution emission reduction strategies or to introduce a low emission zone by excluding specific vehicle types from the fleet.

#### 7.2.1.1. Literature review

The estimation of vehicular emissions is of high importance in urban planning and transport management, as the pollutants emitted by road vehicles are detrimental to air quality. The assessment of environmental impacts of any transport application is critical in the decision-making process under each investigated policy or intervention. Hence, it is important for city planners and authorities to be able to identify and quantify the effects of a mobility

policy on emissions, such as road traffic emissions. Emission levels depend on vehicle characteristics (model size, fuel type, technology) as well as the driving dynamics (e.g., vehicle speed, acceleration, gear selection) depending on the traffic conditions. However, accurate real-world emission measurements are often impractical and cost-prohibitive to obtain at road network level as they would require constant emission measurement of all vehicles in the area and study period (Grote et al., 2016; Smit 2007; Smit et al., 2010). Several methods are used to measure vehicle emissions such as on-board emission measurements (PEMS), remote sensing, near-road air quality measurements, and tunnel studies, each of them associated with some advantages and limitations (Smit et al., 2010). Depending on the measurement technology that is used, emission data may be available for a few locations only, for limited time and vehicle sample or limited range of traffic conditions. Moreover, assumptions are required to convert the measured values to emission factors (Smit et al., 2010).

Therefore, the focus of numerous studies in the literature has been on the empirical estimation and modelling of vehicular emissions (see Smit et al., 2010; Grote et al., 2016; Saedi et al., 2020 for detailed reviews). The existing methodologies for emissions modelling can be broadly split into three categories: microscopic, macroscopic, and mesoscopic modelling. The main difference between the emission modelling approaches lies in the spatial and temporal resolution they offer. A detailed description of the different emission modelling approaches can be found in Samaras et al. (2019) and Saedi et al. (2020). The remaining literature review focuses on a brief summary of macroscopic emission models, as for the scope of this project emissions need to be estimated in a strategic context.

Macroscopic models have been developed that can estimate emissions for large-scale areas and mainly use average speed as an input to predict emissions and fuel consumption (Boulter et al., 2012). The main advantage of the average speed models is that they do not rely on detailed vehicle information, such as trajectories. However, it has been shown in the literature (Samaras et al., 2019) that the usage of average speeds as a single explanatory variable in the emissions models might not be an adequate indicator in predicting accurate emissions. In particular, the emissions could be underestimated for low average speeds, as those could represent different congestion levels. The inaccuracy could result from the averaging out of diverse traffic conditions at different network locations (e.g., stop-and-go and free-flow conditions). One approach to overcome the main limitation of macroscopic average speed models is the utilisation of speed dynamics in the emissions modelling (Tate, 2015). Another limitation of the macroscopic emission models is that they systematically ignore important vehicle operations and interactions, such as vehicle acceleration and braking, that can be accurately represented in microscopic models (Sun et al., 2015; Saedi et al., 2020; Tsanakas et al., 2020).

## 7.2.2. Methodology

The proposed emission model involves the estimation of polynomial functions, which depend on dynamic speed profiles over time and different pollutant types. In addition, the estimated emissions are distinguished per vehicle type (car, bus, taxi, truck, etc.), engine combustion type (diesel and petrol) and vehicle Euro Emission Standard (Euro 0 – Euro 6). Currently, the model estimates two pollutants, namely carbon dioxide ($CO_2$) and nitrogen oxides (NOx). Additional pollutants (such as CO, PM and HC) can be modelled depending on the data availability.

Due to a lack of real emission measurements for the cities involved in the project, synthetic data are obtained from microscopic simulation to estimate and validate the proposed emission model. Based on the synthetic emission and traffic data, regression analyses are performed to fit the observations and estimate emission curves per pollutant and vehicle type as well as for different speed ranges. The estimated curves are, in turn, integrated with the dynamic traffic assignment simulator Aimsun Next (Aimsun, 2020), which can be used to perform simulation-based analyses in order to evaluate the network-wide emission impacts under various scenarios with respect to the network demand and supply.

Figure 50 depicts the proposed framework. The vehicle fleet composition (i.e., the proportions of vehicle and fuel types, Euro segment class) for the given demand and network is defined first. Subsequently, traffic assignment is

performed to generate the required traffic flow indicators (link speeds and flows) over time and can be aggregated at the desired time resolution. Finally, the network emissions estimates are calculated based on the fitted polynomial functions. The emissions can be evaluated for each predefined vehicle fleet composition in the network (e.g., by vehicle type, fuel type, and Euro emission segment). The proposed approach can be seamlessly adopted to fit the emission curves for any real emission data as those become available for a specific city. Subsequently, the aggregate emission indicators can be obtained by performing a simulation analysis for the study area of interest.
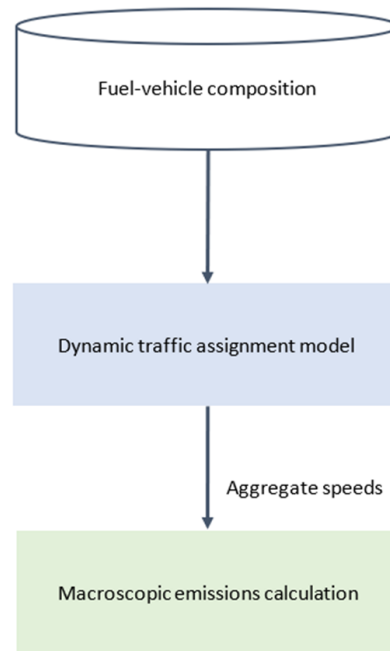


*Figure 50. Framework for estimating a dynamic macroscopic emission model*

### 7.2.2.1. Estimation methodology

As mentioned above, the emissions model estimation was based on average speeds as well as synthetic emission measurements that were obtained from a set of simulated vehicle trajectories from a test network. A combination of two polynomial relationships is chosen to derive the emission factors for CO2 and NOx in order to better describe the patterns observed in the synthetic emissions data. Specifically, depending on a predefined average speed threshold, a second-order and a third-order polynomial functions are used to fit the synthetic data as presented in the equations below:

$$E_p = av^2 + b \text{ for } v < 10 \; km/h \tag{51}$$

$$E_p = av^3 + bv^2 + c \text{ for } v \geq 10 \; km/h \tag{52}$$

where $E_p$ is the emission (grams/km) of pollutant $p \in \{CO_2, NO_x\}$, $v$ is the average speeds (km/h) and $a,b$, and $c$ are the estimated coefficients derived by the regression analysis.

### 7.2.2.2. Estimated emissions and insights

Figure 51 and Figure 52 illustrate indicative examples of estimated speed-emissions curves, for $NO_x$ and $CO_2$, respectively, for specific vehicle euro classes and engine fuel types, derived based on the simulated synthetic data as well as equations(51) and (52). In general, the curves indicate that the emissions of $CO_2$ decrease as the vehicle speed increases, while, for $NO_x$, the emission factors increase with increasing speeds. These trends are consistent across varying vehicle characteristics (i.e., fuel type and Euro class).

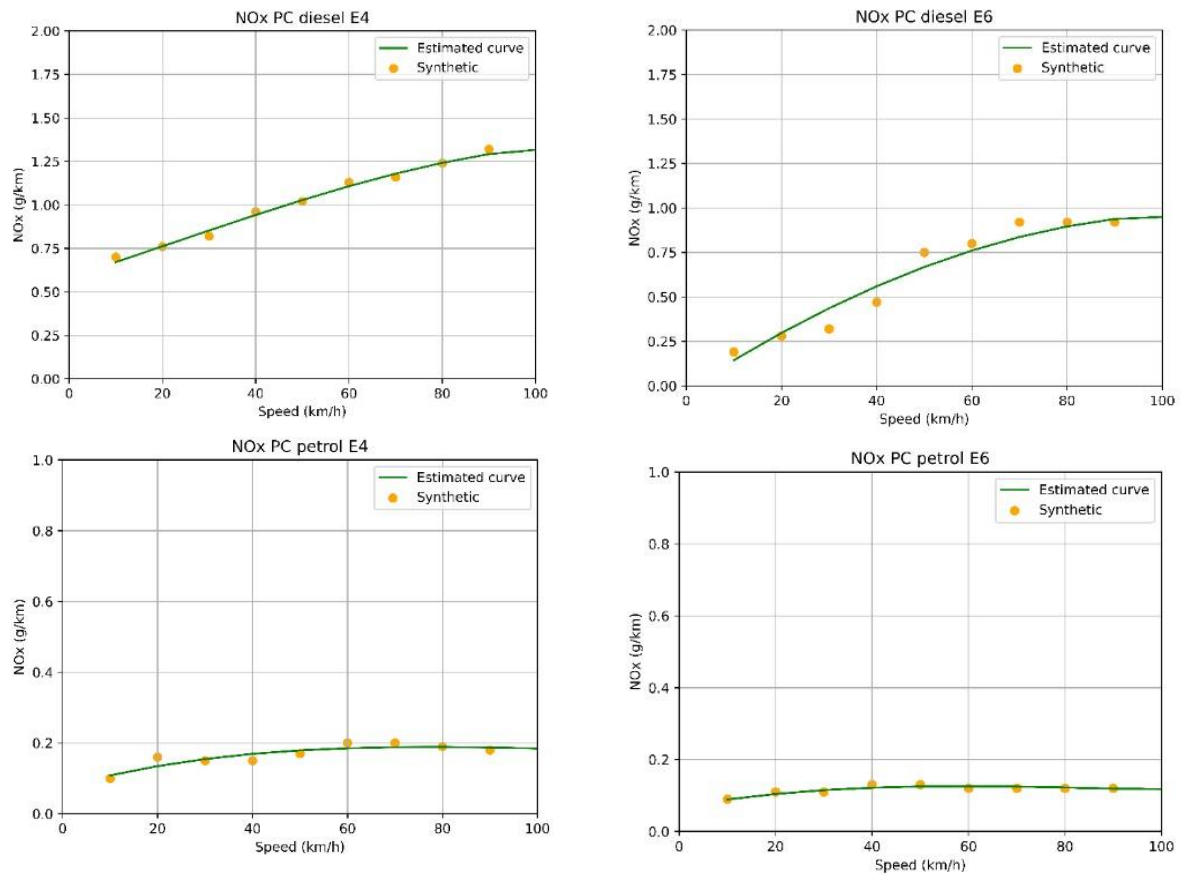*Figure 51. Estimated curves for (g/km) emissions versus speeds (km/h) for (a) diesel passenger cars Euro 4, (b) diesel passenger cars Euro 6, (c) petrol passenger cars Euro 4 and, (d) petrol passenger cars Euro 6.*
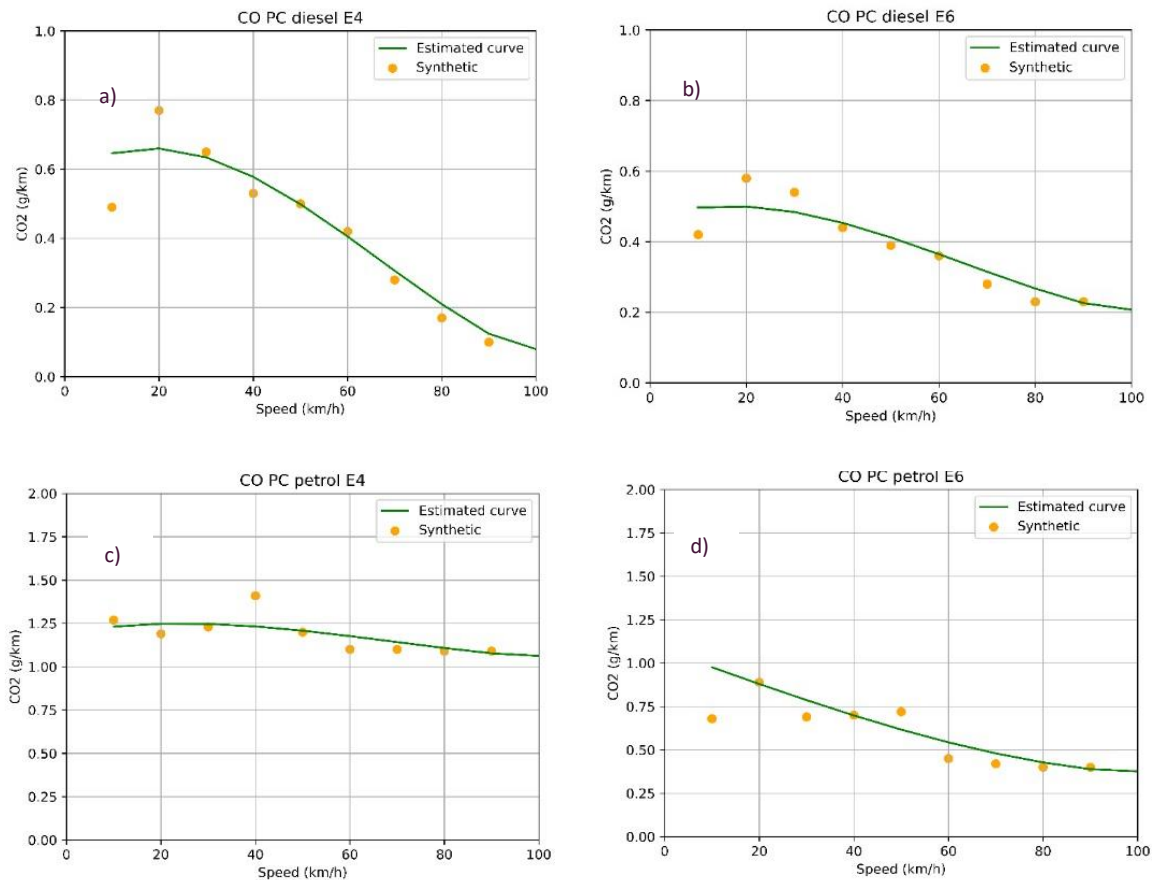
*Figure 52. Estimated curves for (g/km) emissions versus speeds (km/h) for (a) diesel passenger cars Euro 4, (b) diesel passenger cars Euro 6, (c) petrol passenger cars Euro 4 and, (d) petrol passenger cars Euro 6.*

### 7.2.3. Application within MOMENTUM

Within the scope of the MOMENTUM project, the proposed emissions model can be used to assess the impact of new transport modes and services with respect to the network emissions. The estimated emissions curves are integrated into the simulation software Aimsun Next (Aimsun, 2020). As emission observations become available for any city, the estimated curves presented earlier can be adjusted to fit the data of the specific city. Subsequently, simulation analysis can be performed under different investigated scenarios to obtain network-wide emission indicators from each vehicle type and sub-category within the vehicle fleet. The combination of data-driven and simulation-based approach for estimating the emissions can be more adequate for large-scale urban road networks.

As a future direction, evaluation of the accuracy of the simulated emission estimates for the investigated pollutants needs to be conducted against real-world measurements. Moreover, the emissions model can be extended to account for the vehicle acceleration, road gradient and speed limits, in combination with the vehicle speeds. This refined approach is expected to provide more accurate modelling of traffic emissions. For this purpose, a microscopic traffic flow model would be needed to generate the emission value.

# 8. Conclusions

In this deliverable, we have presented the models and algorithms developed in MOMENTUM project, which can properly capture and simulate the impact of emerging mobility concepts and solutions. The presented models and algorithms were designed and developed considering the test cases described in Deliverable 2.2. Besides, the benefits for cities outside the MOMENTUM case studies are also considered.

The main outcomes of this deliverable could be summarized as follows:

1. A modular approach, which encompasses the various developments required to model emerging mobility solutions. This could be used as a basis by the future researchers for extending the research on modelling frameworks for emerging mobility solutions.
2. An intermediate modelling approach, which integrates the principles of agent-based approaches within the traditional four-step approach, providing an opportunity for cities to evaluate and integrate shared mobility systems and form long term planning strategy.
3. A set of models and algorithms for modelling different aspects of the emerging mobility solutions. This set of models and algorithms includes:
   3.1 A model for demand elasticity calculation (i.e., estimation of induced demand), with the functional form based on a logit model.
   3.2 A multi-method framework for the estimation of demand for a small-sized station based round trip sharing system, which are usually utilized for irregular and infrequent trips.
   3.3 OD matrix clustering approaches for selecting the best matching matrix for the specific characteristics of a day or a season of study.
   3.4 A disaggregate mode choice model which can estimate the modal split between conventional-systems-as-a-whole, bike-sharing, car-sharing and ridesharing.
   3.5 A data-driven shared mobility demand model that utilizes general mobility OD matrix, weather observations at each origin zone and land use shares of each zone to predict the number of trips captured by a shared mobility service.
   3.6 Synthetic population generation based on a combination of an iterative proportional update procedure and statistical procedures.
   3.7 Operational research and artificial intelligence tools for planning shared mobility services and mimicking the operations of the services.
   3.8 An aggregate car-ownership model that can be used to calculate car-ownership at the level of traffic zones, which in turn, can be used as a basis for synthetic population generation.
   3.9 A disaggregate car ownership model for the re-estimation of car-ownership for the synthetic population, based on outputs from fleet management modules and traffic assignment.
   3.10 A data-driven traffic assignment method for urban environments, which considers traffic in local roads, circumventing the problems that arise in classical assignment procedures due to centroid connector placement.
   3.11 A hybrid dynamic traffic assignment framework wherein a dynamic mesoscopic model is used in specific area of interest and static macroscopic model in the remainder network.
   3.12 A static emission model based on a simplified COPERT-based EMEP approach, which can be easily integrated with the static traffic assignment models.
   3.13 A dynamic emission model that takes advantage of dynamic speed profiles, in case of availability of a dynamic traffic assignment model.

The outcomes 3.4 and 3.5 have a substitutional nature, since the use of one negates the need for the other. Mode choice models are the commonly used methods in transport models. However, if one wishes to use shared mobility service data, outcome 3.5 can be used to replace the disaggregate mode choice model (i.e., outcome 3.4). The output of outcome 3.5 is an OD matrix of shared mobility and the information of this matrix will get into the

Synthetic population module. Since the entry matrix is already mode specific, the output of the synthetic population does not need to pass through the disaggregate mode choice model, rather it will enter directly to the fleet management module. Similarly, static (outcome 3.12) and dynamic (outcome 3.13) emission models have a substitution nature. Static traffic assignment models are the usual methods employed in the traditional strategic 4-step approach, and hence, a static emission model is a necessity. Nevertheless, there is a growing interest in dynamic traffic assignment, and aiming at such models, a dynamic emission model has also been developed.

# References

Aimsun, 2020, 'Aimsun Next 20 User´s Manual', Aimsun Next Version 20.0.2, Barcelona, Spain.

Anderson, M and Simkins, J, 2012, 'Development of Long Distance Multimodal Passenger Travel Modal Choice Model'. https://www.fhwa.dot.gov/policy/modalchoice/modalchoice.pdf

Bar-Gera, H, 2002, 'Origin-Based Algorithm for the Traffic Assignment Problem', Transportation Science 36, 398–417. doi:10.1287/trsc.36.4.398.549

Bar-Gera, H, 2005, 'Continuous and discrete trajectory models for dynamic traffic assignment', Networks and Spatial Economics 5, 41–70.

Bar-Gera, H, 2010, 'Traffic assignment by paired alternative segments', Transportation Research Part B: Methodological 44, 1022–1046.

Bar-Gera, H, Hellman, F and Patriksson, M, 2013, 'Computational Precision of Traffic Equilibria Sensitivities in Automatic Network Design and Road Pricing', Procedia - Social and Behavioral Sciences 80, 41–60. doi:10.1016/j.sbspro.2013.05.005

Becker, H, Ciari, F and Axhausen, K, 2017, 'Comparing car-sharing schemes in Switzerland: User groups and usage patterns', Transportation Research Part A: Policy and Practice, 97, 17–29. https://doi.org/10.1016/j.tra.2017.01.004

Beckman, R, Baggerly, K and McKay, M, 1996, 'Creating synthetic baseline populations', Transportation Research Part A: Policy and Practice, 30(6), 415-429.

Bellei, G, Gentile, G and Papola, N, 2005, 'A within-day dynamic traffic assignment model for urban road networks', Transportation Research Part B: Methodological 39, 1–29.

Bhat, C and Pulugurta, V, 1998, 'A Comparison of Two Alternative Behavioural Choice Mechanisms for Household Auto Ownership Decisions', Transportation Research Part B: Methodological Vol. 32, No. 1, pp. 61-75.

Bierlaire, M, 2020, 'A Short Introduction to PandasBiogeme', Technical Report TRANSP-OR 200605. Transport and Mobility Laboratory, ENAC, EPFL.

Boulter, P, McCrae, I, Price, J and Emmerson, P, 2012, 'A city-wide road traffic emission model for Oxford–Scoping report' (No. PPR473).

Cantarella, G, de Luca, S, Di Gangi, M, and Di Pace, R, 2013, 'Stochastic Equilibrium Assignment With.', WIT Trans. Built Environ. 130 (May). https://doi.org/10.2495/UT130271.

Cascetta, E 2009, 'Transportation Systems Analysis', Springer-Verlag US: Springer US. https://doi.org/10.1007/978-0-387-75857-2.

Chawla, N, Bowyer, K, Hall, L and Kegelmeyer, W, 2002, 'SMOTE: Synthetic Minority Over-sampling Technique', Journal of Artificial Intelligence Research, 16, 321–357. https://doi.org/10.1613/jair.953

Chemlaa, D, Meuniera, F and Wolfler, R, 2013, 'Bike-sharing systems: Solving the static rebalancing problem.'

Cheng, L, Chen, X, Wei, M, Wu, J and Hou, X, 2014, ' Modeling mode choice behavior incorporating household and individual sociodemographics and travel attributes based on rough sets theory', Computational Intelligence and Neuroscience. Advance online publication. https://doi.org/10.1155/2014/560919

Ciari, F, Balac, M and Axhausen, K, 2016, 'Modeling Carsharing with the Agent-Based Simulation MATSim: State of the Art, Applications, and Future Developments', Transportation Research Record: Journal of the Transportation Research Board, 2564(1), 14–20. https://doi.org/10.3141/2564-02

Clewlow, R, 2016, 'Carsharing and sustainable travel behavior: Results from the San Francisco Bay Area', Transport Policy, 51, 158–164. https://doi.org/10.1016/j.tranpol.2016.01.013

Cordeau, J and Laporte, G, 2007, 'The dial-a-ride problem (DARP): Models and algorithms', Annals OR 153.

Croissant, Y, 2020, 'Estimation of Random Utility Models in R: The mlogit Package', Journal of Statistical Software, 95(11), 1–41. doi: 10.18637/jss.v095.i11

de Jong, G, Fox, J, Pieters, M, Daly, A and Smith, R, 2004, 'A comparison of car-ownership models', Transport Reviews 24(4), pp.379-408

de Nunzio, G, Laraki, M and Thibault, L, 2021, 'Road Traffic Dynamic Pollutant Emissions Estimation: From Macroscopic Road Information to Microscopic Environmental Impact', Atmosphere, 12(1). https://doi.org/10.3390/atmos12010053

Dell'Amico, M, Hadjicostantinou, E, Iori, M and Novellani, S, 2014, 'The bike-sharing rebalancing problem: Mathematical formulations and benchmark instances', Omega-international Journal of Management Science 7-19.

Dial, R, 1971, 'A probabilistic multipath traffic assignment model which obviates path enumeration', Transportation Research, 5, 83–111. doi:10.1016/0041-1647(71)90012-8

Dial, R, 2006, 'A path-based user-equilibrium traffic assignment algorithm that obviates path storage and enumeration', Transportation Research Part B: Methodological, 40, 917–936.

D'Orazio, M, Di Zio, M and Scanu, M, 2006, 'Statistical matching: Theory and practice', John Wiley & Sons.

Farooq, B, Bierlaire, M, Hurtubia, R and Flötteröd, G, 2013, 'Simulation based population synthesis', Transportation Research Part B: Methodological, 58, 243-263.

Felbermair, S, Lammer, F, Trausinger-Binder, E and Hebenstreit, C, 2020, 'Generating synthetic population with activity chains as agent-based model input using statistical raster census data', Procedia Computer Science, 170, 273-280.

Florian, M, Mahut, M and Tremblay, N, 2005, 'Application of a simulation-based dynamic traffic assignment model', Simulation Approaches in Transportation Analysis, 1–22.

Frade, I and Ribeiro, A, 2015, 'Bike-sharing stations: A maximal covering location approach', Transportation Research Part A-policy and Practice 216-227.

Friedrich, M and Noekel, K, 2017, 'Modeling intermodal networks with public transport and vehicle sharing systems', EURO Journal on Transportation and Logistics, 6(3), 271–288. https://doi.org/10.1007/s13676-015-0091-7

Friedrich, M, Hartl, M and Magg, C, 2018, 'A modelling approach for matching ridesharing trips within macroscopic travel demand models', Transportation, 45(6), 1639–1653. https://doi.org/10.1007/s11116-018-9957-5

Fromm, H, Ewald, L, Frankenhauser, D, Ensslen, A and Jochem, P, 2019, 'A Study on Free-floating Carsharing in Europe : Impacts of car2go and DriveNow on modal shift, vehicle ownership, vehicle kilometers traveled, and $CO_2$ emissions in 11 European cities', https://doi.org/10.5445/IR/1000104216

Furuhata, M, Dessouky, M, Ordóñez, F, Brunet, M, Wang, X and Koenig, S, 2013, 'Ridesharing: The state-of-the-art and future directions', Transportation Research Part B: Methodological 28-46.

Geilenkirchen, G, Geurs, K, Van Essen, H, Schroten, A  and Boon, B, 2010, 'Effecten van Prijsbeleid in Verkeer En Vervoer. Kennisoverzicht', PBL Planbureau Voor de Leefomgeving, October. https://www.pbl.nl/sites/default/files/downloads/500076011.pdf.

Gentile, G, 2014, 'Local User Cost Equilibrium: a bush-based algorithm for traffic assignment', Transportmetrica A: Transport Science 10, 15–54. doi:10.1080/18128602.2012.691911

Goyal, P and Ferrara, E, 2018, 'Graph embedding techniques, applications, and performance: A survey. Knowledge-Based Systems', 151, 78-94.

Grote, M, Williams, I, Preston, J and Kemp, S, 2016, 'Including congestion effects in urban road traffic $CO_2$ emissions modelling: Do Local Government Authorities have the right options?', Transportation Research Part D: Transport and Environment, 43, 95-106.

Grover, A and Leskovec, J 2016, 'Node2Vec: Scalable feature learning for networks', Proceedings of the 22nd ACM SIGKDD international conference on Knowledge discovery and data mining (pp. 855-864).

Guo, J and Bhat, C, 2007, 'Population synthesis for microsimulating travel behavior', Transportation Research Record, 2014(1), 92-101.

Häll, C, Andersson, H, Lundgren, Jand Värbrand, P, 2009, 'The Integrated Dial-a-Ride Problem.', Public Transport 39-54.

He, B, Zhou, J, Ma, Z, Chow, J and Ozbay, K, 2020, 'Evaluation of city-scale built environment policies in New York City with an emerging-mobility-accessible synthetic population', Transportation Research Part A: Policy and Practice, 141, 444-467.

Heilig, M, Mallig, N, Schröder, O, Kagerbauer, M and Vortisch, P, 2015, 'Multiple-day Agent-based Modeling Approach of Station-based and Free-floating Carsharing', 94th Annual Meeting of the Transport Research Board.

Hörl, S and Balac, M, 2020, 'Open data travel demand synthesis for agent-based transport simulation: A case study of Paris and Ile-de-France', Arbeitsberichte Verkehrsund Raumplanung, 1499.

Jafari, E, Gemar, M, Juri, N and Duthie, J, 2015, 'Investigation of Centroid Connector Placement for Advanced Traffic Assignment Models with Added Network Detail', Transportation Research Record: Journal of the Transportation Research Board, 2498(1), pp.19-26.

Jain, S, Ronald, N and Winter, S, 2015, 'Creating a synthetic population: A comparison of tools', Proceedings of the 3rd Confer-ence Transportation Reserch Group, Kolkata, India, 17-20.

Jiang, Y, Ma, P and Zhou, S, 2018, 'Macroscopic modeling approach to estimate traffic-related emissions in urban areas', Transportation Research Part D: Transport and Environment, 60, 41-55.

Junming, L, Qiao, L, Meng, Q, Weiwei, C, Jingyuan, Y, Hui, X, Hao, Z and Yanjie, F, 2015, 'Station Site Optimization in Bike-sharing Systems', IEEE International Conference on Data Mining. Atlantic City, NJ, USA. 883-888.

Konduri, K, You, D, Garikapati, V and Pendyala, R, 2016, 'Enhanced synthetic population generator that accommodates control variables at multiple geographic resolutions', Transportation Research Record, 2563(1), 40-50.

Lee, D, Klein, L and Camus, G, 1999, 'Induced Traffic and Induced Demand', Transp. Res. Rec. 1659 (1): 68–75. https://doi.org/10.3141/1659-09.

Lejri, D, Can, A, Schiper, N and Leclercq, L, 2018, 'Accounting for traffic speed dynamics when calculating COPERT and PHEM pollutant emissions at the urban scale', Transportation research part D: Transport and Environment, 63, 588-603.

Liang, L, Xu, M, Grant-Muller, S and Mussone, L, 2020, 'Household travel mode choice estimation with large-scale data—an empirical analysis based on mobility data in Milan', International Journal of Sustainable Transportation, 15(1), 70–85. https://doi.org/10.1080/15568318.2019.1686782

Lim, P and Gargett, D, 2013, 'Population synthesis for travel demand forecasting', Proceedings of the 36th Australasian Transport Research Forum (ATRF), Brisbane, Australia (pp. 2-4).

Litman, T, 2017, 'Generated Traffic and Induced Travel: Implications for Transport Planning', Victoria Transport Policy Institute Canada. https://www.vtpi.org/gentraf.pdf.

Manout, O, Bonnel P and Pacull, F, 2020, 'Spatial Aggregation Issues in Traffic Assignment Models'

Manout, O, Bonnel, P and Pacull, F, 2021, 'Spatial Aggregation Issues in Traffic Assignment Models'

MARG, 2016, 'PopGen: Synthetic Population Generator', Mobility Analytics Research Group, http://www.mobilityanalytics.org/popgen.html.

Martínez, L, Correia, G, Moura, F and Mendes Lopes, M, 2017, ' Insights into car-sharing demand dynamics: Outputs of an agent-based model application to Lisbon, Portugal', International Journal of Sustainable Transportation, 11(2), 148–159. https://doi.org/10.1080/15568318.2016.1226997

Müller, K and Axhausen, K 2011, 'Hierarchical IPF: Generating a synthetic population for Switzerland', Arbeitsberichte Verkehrs-und Raumplanung, 718.

Müller, K and Axhausen, K, 2011, 'Population synthesis for microsimulation: State of the art', Transportation Research Board 90th Annual Meeting.

Nikiforiadis, A, Aifadopoulou, G, Salanova J and Boufidis, N, 2021, 'Determining the optimal locations for bike-sharing stations: methodological approach and application in the city of Thessaloniki, Greece.' Transportation Research Procedia 557-564.

Panis, L, Broekx, S and Liu, R, 2006, 'Modelling instantaneous traffic emission and the influence of traffic speed limits', Science of the total environment, 371(1-3), 270-285.

Polyak, B, 1990, 'New method of stochastic approximation type'

Pritchard, D and Miller, E, 2012, 'Advances in population synthesis: fitting many attributes per agent and fitting to household and person margins simultaneously', Transportation, 39(3), 685-704.

Psaraftis, H, Wen, M and Kontovas, C, 2016, 'Dynamic vehicle routing problems: Three decades and counting', Networks 3-31.

Raviv, T, Kolka, O, 2013, 'Optimal inventory management of a bike-sharing station', IIE Transactions 1077-1093.

Saedi, R, Verma, R, Zockaie, A, Ghamami, M and Gates, T, 2020, 'Comparison of Support Vector and Non-Linear Regression Models for Estimating Large-Scale Vehicular Emissions, Incorporating Network-Wide Fundamental Diagram for Heterogeneous Vehicles', Transportation Research Record, 2674(5), 70-84.

Salanova, J and Estrada, M, 2015 'Agent Based Modelling for Simulating Taxi Services', ANT/SEIT.

Salanova, J, Estrada, M, Aifadopoulou, G and Mitsakis, E, 2011, 'A Review of the Modeling of Taxi Services', Procedia - Social and Behavioral Sciences 150-161.

Samaras, C, Tsokolis, D, Toffolo, S, Magra, G, Ntziachristos, L and Samaras, Z, 2019, 'Enhancing average speed emission models to account for congestion impacts in traffic network link-based simulations', Transportation Research Part D: Transport and Environment, 75, 197-210.

Smit, R, Ntziachristos, L and Boulter, P, 2010, 'Validation of road vehicle and traffic emission models–A review and meta-analysis', Atmospheric environment, 44(25), 2943-2953.

Smit, R, Smokers, R and Rabé, E, 2007, 'A new modelling approach for road traffic emissions: VERSIT+', Transportation Research Part D: Transport and Environment, 12(6), 414-422.

Stephan, F, 1942, 'An iterative method of adjusting sample frequency tables when expected marginal totals are known', The Annals of Mathematical Statistics, 13(2), 166-178.

Sun, L, Erath, A, and Cai, M, 2018, 'A hierarchical mixture modeling framework for population synthesis', Transportation Research Part B: Methodological, 114, 199-212.

Sun, Z, Hao, P, Ban, X and Yang, D, 2015, 'Trajectory-based vehicle energy/emissions estimation for signalized arterials using mobile sensing data', Transportation Research Part D: Transport and Environment, 34, 27-40.

Sutton, R, Barto, A, 1998, 'Introduction to Reinforcement Learning'

Tate, J, 2015, 'Wakefield Modelling of Action Plan Measures-Vehicle Emission Modelling', Institute For Transport Studies, University of Leeds.

Train, K, 2009, 'Discrete Choice Methods with Simulation', Cambridge university press.

Tsanakas, N, Ekström, J and Olstam, J, 2020, 'Estimating Emissions from Static Traffic Models: Problems and Solutions', Journal of Advanced Transportation, 2020.

van der Loop, H, van der Waard, J and van Mourik, H, 2014, 'De Latente Vraag in Het Wegverkeer'

Voas, D and Williamson, P, 2000. 'An evaluation of the combinatorial optimisation approach to the creation of synthetic microdata', International Journal of Population Geography, 6(5), 349-366.

Williams, H and Yamashita, Y, 1992, 'Travel Demand Forecasts and the Evaluation of Highway Schemes Under Congested Conditions', Journal of Transport Economics and Policy, 261–82.

Xiao, G, Wang, R, Zhang, C and Ni, A, 2020, 'Demand prediction for a public bike sharing program based on spatio-temporal graph convolutional networks', Multimed Tools Appl, https://doi.org/10.1007/s11042-020-08803-y

Yameogo, B, Vandanjon, P, Gastineau, P and Hankach, P, 2021, 'Generating a two-layered synthetic population for French municipalities: Results and evaluation of four synthetic reconstruction methods', JASSS-Journal of Artificial Societies and Social Simulation, 24, 27p.

Ye, X, Konduri, K, Pendyala, R, Sana, B and Waddell, P, 2009, 'A methodology to match distributions of both household and person attributes in the generation of synthetic populations', 88th Annual Meeting of the Transportation Research Board, Washington, DC.

Ziliaskopoulos, A, Waller, S, Li, Y and Byram, M, 2004, 'Large-Scale Dynamic Traffic Assignment: Implementation Issues and Computational Analysis', Journal of Transportation Engineering 130, 585–593. doi:10.1061/(ASCE)0733-947X(2004)130:5(585)

# Annex

## A1.    Induced demand calibration details

### Multidimensional linear

The definition of elasticity can be written as

$$\eta_j \frac{D^j}{x} = \frac{\partial D^j}{\partial x} = \sum_{k \in B\setminus\{i\}} \frac{\partial D^j}{\partial U^k}\frac{\partial U^k}{\partial x} + \frac{\partial D^j}{\partial U^i}\frac{\partial U^i}{\partial x}, \tag{1}$$

from which it immediately follows that

$$\frac{\partial D^j}{\partial U^i} = \left(\frac{\partial U^i}{\partial x}\right)^{-1}\left[\eta_j \frac{D^j}{x} - \sum_{k \in B\setminus\{i\}} \frac{\partial D^j}{\partial U^k}\frac{\partial U^k}{\partial x}\right]. \tag{2}$$

In the general case, this is a set of equations that need to be solved consistently for $\partial D^j / \partial U^i$ for every $i \in B$. If all $U^k$, except for $U^i$, are independent of $x$, the formula reduces to

$$\frac{\partial D^j}{\partial U^i} = \left(\frac{\partial U^i}{\partial x}\right)^{-1}\eta_j \frac{D^j}{x}. \tag{3}$$

### One-dimensional linear

The quantity $\partial D / \partial x|_{T=0}$ should be obtained through calibration. From the second expression for elasticity, it can be derived that

$$\frac{\partial D}{\partial x} = \frac{1}{P^j}\left[\frac{D^j}{x}\eta_j - D\frac{\partial P^j}{\partial x}\right] \tag{4}$$

Since the Taylor-expansion is only one-dimensional, only one parameter needs to be calibrated. Which alternative $j$ is used for this calibration, is dependent on the availability of the corresponding (cross-)elasticities $\eta_j$. The result

$$D = D_0 + (U - U_0)\frac{\left[\frac{D^j}{x}\eta_j - D\frac{\partial P^j}{\partial x}\right]}{P^j\,\partial U / \partial x}\Bigg|_{T=0} \tag{5}$$

is obtained, where

$$\frac{\partial U}{\partial x} = \frac{\sum_{k \in B} \left[ e^{U^k} \frac{\partial U^k}{\partial x} \right]}{\sum_{l \in B} e^{U^l}} = \sum_{k \in B} P^k \frac{\partial U^k}{\partial x}. \tag{6}$$

Up to this point, all $U^k$ could depend on $x$. If only $U^j$ is dependent on $x$, one can use the relation

$$\frac{\partial P^j}{\partial x} = P^j \left( \frac{\partial U^j}{\partial x} - \frac{dU}{dx} \right), \tag{7}$$

to further reduce the demand expression to

$$D = D_0 \left( 1 + (U - U_0) \left( 1 + \left. \frac{\left[ \frac{1}{x} \eta_j - \frac{\partial U^j}{\partial x} \right]}{\partial U / \partial x} \right|_{T=0} \right) \right). \tag{8}$$

## Logit-like

Using $D = \frac{P^t}{P_0^t} D_0$, the second expression for elasticity can be transformed into

$$\eta_j \frac{D^j}{x} - D \frac{dP^j}{dx} = P^j \frac{d}{dx} \left[ \frac{P^t}{P_0^t} D_0 \right]. \tag{9}$$

Notice that $P^j$ and $P^t$ are functions, while $P_0^t$ and $D_0$ are function evaluations of $P^t$ and $D$ for the base scenario. The expression is then

$$\eta_j \frac{D^j}{x} - D \frac{dP^j}{dx} = P^j \frac{D_0}{P_0^t} \frac{dP^t}{dx}. \tag{10}$$

The derivative of the share of travellers $P^t = e^U / (K + e^U)$ is easily obtained:

$$\frac{dP^t}{dx} = P^t (1 - P^t) \frac{dU}{dx} \tag{11}$$

The remaining derivative of the generalized utility function $U$ is

$$\frac{dU}{dx} = \frac{d}{dx} [W + \lambda I] = \lambda \frac{dI}{dx} = \sum_k P^k \frac{dU^k}{dx}, \tag{12}$$

where the last step employs the corresponding derivative of the aggregated utility logsum for the alternatives

$$\frac{\mathrm{d}I}{\mathrm{d}x} = \frac{\mathrm{d}}{\mathrm{d}x}\ln\left(\sum_j e^{U^j/\lambda}\right) = \frac{1}{\lambda}\sum_k \frac{e^{U^k/\lambda}}{\sum_j e^{U^j/\lambda}}\frac{\mathrm{d}U^k}{\mathrm{d}x} = \frac{1}{\lambda}\sum_k P^k \frac{\mathrm{d}U^k}{\mathrm{d}x}. \tag{13}$$

In the last equality, the share $P^k$ of travellers choosing for alternative $k$ was recognized.

Combining above expressions gives

$$\eta_j \frac{D^j}{x} - D\frac{\mathrm{d}P^j}{\mathrm{d}x} = P^j \frac{D_0}{P_0^{\mathrm{t}}} P^{\mathrm{t}}(1-P^{\mathrm{t}})\sum_k P^k \frac{\mathrm{d}U^k}{\mathrm{d}x}. \tag{14}$$

Since $K$ is assumed to remain constant, calibration can be done using the base scenario. Evaluating the expression for the base scenario yields

$$\eta_j \frac{D^j}{x}\bigg|_{T=0} - D_0\frac{\mathrm{d}P^j}{\mathrm{d}x}\bigg|_{T=0} = P_0^j D_0 (1-P_0^{\mathrm{t}})\sum_k P_0^k \frac{\mathrm{d}U^k}{\mathrm{d}x}\bigg|_{T=0}. \tag{15}$$

Further, using the relation

$$\frac{\mathrm{d}P^j}{\mathrm{d}x} = P^j\left(\frac{\partial U^j}{\partial x} - \sum_k P^k \frac{\mathrm{d}U^k}{\mathrm{d}x}\right) \tag{16}$$

simplifies the expression to

$$\eta_j \frac{D_0^j}{x_0} - D_0 P_0^j \frac{\partial U^j}{\partial x}\bigg|_{T=0} = -P_0^j D_0 P_0^{\mathrm{t}}\sum_k P_0^k \frac{\mathrm{d}U^k}{\mathrm{d}x}\bigg|_{T=0}. \tag{17}$$

The share of travellers in the base scenario can be extracted and equated to its definition:

$$P_0^{\mathrm{t}} = \frac{D_0 P_0^j \frac{\partial U^j}{\partial x}\big|_{T=0} - \eta_j \frac{D_0^j}{x_0}}{P_0^j D_0 \sum_k P_0^k \frac{\mathrm{d}U^k}{\mathrm{d}x}\big|_{T=0}} = \frac{e^{U_0}}{K + e^{U_0}}. \tag{18}$$

Elementary algebra and the relation $D_0^j = D_0 P_0^j$ then lead to

**Deliverable 4.1**

Copyright © 2021 by MOMENTUM

New transport modelling approaches
for emerging mobility solutions

Version: Issue 1 Draft 2

Page **133** of **137**

$$K = \mathrm{e}^{U_0} \left[ \frac{\sum_k P_0^k \left. \dfrac{\mathrm{d}U^k}{\mathrm{d}x} \right|_{T=0}}{\left. \dfrac{\mathrm{d}U^j}{\mathrm{d}x} \right|_{T=0} - \dfrac{\eta_j}{x_0}} - 1 \right]. \tag{19}$$

This relation can be used to calibrate $K$ (and thus $U^{\mathrm{nt}}$), given the $x$-elasticity of the demand $D^j$ of alternative $j$ with as boundary conditions:

- the base-scenario share $P_0^k$ of alternative $k$
- the base-scenario total utility of travelling $U_0$
- the base-scenario $x$-sensitivity of the utility $U^j$ for alternative $j$

## A2.  Synthetic population generation

### The Iterative Proportional Updating (IPU)

A brief description of the generalised procedure of the IPU heuristic method is presented below using a simple example illustrated on Table 21. A detailed description can be found in Ye et al. (2009). In summary, the algorithm consists of the following main steps:

1. Generate a frequency matrix showing the household type and the frequency of different person types within each household for the sample.
2. Initially it assumes equal weights (1.0) for all households in the sample, in a specific geographic area.
3. The algorithm then updates the weights for each household type in an iterative process in order to match the aggregate distributions. For example, the weights for the first household level constraint are adjusted by dividing the number of households in that category (i.e., defined by the constraint value) by the weighted sum of the first household type column.
4. The weights for all households of each household type are multiplied by the respective ratios to satisfy the constraints.
5. The weights are then updated to satisfy person-level variable constraints. For example, the weights for households containing persons of type 1 are updated and adjusted to match the distribution of person type 1.
6. An iteration is defined as the completion of weight updating for all types of households and persons.
7. Finally, the absolute value of the relative difference between the weighted sum and the corresponding constraint are used as a goodness-of-fit measure as a means of assessing the process.

After the calibration of weights using the IPU algorithm, households may be randomly drawn from the sample data to generate the synthetic population.

| Household ID | Weights | Household Type 1 | Household Type 2 | Person Type 1 | Person Type 2 | Person Type 3 | Weights 1 | Weights 2 | Weights 3 | Weights 4 | Weights 5 | Final Weights |
|---|---|---|---|---|---|---|---|---|---|---|---|---|
| 1 | 1 | 1 | 0 | 1 | 1 | 1 | 11.67 | 11.67 | 9.51 | 8.05 | 12.37 | 1.36 |
| 2 | 1 | 1 | 0 | 1 | 0 | 1 | 11.67 | 11.67 | 9.51 | 9.51 | 14.61 | 25.66 |
| 3 | 1 | 1 | 0 | 2 | 1 | 0 | 11.67 | 11.67 | 9.51 | 8.05 | 8.05 | 7.98 |
| 4 | 1 | 0 | 1 | 1 | 0 | 2 | 1.00 | 13.00 | 10.59 | 10.59 | 16.28 | 27.79 |
| 5 | 1 | 0 | 1 | 0 | 2 | 1 | 1.00 | 13.00 | 13.00 | 11.00 | 16.91 | 18.45 |
| 6 | 1 | 0 | 1 | 1 | 1 | 0 | 1.00 | 13.00 | 10.59 | 8.97 | 8.97 | 8.64 |
| 7 | 1 | 0 | 1 | 2 | 1 | 2 | 1.00 | 13.00 | 10.59 | 8.97 | 13.78 | 1.47 |
| 8 | 1 | 0 | 1 | 1 | 1 | 0 | 1.00 | 13.00 | 10.59 | 8.97 | 8.97 | 8.64 |
| Weighted Sum | | 3.00 | 5.00 | 9.00 | 7.00 | 7.00 | | | | | | |
| Constraints | | 35.00 | 65.00 | 91.00 | 65.00 | 104.00 | | | | | | |
| $\delta_b$ | | 0.9143 | 0.9231 | 0.9011 | 0.8923 | 0.9327 | | | | | | |
| Weighted Sum 1 | | 35.00 | 5.00 | 51.67 | 28.33 | 28.33 | | | | | | |
| Weighted Sum 2 | | 35.00 | 65.00 | 111.67 | 88.33 | 88.33 | | | | | | |
| Weighted Sum 3 | | 28.52 | 55.38 | 91.00 | 76.80 | 74.39 | | | | | | |
| Weighted Sum 4 | | 25.60 | 48.50 | 80.11 | 65.00 | 67.68 | | | | | | |
| Weighted Sum 5 | | 35.02 | 64.90 | 104.84 | 85.94 | 104.00 | | | | | | |
| $\delta_u$ | | 0.0006 | 0.0015 | 0.1521 | 0.3222 | 0.0000 | | | | | | |
| Final Weighted Sum | | 35.00 | 65.00 | 91.00 | 65.00 | 104.00 | | | | | | |

*Table 21. An Example of the Iterative Proportional Updating (IPU) Algorithm (source: Ye et al., 2009)*

*Control variables*

Table 22 presents an example of the commonly used control variables in the literature.

| Analysis unit | Variable name | Variable description |
|---|---|---|
| Household | Household type | The group of the household type (e.g., family with children, without children, single person) |
| | Household size | Number of people in the household |
| | Income | Income group of the household |
| Person | Age groups | Age group of a person |
| | Gender | Female, Male or other |
| | Education | The education level (e.g., primary, bachelor) |
| | Car-ownership | Number of cars owned by household |
| | Employment | The employment status of a person |
| | Public Transport subscription | PT subscription available or not |

*Table 22. Example of control variables*

## A3.   Ridesharing: planning

Objective function of the ridesharing planning model is as follows:

$$\min f(system) = \left( \sum_{\forall i \in PR} \text{Access Duration}_i + \sum_{\forall i \in PR} \text{Waiting Duration}_i \right.$$
$$\left. + \sum_{\forall i \in PR} \text{Trip Duration}_i \right) \times \text{Value Of Time}$$
$$+ \left( \sum_{\forall i \in DR} \text{Waiting Duration}_i + \sum_{\forall i \in DR} \text{Trip Duration}_i \right) \times \text{Value Of Driver's Time}$$
$$+ \sum_{\forall i \in Requests} \text{Rejected Request}_i \times \text{Revenue}_i \qquad (20)$$
$$+ \sum_{\forall j \in DR} \text{Maintenance}_j \times \text{Distance}_j \div \text{Utilization}_j$$
$$+ \sum_{\forall j \in DR} \text{Fixed Cost}_j \times \text{Driver}_j \times \text{Duration}_j \div \text{Utilization}_j$$
$$+ \sum_{\forall j \in DR \cup OTF} f(\text{Distance}_j, \text{Duration}_j) \times fuel\ Price$$
$$+ \sum_{\forall j \in OTF} \text{Renting Duration}_j \times hourly\ renting\ fee$$

## A4.    Bike-sharing: planning

Objective function of the bike-sharing planning model is as follows:

$$\min f(system) = \left( \sum_{\forall i \in Trip} \text{Access Duration}_i + \sum_{\forall i \in Trip} \text{Trip Duration}_i \right)$$
$$\times \text{Value Of Time}$$
$$+ \sum_{\forall j \in RebalancingRoute} \text{Maintenance}_j \times \text{Distance}_j$$
$$+ \sum_{\forall j \in RebalancingRoute} \text{Fixed Cost}_j \times \text{Driver}_j \times \text{Duration}_j \qquad (21)$$
$$\div \text{Utilization}_j$$
$$+ \sum_{\forall j \in RebalancingRoute} f(\text{Distance}_j, \text{Duration}_j) \times fuel\ Price$$
$$+ \sum_{\forall j \in Stations} \text{Station Fixed Cost}_j$$

## A5.    Car-sharing: planning

Objective function of the car-sharing planning model is as follows:

$$
\begin{aligned}
\min \mathrm{f}(system) = {} & \left( \sum_{\forall\, i\, \in\, Trip} \text{Access Duration}_i \;+\; \sum_{\forall\, i\, \in\, Trip} \text{Trip Duration}_i \right) \\
& \times \text{Value Of Time} \\[4pt]
& + \sum_{\forall\, j\, \in\, RebalancingRoute} \text{Maintenance}_j \times \text{Distance}_j \\
& + \sum_{\forall\, j\, \in\, RebalancingRoute} \text{Fixed Cost}_j \times \text{Driver}_j \times \text{Duration}_j \\
& \div \text{Utilization}_j \\
& + \sum_{\forall\, j\, \in\, RebalancingRoute} \mathrm{f}\left( \text{Distance}_j, \text{Duration}_j \right) \times fuel\ Price \\
& + \sum_{\forall\, j\, \in\, Stations} \text{Station Fixed Cost}_j \\[4pt]
& + \sum_{\forall\, j\, \in\, CarTrip} \text{Maintenance}_j \times \text{Distance}_j \;+\; \text{fixed Cost}_j \times \text{Distance}_j
\end{aligned}
\tag{22}
$$